

# Tropospheric Ozone Production Pathways with Detailed Chemical Mechanisms

Dissertation zur Erlangung des akademischen Grades  
des Doktors der Naturwissenschaften  
am Fachbereich Geowissenschaften  
an der Freien Universität Berlin

Vorgelegt von  
Jane Coates  
im April 2016

Freie Universität  Berlin

---



1. Gutachter: Prof. Dr. Peter Bultjes
2. Gutachter: Prof. Dr. Martijn Schaap

Tag der Disputation: 12.07.2016



# Acknowledgements

First and foremost, I would like to thank Tim Butler. Thanks for giving me the opportunity to pursue my PhD, bringing me up to speed on the skills I needed for the work and always being there to offer advice. I also appreciate the criticism which helped me improve my work, your sense of humour and that we make a good basis for a successful pub quiz team!

I would like to thank Mark Lawrence and the IASS for scientific and financial support of the project. Working at the IASS helped me develop the mindset of applying scientific research within the wider framework of societal transformation. I could not have truly appreciated this without working at the IASS and the guidance of Mark Lawrence.

I thank Peter Bultjes for the collaboration and support during the project. Your pleasant comments and input during the many PAC meetings were greatly appreciated.

Thanks also goes to all my colleagues, past and present, at the IASS. All the discussions, translations, runs around the lake and coffee breaks helped me get through this time!

Last but not least, I must thank Nadja Menz: you have sat through so many trial presentations, proofread texts and supplied an adequate amount of coffee and baked goodies to fuel me through this work. For your unwaivering support that takes on many forms - thanks!



# Table of Contents

<b>1</b>	<b>Introduction</b>	<b>1</b>
1.1	Ozone . . . . .	2
1.2	Ozone Chemistry . . . . .	3
1.2.1	VOC and NO <sub>x</sub> Chemistry . . . . .	7
1.2.2	Representing Atmospheric Chemistry in Models . . . . .	9
1.3	Source and Sinks of Ozone Precursors . . . . .	10
1.3.1	NO <sub>x</sub> . . . . .	10
1.3.2	VOCs . . . . .	11
1.3.3	Representing NMVOC Emissions in Models . . . . .	13
1.4	Effects of Meteorology on Ozone Production . . . . .	14
1.5	Research Questions and Objectives of this Thesis . . . . .	17
<b>2</b>	<b>Methodology</b>	<b>19</b>
2.1	Air Quality Modelling . . . . .	19
2.1.1	Model Description and Setup . . . . .	20
2.2	Chemical Mechanisms . . . . .	21
2.2.1	Implementing Chemical Mechanisms in MECCA . . . . .	22
2.2.2	Tagging of Chemical Mechanisms . . . . .	22
2.3	Initial and Boundary Conditions . . . . .	23

<b>3</b>	<b>Presentation of Papers</b>	<b>27</b>
3.1	Paper I: A Comparison of Chemical Mechanisms using Tagged Ozone Production Potential (TOPP) Analysis . . . . .	27
3.2	Paper II: Variation of the NMVOC Speciation in the Solvent Sector and the Sensitivity of Modelled Tropospheric Ozone . . . . .	29
3.3	Paper III: The Influence of Temperature on Ozone Production under varying NO <sub>x</sub> Conditions – A Modelling Study . . . . .	30
<b>4</b>	<b>Overall Discussion and Conclusions</b>	<b>33</b>
<b>5</b>	<b>Outlook</b>	<b>37</b>
<b>6</b>	<b>Summary and Zusammenfassung</b>	<b>41</b>
6.1	Summary . . . . .	41
6.2	Zusammenfassung . . . . .	42
	<b>References</b>	<b>45</b>
<b>7</b>	<b>Paper I: A comparison of chemical mechanisms using tagged ozone production potential (TOPP) analysis</b>	<b>55</b>
<b>8</b>	<b>Paper II: Variation of the NMVOC Speciation in the Solvent Sector and the Sensitivity of Modelled Tropospheric Ozone</b>	<b>81</b>
<b>9</b>	<b>Paper III: The Influence of Temperature on Ozone Production under varying NO<sub>x</sub> Conditions – a modelling study</b>	<b>103</b>
<b>10</b>	<b>Publication List</b>	<b>147</b>
10.1	Scientific Articles . . . . .	147
10.2	Presentations . . . . .	147
10.3	Posters . . . . .	148
	<b>Appendix</b>	<b>149</b>

# List of Tables

1.1	Categories of emission source sectors . . . . .	14
1.2	Influence of meteorological variables on ozone production . . . . .	15
2.1	MECCA box model settings. . . . .	20
2.2	Chemical mechanisms used in this work. . . . .	21
2.3	Solvent sector emission inventories compared in this work. . . . .	24



# List of Figures

1.1	Methane degradation pathways . . . . .	5
1.2	Schematic of general secondary degradation of VOCs . . . . .	6
1.3	Ozone mixing ratios as a function of NO <sub>x</sub> and VOCs . . . . .	8
1.4	NO <sub>x</sub> sources and sinks . . . . .	11



# Chapter 1

## Introduction

Air pollution is the leading environmental health risk in many areas around the world. The effects of air pollution to the general population range from chronic to less severe health impacts and reduced growth rates of vegetation resulting in economic losses of billions of euros (EEA, 2015). Moreover, the International Agency for Research on Cancer labelled air pollution as carcinogenic (IARC, 2013). Due to these impacts, many governed areas introduced legislation designed to reduce concentrations of many air pollutants.

Tropospheric ozone ( $O_3$ ) is one of the most problematic air pollutants over Europe with up to 98 % of Europe's urban population exposed to concentrations of ozone above the WHO guidelines (EEA, 2015). Furthermore, in 2011 the EU ozone target value for human health (the EU has no limit value for ozone) was exceeded in 65 % of the EU member states and Europe's ozone target value for vegetation was exceeded in 27 % of the EU-28 agricultural areas (EEA, 2013).

Reducing atmospheric concentrations of tropospheric ozone is a complex problem as ozone is not directly emitted into the troposphere. Tropospheric ozone is produced from the reactions of volatile organic compounds (VOCs) in the presence of nitrogen oxides ( $NO_x \equiv NO + NO_2$ ) and sunlight (Atkinson, 2000). Meteorology and transport also influence tropospheric ozone levels (Jacob and Winner, 2009).

Air quality (AQ) models are an important tool for understanding ozone pollution and predicting future air quality. Many AQ models are available with different scales and dimensions depending on the scope of the modelling experiment. Accurately representing the complexity of ozone production in a computationally efficient model is an ongoing challenge for the modelling community (Russell and Dennis, 2000).

Model intercomparison projects (MIPs) compare the outputs from different models showing differences in tropospheric ozone due to differing representations of key processes. For example, the Atmospheric Chemistry and Climate Model Intercomparison Project (ACCMIP) showed different magnitudes of future ozone burden in the same region (Young et al., 2013). A current MIP, the Chemistry Climate Model Initiative (CCMI), aims to investigate differences in the representation of chemistry, emissions and transport processes between models to understand the differences between predictions from global models (Eyring et al., 2013).

Detailed process studies are key to understanding the differences between simulated ozone levels using different models. This thesis focuses on the influence of the representation of VOC degradation chemistry, VOC emissions and the ozone-temperature relationship within models on ozone production, with the research questions framing this work found in Sect. 1.5. This assessment is expected to be beneficial to the modelling community in understanding potential differences between model outputs and improving AQ models. The remainder of this introduction discusses ozone in the atmosphere, the chemistry and sources of ozone as well as the effects of meteorology on ozone production.

## 1.1 Ozone

Ozone is an atmospheric gas found in the stratosphere and troposphere, however its atmospheric effects are very different in these regions. The stratosphere contains  $\sim 90\%$  of the atmospheric ozone with a peak mixing ratio of  $\sim 12$  ppm (Seinfeld and Pandis, 2006). Stratospheric ozone absorbs the sun's ultraviolet radiation which is important due to the adverse effects of excess UV radiation on humans and ecosystems.

In contrast, tropospheric (or surface) ozone is both a pollutant and a greenhouse gas. Increased levels of tropospheric ozone are harmful to humans, plants and other living systems. High ozone exposure may lead to pulmonary problems in humans and can decrease both crop yields and forest growth (World Meteorological Organisation, 2011).

Tropospheric ozone is formed via photochemical production from the reactions between VOCs and  $\text{NO}_x$ , described in Sect. 1.2, while meteorology and transport also influence ozone concentrations. For example, a spring-time peak in tropospheric ozone is common in the Northern Hemisphere mid-latitudes, originally

attributed to transport of ozone from the stratosphere into the troposphere via the Stratosphere-Troposphere Exchange (STE) (Monks, 2000). However, ozone transported via STE rarely influences surface ozone levels (Lelieveld and Dentener, 2000) and the spring maximum is due to the photochemical reactions occurring in the Northern Hemisphere spring after the buildup of reservoir species over winter (Penkett and Brice, 1986). For the rest of this thesis, ozone refers to tropospheric ozone.

Understanding the intricacies of surface ozone pollution requires a combined effort from the modelling, observational and chemical kinetic communities – called the “three-legged stool” approach by Abbatt et al. (2014). Modelling of ozone production has helped understand the complexity of atmospheric chemistry, such as the non-linear relationship of ozone production with precursor (VOC and  $\text{NO}_x$ ) emissions. Modelling studies attempt to reproduce observational trends of surface ozone and model predictions may inform new observational studies. Chemical kinetic studies performed by laboratories give insights to missing or incorrect representations of atmospheric chemistry to be included in updated models.

## 1.2 Ozone Chemistry

Ozone absorbs UV radiation producing either ground-state atomic oxygen ( $\text{O}(^3\text{P})$ ) or excited singlet ( $\text{O}(^1\text{D})$ ) oxygen atoms.



Ground-state oxygen quickly reacts with oxygen to reform ozone.



Thus, there is no net loss or production of ozone through (R1) and (R3).  $\text{O}(^1\text{D})$  may collide with  $\text{N}_2$  or  $\text{O}_2$  (represented as M in chemical reactions) stabilising to the ground-state. This process again leads to a null cycle with ozone destruction balanced by production. However,  $\text{O}(^1\text{D})$  can react with water vapour producing hydroxyl (OH) radicals. The OH radical is a highly reactive chemical species reacting with almost all trace chemical species in the troposphere. (Seinfeld and Pandis, 2006; Monks, 2005)



The initial oxidation of VOCs by OH initiates a reaction chain which may lead to net production or loss of ozone depending on the atmospheric conditions. For example, when carbon monoxide (CO) reacts with OH in the presence of oxygen, carbon dioxide and the hydroperoxy (HO<sub>2</sub>) radical are formed. In polluted areas with high-NO<sub>x</sub> concentrations, HO<sub>2</sub> readily reacts with nitrogen oxide (NO) regenerating OH and producing nitrogen dioxide (NO<sub>2</sub>).



Photolysis of NO<sub>2</sub> produces ground-state atomic oxygen leading to ozone production via (R3).



The reaction between OH and NO<sub>2</sub> produces nitric acid (HNO<sub>3</sub>), limiting the recycling of OH and NO<sub>2</sub>. Nitric acid may be removed through deposition and is a sink for both OH and NO<sub>2</sub>.



In low-NO<sub>x</sub> conditions away from polluted areas, OH and HO<sub>2</sub> are interconverted through reactions with ozone.



OH and HO<sub>2</sub> may also react in a termination reaction producing water vapour and oxygen.



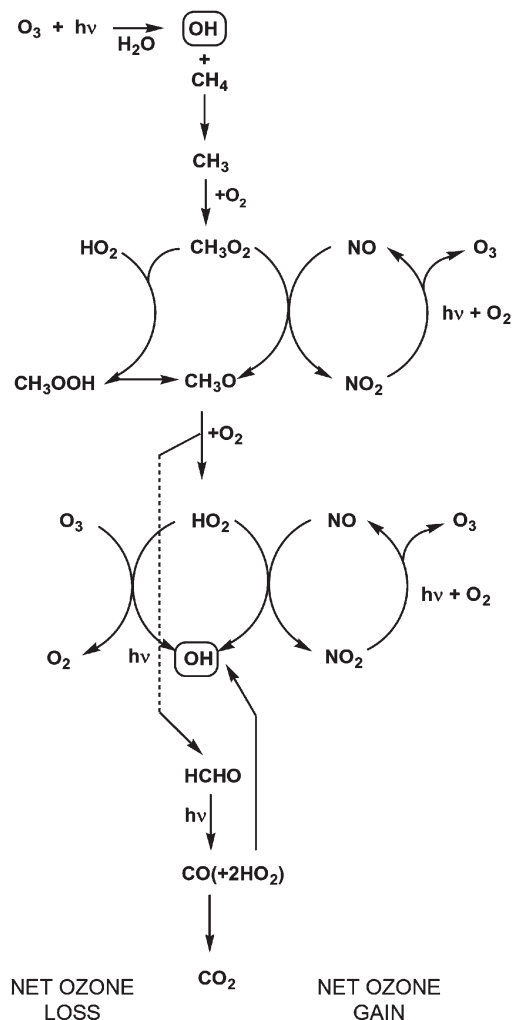
Other termination reactions involve combination reactions of HO<sub>2</sub> radicals producing hydrogen peroxide (H<sub>2</sub>O<sub>2</sub>).



Hydrogen peroxide may be removed through deposition (Gunz and Hoffmann, 1990) but may also be a temporary sink for the odd-oxygen species OH and HO<sub>2</sub>.



Figure 1.1: Methane degradation pathways in low- $\text{NO}_x$  and high- $\text{NO}_x$  conditions. Taken from Monks (2005).



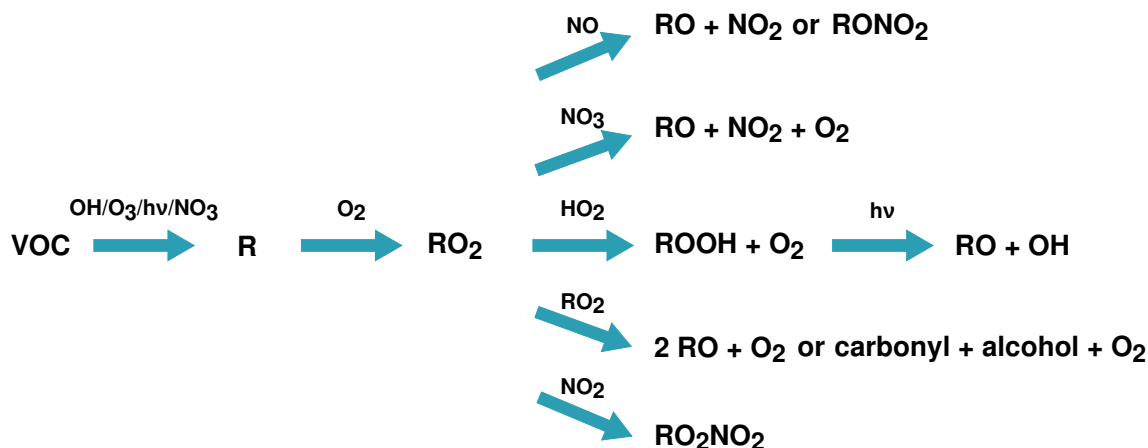
In summary, the secondary degradation of CO produces ozone in high- $\text{NO}_x$  conditions while in low- $\text{NO}_x$  conditions ozone is destroyed. (Seinfeld and Pandis, 2006; Monks, 2005)

The secondary degradation of more complex VOCs has similar features to that of CO. Methane ( $\text{CH}_4$ ), with a mixing ratio of  $\sim 1.7$  ppmv, is the most abundant VOC in the troposphere. The reaction of  $\text{CH}_4$  with  $\text{OH}$ , in the presence of  $\text{O}_2$ , produces the methyl peroxy radical ( $\text{CH}_3\text{O}_2$ ) – the simplest organic peroxy radical ( $\text{RO}_2$ ).



Similar to CO oxidation,  $\text{NO}_x$  conditions play a crucial role in the fate of  $\text{CH}_3\text{O}_2$  and whether ozone is produced or destroyed, depicted in Fig. 1.1.

Figure 1.2: Schematic diagram outlining general pathways of the secondary degradation of an emitted VOC.



The general types of secondary degradation products formed during  $\text{CH}_4$  degradation can be extended to more complex non-methane VOCs (NMVOCs). Initial oxidation pathways of NMVOCs are reactions with OH, while unsaturated VOCs, such as alkenes, may react with ozone and photolysis is important for carbonyl species. During the night-time, reaction with the nitrate ( $\text{NO}_3$ ) radical is typically more important than OH-oxidation due to the relatively higher night-time concentrations of  $\text{NO}_3$ .

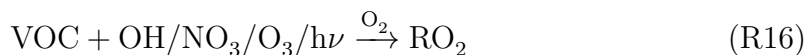
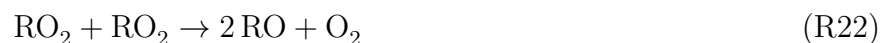
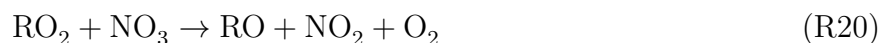


Figure 1.2 represents a general and simplified reaction scheme for VOCs in the troposphere. The initial oxidation of NMVOCs produces  $\text{RO}_2$  radicals and the fate of the  $\text{RO}_2$  determines whether net loss or production of ozone occurs.



All degradation pathways of  $\text{RO}_2$  that produce  $\text{NO}_2$  result in  $\text{O}_3$  formation due to (R7) and (R3). Reaction with  $\text{HO}_2$  forms a hydroperoxide ( $\text{ROOH}$ ) which may either be deposited or photolysed producing an alkoxy ( $\text{RO}$ ) radical and  $\text{OH}$ . The carbonyl and alcohol products resulting from reactions between  $\text{RO}_2$  radicals follows a similar sequence of reactions and can produce further  $\text{O}_3$ . Thus the subsequent reactions of secondary degradation products of a NMVOC may lead to further production of ozone.

Reaction of  $\text{RO}_2$  with  $\text{NO}_2$  (R19) forms peroxy nitrates ( $\text{RO}_2\text{NO}_2$ ) which are a temporary reservoir for  $\text{RO}_2$  and  $\text{NO}_x$ . The thermal decomposition rate of  $\text{RO}_2\text{NO}_2$  is highly temperature dependent. At lower temperatures,  $\text{RO}_2\text{NO}_2$  builds up and may be transported away from the region of formation. Thus releasing  $\text{RO}_2$  and  $\text{NO}_2$  in areas away from large sources of  $\text{NO}_x$  and fuelling ozone production.

The reaction between  $\text{NO}$  and ozone is another important reaction in polluted regions.



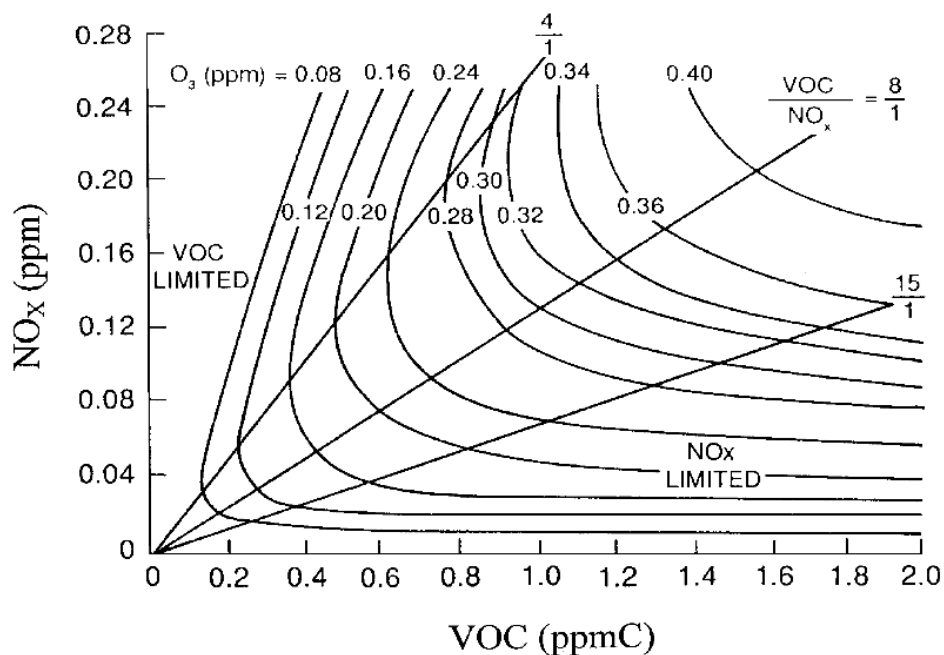
Together with (R7) and (R3), (R24) forms a null cycle of ozone production and destruction which limits ozone levels. On the local urban scale close to  $\text{NO}$  sources, (R24) decreases ozone levels called ozone titration. Ozone titration is also important during the night where the lack of photochemistry does not regenerate ozone. Urban measurement studies have confirmed the importance of ozone titration near sources of  $\text{NO}$  (Syri et al., 2001).

### 1.2.1 VOC and $\text{NO}_x$ Chemistry

The chemistry in low- $\text{NO}_x$  and high- $\text{NO}_x$  conditions indicates that ozone production is a non-linear process. Figure 1.3, taken from Jenkin and Clemitshaw (2000), depicts the non-linear relationship between ozone as a function of VOC and  $\text{NO}_x$ . This relationship can be divided into distinct regimes of ozone production:  *$\text{NO}_x$ -sensitive* (or  *$\text{NO}_x$ -limited*),  *$\text{NO}_x$ -saturated* (or *VOC-limited*) and *VOC-and- $\text{NO}_x$ -sensitive* regimes.

In regions with low- $\text{NO}_x$  concentrations,  $\text{RO}_2$  are more likely to react with other radicals rather than convert  $\text{NO}$  to  $\text{NO}_2$ . Increasing  $\text{NO}_x$  levels increases the number of  $\text{NO}$  to  $\text{NO}_2$  conversions by peroxy radicals leading to ozone production. However, increasing VOC levels has little effect on  $\text{O}_3$  production due to increased radical-radical reactions. This is  *$\text{NO}_x$ -sensitive* chemistry.

Figure 1.3: Ozone isopleth plots for various initial mixing ratios of  $\text{NO}_x$  and VOCs. Taken from Jenkin and Clemitshaw (2000).



On the other hand, in regions with high levels of  $\text{NO}_x$ , reactions between radicals and  $\text{NO}_x$  are more likely to occur. The production of  $\text{HNO}_3$  increases through (R8) removing OH and  $\text{NO}_2$ . Higher levels of VOC increase the likelihood of  $\text{RO}_2$  converting NO to  $\text{NO}_2$  leading to ozone production while higher  $\text{NO}_x$  levels will not increase  $\text{O}_3$  production. This is  $\text{NO}_x$ -saturated or *VOC-limited* chemistry.

The VOC-and- $\text{NO}_x$ -sensitive regime (contour ridges in Fig. 1.3) is characterised by  $\text{O}_3$  production being sensitive to both VOC and  $\text{NO}_x$  levels. Moreover, it is in this atmospheric regime that the maximum amount of ozone is produced. Kleinman (1994) showed that this non-linear relationship can be thought of as a titration process between radicals and  $\text{NO}_x$  with the VOC-and- $\text{NO}_x$ -sensitive regime being the turning point.

The non-linear nature of ozone production is one of the challenges in controlling ozone levels. The difficulty is exacerbated by the fact that the troposphere can alternate between these regimes depending on the meteorological conditions. Moreover, fresh emissions tend to occur in  $\text{NO}_x$ -saturated areas before being transported to VOC-and- $\text{NO}_x$ -sensitive and  $\text{NO}_x$ -sensitive regions.

## 1.2.2 Representing Atmospheric Chemistry in Models

Representing the degradation chemistry for each VOC in a chemical transport model is unrealistic. Even if all the secondary degradation pathways and products were known for every VOC, a chemical transport model would be unable to efficiently solve the system of differential equations.

The representation of atmospheric chemistry in a chemical transport model is called a chemical mechanism. Chemical mechanisms are developed by simplifying and aggregating VOCs, degradation products and reactions. Less aggressive simplification approaches may result in a chemical mechanism having thousands of species while more aggressive simplification approaches may result in only a hundred species. Chemical mechanisms are verified by comparing the concentrations of field studies or controlled chamber study experiments to model simulations (Stockwell et al., 2012). Section 2.2 includes further details of the simplification techniques used to develop chemical mechanisms.

Chemical mechanism comparison studies, such as Kuhn et al. (1998), Emmerson and Evans (2009) and Archibald et al. (2010), compared the outputs of different chemical mechanisms using the same model setup and initial conditions. These studies showed that the differences between chemical mechanisms led to large differences in simulated ozone concentrations. While these comparisons indicate that chemical mechanisms lead to differences in ozone levels, they do not point out the root cause of the differences.

Determining the source of differences between chemical mechanisms is a difficult task due to the interlinked chemistry of many key species. The first part of this work compares the ozone production from different chemical mechanisms determining the differences in the treatment of VOC degradation chemistry. The research questions framing this comparison are presented in Sect. 1.5 and the results are described in Sect. 3.1.

## 1.3 Source and Sinks of Ozone Precursors

Ozone precursors are emitted from many anthropogenic and biogenic sources with varying emissions throughout the year, month and day. In many regions, reduced road transport during the weekend leads to a noticeable reduction in  $\text{NO}_x$  emissions influencing ozone levels. This is called the “weekend-effect”. For example, ozone production is  $\text{NO}_x$ -saturated during weekdays in San Joaquin Valley, California but during the weekend higher ozone levels are recorded as the reduction in  $\text{NO}_x$  levels leads to VOC-and- $\text{NO}_x$ -sensitive chemistry (Pusede et al., 2014). Many sources of NMVOC also have a reduction of activities during the weekend, such as industry and solvent use, and residential combustion is highest during the winter months and lowest during the summer (Denier van der Gon et al., 2011).

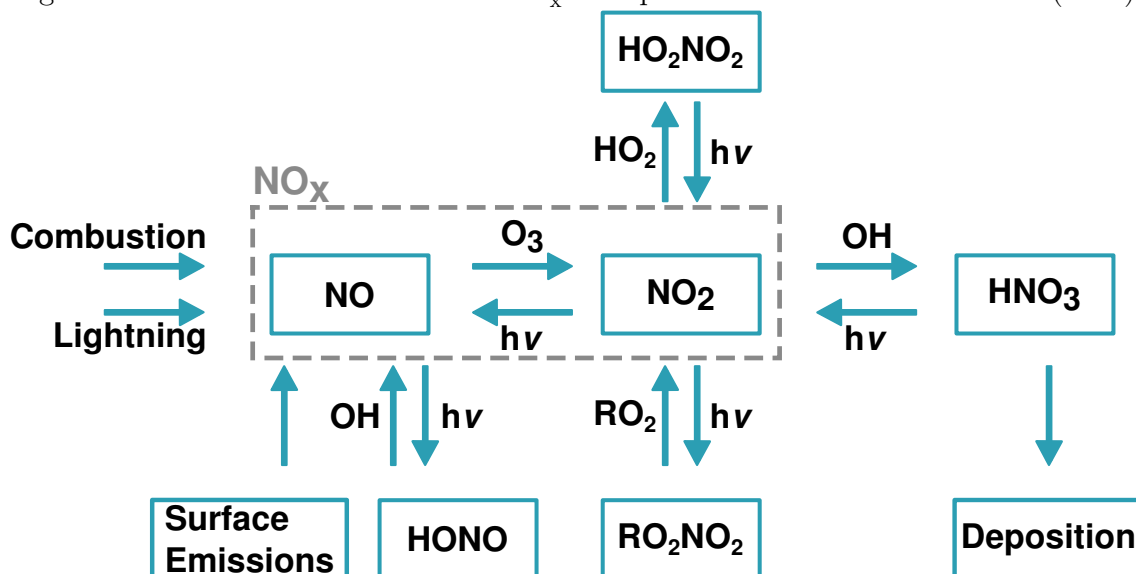
### 1.3.1 $\text{NO}_x$

Anthropogenic activities are the main source of  $\text{NO}_x$  emissions into the atmosphere. In the year 2000, almost 52 Tg N were emitted with 65 % fossil fuel combustion (Seinfeld and Pandis, 2006). Examples of fossil fuel combustion are diesel and petrol vehicles, industrial activities and domestic heating (von Schneidemesser et al., 2015).

Up to 95 % of  $\text{NO}_x$  emissions from combustion are emitted as NO, which is oxidised to form  $\text{NO}_2$  through (R24) and (R6). However, the increase in diesel vehicles and the implementation of diesel filters increased the fraction of emitted  $\text{NO}_2$  from vehicles. Grice et al. (2009) showed that over Europe, emissions of  $\text{NO}_2$  from diesel vehicles have increased from 8.6 % in 2000 to 12.4 % in 2004.

Despite the majority of  $\text{NO}_x$  emissions coming from human activities, there are also natural sources of  $\text{NO}_x$ . Lightning is an important source of  $\text{NO}_x$  in the free troposphere, while emissions of  $\text{NO}_x$  from soils are important in remote regions with little anthropogenic influence. Lightning and soils each contributed  $\sim 10$  % to global  $\text{NO}_x$  emissions in 2000 (Seinfeld and Pandis, 2006).

The main sink of  $\text{NO}_x$  is through deposition of nitric acid, formed via (R8). Temporary reservoirs, such as peroxy nitrates and HONO, may be transported away from sources into remote areas and their decomposition is an important source of  $\text{NO}_x$  fuelling ozone production in these areas. These sources and sinks of  $\text{NO}_x$  are illustrated in Fig. 1.4.

Figure 1.4: The sources and sinks of  $\text{NO}_x$ . Adapted from Seinfeld and Pandis (2006).

### 1.3.2 VOCs

This section looks at the sources and sinks of methane, non-methane VOCs and CO. Although CO is not actually a VOC, its photochemistry is important for ozone production. The main sink of VOCs is the oxidation chemistry (Sect. 1.2) leading to  $\text{CO}_2$  and  $\text{H}_2\text{O}$ . The degradation of VOCs plays an important role in secondary organic aerosol formation as well as ozone production (Hallquist et al., 2009).

The degradation of a VOC yields the maximum possible amount of ozone when every peroxy radical converts  $\text{NO}$  to  $\text{NO}_2$  called the *ozone production potential* (OPP) of a VOC. In reality, the OPP of a VOC is never achieved as other reactions with peroxy radicals occur. However, the OPP is useful for assessing the amount of ozone produced from emitted VOCs.

#### Carbon Monoxide

Carbon monoxide is emitted directly into the troposphere through combustion and industrial processes. An equally important source of CO is its formation during VOC degradation. Hauglustaine et al. (1998) estimated that  $881 \text{ Tg yr}^{-1}$  of CO was produced globally from chemical oxidation of VOC, while  $1219 \text{ Tg yr}^{-1}$  of CO was directly emitted.

The reaction between CO and OH (R5) is the main sink of CO. The OPP of CO is one, as the degradation of CO produces one peroxy radical ( $\text{HO}_2$ ), thus a maximum of one molecule of ozone may be produced during CO degradation.

## Methane

Emissions of methane range between 500 and 600 Tg CH<sub>4</sub> yr<sup>-1</sup> with ~60 % of the emissions from anthropogenic sources. The main anthropogenic sources of CH<sub>4</sub> are agriculture, fossil fuels and biomass burning with agriculture contributing 60 % of the anthropogenically emitted CH<sub>4</sub>. Emissions from wetlands are the main natural source of methane emissions (Kirschke et al., 2013).

Methane has a lifetime in the atmosphere of about 10 years, significantly longer than other VOCs (Voulgarakis et al., 2013). The lifetime of a chemical species is the time required for the concentration of the species to decrease by  $\frac{1}{e}$  (Seinfeld and Pandis, 2006). Thus, methane influences ozone production on the global rather than the regional scale and is important for background levels of ozone.

Reaction with OH (R15) is the main sink of methane and the secondary degradation of CH<sub>4</sub> (Fig. 1.1) produces CO and four peroxy radicals (1× CH<sub>3</sub>O<sub>2</sub>, 3× HO<sub>2</sub>). Thus the OPP of methane is five, as methane degradation can produce a maximum five molecules of O<sub>3</sub> per molecule of CH<sub>4</sub> oxidised.

## NMVOCs

A wide variety of NMVOCs are emitted from anthropogenic activities directly into the troposphere. Solvent use, industry, fossil fuel burning and transportation are all major activities emitting NMVOCs of varying functional groups, carbon numbers and reactivity. Emissions of NMVOC from vegetation depend on meteorological variables (such as temperature and radiation) and biological variables (such as leaf age and leaf area index) (Guenther et al., 2012).

Lamarque et al. (2010) estimated that in 2000, 130 Tg NMVOC were globally emitted from anthropogenic sources. This amount is dwarfed by emissions from biogenic sources – 1000 Tg NMVOC yr<sup>-1</sup> (Guenther et al., 2012). Isoprene (C<sub>5</sub>H<sub>8</sub>) emitted from vegetation dominates at the global scale; however, emissions of other NMVOC from vegetation, such as monoterpenes and sesquiterpenes, may be significant on the regional scale.

Although isoprene is considered as a biogenic VOC (BVOC), it has been measured in the urban areas of London and Paris away from biogenic emission sources and during times where biogenic emissions are not important, such as freezing conditions in winter. Transport of isoprene is unlikely, as isoprene is a highly reactive NMVOC indicating anthropogenic sources of isoprene (von Schneidmesser et al., 2011). Other NMVOC emitted from anthropogenic sources, such as methanol and acetaldehyde, are also emitted from vegetation (Guenther et al., 2012).

The maximum number of molecules of O<sub>3</sub> produced per degradation of an emitted NMVOC depends on the type and the number of carbons of the NMVOC leading to a wide range of OPPs for different NMVOC. Unsaturated NMVOC, such as alkenes, tend to have larger OPPs than alkanes (saturated NMVOC). Even within a functional group of NMVOC, different OPPs are calculated. For example, benzene and xylene are both aromatic compounds but as benzene is a more chemically stable molecule it has a lower OPP than xylene (Carter, 1994).

OPPs for complex NMVOCs have been calculated using models by incrementally varying the concentration of an NMVOC and calculating the change in ozone. Different OPP scales have been developed using different NO<sub>x</sub> conditions. The Maximum Incremental Reactivity (MIR) and Maximum Ozone Incremental Reactivity (MOIR) scales of Carter (1994) and the Tagged Ozone Production Potential (TOPP) of Butler et al. (2011) are examples of OPP scales for NMVOCs.

### 1.3.3 Representing NMVOC Emissions in Models

Emissions of NMVOC species are a critical input in models and emission inventories are used to specify the type and quantity of emissions from source categories. Table 1.1 lists the source sectors of emissions used by the TNO-MACCII emission inventory (Kuenen et al., 2014). Emission inventories are available for global or regional emissions. For example, EDGAR (Olivier et al., 2001) specifies global emissions while TNO-MACCII (Kuenen et al., 2014) specifies European emissions.

Many uncertainties are associated with emission inventories. For example, Coll et al. (2010) showed that large discrepancies arise between ambient measurements and emission inventories. Often temporal variation of emissions are not captured by emission inventories (Boynard et al., 2014).

BVOC emissions depend on meteorological and biological variables and algorithms estimating BVOC emissions may be calculated as part of the model simulation instead of an emission inventory. Emissions of AVOCs may also depend on meteorological variables, for example, evaporative emissions increase with temperature (Rubin et al., 2006). The Model of Emissions of Gases and Aerosols from Nature (MEGAN, Guenther et al. (2006, 2012)) calculates BVOC emissions using the temperature and radiation values determined from the model. Specifying BVOC emissions using an algorithm or emission inventory influences modelled ozone concentrations. For example, Curci et al. (2009) noted large differences in summertime ozone concentrations over Europe when using a gridded emission inventory or an on-line algorithm for BVOC emissions.

Table 1.1: Emission source sectors for anthropogenic emissions listed in the TNO-MACCII inventory (Kuenen et al., 2014).

<b>Emission Source Category</b>	<b>Emission Source Category</b>
Public Power	Road Transport: Others
Residential Combustion	Road Transport: Evaporation
Industry	Road Transport: Wear
Fossil Fuel	Non-road Transport
Solvent Use	Waste
Road Transport: Gasoline	Agriculture
Road Transport: Diesel	

Emissions of the NMVOCs specified by an emission inventory are mapped to the chemical mechanism species used in the model. This mapping is not standardised throughout the modelling community with the same NMVOC emissions possibly being allocated to different chemical species even if using the same chemical mechanism (Carter, 2015).

The influence of the speciation of NMVOC emissions on modelled ozone production is determined in the second part of this work. Moreover, the effect of using the same speciations of NMVOC emissions with different chemical mechanisms is also explored. Section 1.5 outlines the research questions and the results are presented in Sect. 3.2.

## 1.4 Effects of Meteorology on Ozone Production

Meteorological conditions influence the production of ozone with clear and calm summer days typically having high ozone levels (Dueñas et al., 2002). Comrie (1997) noted a complex relationship between meteorology and ozone due to competing positive and negative effects on ozone production. Table 1.2, taken from Jacob and Winner (2009), details the effects of specific meteorological variables on ozone production.

Climate change is predicted to influence many meteorological variables and increase the number of heatwaves (Karl and Trenberth, 2003). Thus, understanding the influence of meteorology on ozone production is particularly important for future predictions of air quality and tackling ozone pollution in a changing climate.

Table 1.2: Influence of meteorological variables on ozone production, taken from Jacob and Winner (2009).

Meteorological Variable	Influence on Ozone
Temperature	Consistently positive
Stagnation	Consistently positive
Wind Speed	Generally negative
Mixing Height	Weak or variable
Humidity	Weak or variable
Cloud Cover	Generally negative
Precipitation	Weak or variable

### Humidity

Humidity influences ozone production both positively and negatively. When  $O(^1D)$ , originating from ozone photolysis (R2), reacts with water vapour (R4), the production of OH radicals leads to ozone loss. However, the initiation of VOC degradation through reaction with OH can lead to ozone production (Sect. 1.2). These competing effects of water vapour on ozone production lead to a weak correlation of ozone production with water vapour (Jacob and Winner, 2009).

### Wind Speed

High wind speeds transport ozone precursors away from their sources leading to a generally negative effect on ozone pollution over a region. Model projections of Doherty et al. (2013) showed that while climate change is expected to change large-scale atmospheric transport, there is little influence on the spatial patterns of mean concentrations of ozone.

### Stagnation

During periods of low wind speeds, emissions of ozone precursors remain close to their sources. These stagnant conditions over polluted urban areas are highly correlated with increased ozone production over urban areas (Jacob and Winner, 2009). Heatwaves result from stagnant conditions along with high temperatures enhancing the ozone pollution over a region.

## Mixing Height

The effects of the mixing height of the planetary boundary layer (PBL) with the free troposphere depend on the region. For example, Dawson et al. (2007) found that over the Eastern U.S., regions with low ozone are positively correlated with a higher mixing height, whereas regions with high ozone levels are negatively affected. This spatial effect of mixing height on ozone production depends on the difference between ozone levels within the PBL and the free troposphere (Jacob and Winner, 2009).

Mixing between the PBL and free troposphere into regions with levels of surface ozone lower than the free troposphere is an additional source of ozone. Conversely, mixing of the elevated levels of ozone from polluted areas into the free troposphere reduces the burden of surface ozone.

## Cloud Cover

Cloud cover negatively affects the photochemistry of ozone production with increased cloud cover reducing the amount of sunlight reaching the troposphere. Korsog and Wolff (1991) showed a negative correlation between cloud cover and ozone. Also, ozone levels in the study of Dawson et al. (2007) were not significantly influenced by changes in cloud cover.

## Precipitation

Precipitation influences the wet deposition rates of ozone and other chemical species. The studies of Dawson et al. (2007) and Murazaki and Hess (2006) noted a minor influence of precipitation on ozone levels.

## Temperature

Temperature is positively correlated with ozone in many areas. Otero et al. (2016) showed that temperature was the main driver of summertime ozone values over many areas of central Europe while Camalier et al. (2007) correlated ozone with temperature over the Eastern US. Sillman and Samson (1995) illustrated that only ozone pollution produced from the chemistry described in Sect. 1.2 is correlated with temperature rather than background ozone, the ozone levels without the influence of local emissions of anthropogenic NMVOCs.

Temperature directly influences ozone levels in two ways: increasing the emissions of VOCs from vegetation and speeding up the rates of chemical reactions. The review of Pusede et al. (2015) showed that the temperature dependence of radical production, organic reactivity, the shorter lifetime of  $\text{RO}_2\text{NO}_2$  and the formation of alkyl nitrates (R18) affects ozone production. Pusede et al. (2015) also highlighted a lack of modelling studies considering the relationship between ozone production and temperature with different  $\text{NO}_x$  conditions.

The final part of this work simulates this relationship between ozone, temperature and  $\text{NO}_x$  and determines whether temperature-dependent BVOC emissions or temperature-dependent chemistry is more important for ozone production in urban areas. The research questions for this study are detailed in Sect. 1.5 and results are presented in Sect. 3.3.

## 1.5 Research Questions and Objectives of this Thesis

The detailed chemistry producing ozone cannot be fully represented in models for reasons of computational efficiency. Thus, models select a particular representation of atmospheric chemistry raising the overarching research questions for this thesis:

- How do representations of detailed atmospheric chemistry influence simulated ozone production?
- What are the most important chemical processes when simulating ozone production?

This work addresses these questions through detailed modelling studies. Three studies were designed to highlight the chemical processes having the largest impact on simulated ozone production.

Firstly, different simplified versions of the ozone production chemistry are available to the modelling community with comparison studies showing that ozone concentrations vary between chemical mechanisms. These chemical mechanism comparison studies do not determine the root causes of the differences between chemical mechanisms, leading to the research questions:

- How do the simplification techniques used by different chemical mechanisms affect ozone production?
- Which processes are responsible for differences in ozone production with different chemical mechanisms?

Secondly, NMVOC emissions are a known source of uncertainty in modelling experiments. The choice of emission inventory influences the speciation of individual NMVOC emissions, possibly influencing ozone production. By comparing the ozone produced using different emission inventories, the following research questions are addressed:

- What is the influence on modelled ozone production when using different speciations of emitted NMVOCs?
- Does this influence change when using different chemical mechanisms?

Finally, meteorology influences ozone production with temperature having the strongest positive correlation with ozone. Temperature directly influences ozone production through increasing biogenic emissions and speeding up the reaction rates of chemical reactions.

- Are temperature-dependent emissions or chemical processes more important for ozone production with increasing temperature?
- How is the ozone-temperature relationship treated by different chemical mechanisms?

Detailed processed studies were performed using a box model to address these research questions, details of the experimental setup are presented in Chap. 2. The results of the experiments are found in Chap. 3, the general discussion and conclusions of the thesis are in Chap. 4.

# Chapter 2

## Methodology

This chapter details the methodology used to address the research questions of this work (Sect. 1.5). A brief description of AQ modelling is followed by the model set-up used in the separate studies (Sect. 2.1). The chemical mechanisms used in this work are introduced in Sect. 2.2 and the required initial and boundary conditions are described in Sect. 2.3.

### 2.1 Air Quality Modelling

AQ models are mathematical representations of the atmosphere designed to produce continuous output fields that aid in explaining sources of air pollution. All models numerically solve the system of differential equations describing the conservation of chemical species used by the model (Russell and Dennis, 2000).

Solving the system of differential equations requires initial and boundary conditions for each chemical species. Initial conditions fix the starting concentrations of each species in every grid-box. Boundary conditions require knowledge of the concentration and transport of each species at the boundary edges of the model grid.

Eulerian models are the most common type of AQ model (Russell and Dennis, 2000). These models describe the atmosphere by fixed grid-boxes where species are transported in and out of the boxes (Seinfeld and Pandis, 2006). Box models are the simplest type of model (zero-dimensional) having uniform atmospheric concentrations that are a function of time. On the other hand, 3D models describe atmospheric concentrations as a function of time, latitude, longitude and height requiring more computing power than a box model (Seinfeld and Pandis, 2006). Box models may lack realism but are useful for studying detailed processes influencing air quality.

Table 2.1: MECCA box model settings.

Model Parameter	Setting
Pressure	1013 hPa
Relative Humidity	81 %
Starting Date and Time	27th March 06:00
Model Time Step	20 mins

### 2.1.1 Model Description and Setup

The MECCA (Module Efficiently Calculating the Chemistry of the Atmosphere) box model was used throughout this work. MECCA was developed by Sander et al. (2005) and adapted to include MCM v3.1 chemistry by Butler et al. (2011). MECCA was used in the published studies of Kubistin et al. (2010) and Lourens et al. (2016).

MECCA is written in Fortran code and runs on UNIX/Linux platforms. The Kinetic Pre-Processor (KPP, Damian et al. (2002)) processed the chemical mechanism and generated Fortran code further compiled within MECCA. KPP has many choices of numerical solvers for solving the differential equations, out of which a Rosenbrock solver (ros3 option) was used for this work.

Emissions of species into the box and deposition of species out of the box were handled by KPP. The chemical mechanism included pseudo-unimolecular reactions specifying the emissions and dry deposition of chemical species with the relevant rate. The emitted chemical species and emission rates were read into the model using a namelist file. Namelist files also specified the initial and boundary conditions of chemical species.

The physical parameters used in MECCA throughout this work are detailed in Table 2.1. In the first two studies, temperature was held constant at 293 K (20 °C) and the boundary layer height was fixed at 1000 m. In the final study, MECCA was updated to include a variable diurnal boundary layer height and temperature was systematically varied between 288 K and 313 K (15–40 °C). These changes to the model setup for the final study are outlined in Paper III (Chap. 9).

Photolysis rates were parameterised as a function of the solar zenith angle based on the approach of the MCM (Jenkin et al., 1997). This parameterisation utilises the degree of latitude and in the first two studies 34 °N, roughly the city of Los Angeles, was used. In the final study, the latitude was set to 51 °N, simulating central European conditions.

Table 2.2: Chemical mechanisms used in this work.

Chemical Mechanism	Lumping Type	Reference
MCM v3.1 and v3.2	No lumping	Jenkin et al. (1997), Jenkin et al. (2003) Saunders et al. (2003), Bloss et al. (2005) Rickard et al. (2015)
CRIv2	Lumped intermediate	Jenkin et al. (2008)
MOZART-4	Lumped molecule	Emmons et al. (2010)
RADM2	Lumped molecule	Stockwell et al. (1990)
RACM	Lumped molecule	Stockwell et al. (1997)
RACM2	Lumped molecule	Goliff et al. (2013)
CBM-IV	Lumped structure	Gery et al. (1989)
CB05	Lumped structure	Yarwood et al. (2005)

## 2.2 Chemical Mechanisms

The chemical mechanisms used in this study are listed in Table 2.2 with more details found in Paper I (Sect. 3.1). These chemical mechanisms were chosen as they are commonly used by the AQ modelling community as outlined by the review of European modelling groups by Baklanov et al. (2014).

The Master Chemical Mechanism (MCM, Jenkin et al. (1997, 2003); Saunders et al. (2003); Bloss et al. (2005); Rickard et al. (2015)) is a near-explicit chemical mechanism with a high level of detail making it ideal as the reference chemical mechanism in each study of this work. The Common Representative Intermediates (CRI) chemical mechanism (Jenkin et al., 2008) is a lumped-intermediate mechanism where the degradation productions are aggregated (lumped) rather than the emitted VOC.

Lumped-molecule chemical mechanisms aggregate primary VOCs into mechanism species and is the most commonly used simplification approach. The lumped-molecule chemical mechanisms used in this work were Model for Ozone and Related chemical Tracers (MOZART, Emmons et al. (2010)), Regional Acid Deposition Model (RADM2, Stockwell et al. (1990)), Regional Atmospheric Chemistry Mechanism (RACM, Stockwell et al. (1997)) and RACM2 (Goliff et al., 2013). Lumped-structure chemical mechanisms represent emissions of NMVOC through emissions of mechanism species representing the bonds present in the NMVOC. Two versions of the Carbon Bond mechanisms (CBM-IV, (Gery et al., 1989) and CB05, (Yarwood et al., 2005)) were the lumped-structure chemical mechanisms used in this work.

### 2.2.1 Implementing Chemical Mechanisms in MECCA

Each chemical mechanism listed in Table 2.2 was adapted to the KPP format used in the MECCA box model. The Weather Research and Forecasting-Chemistry (WRF-Chem) model (Grell et al., 2005) includes KPP versions of RADM2, RACM and CBM-IV and this was the source for these chemical mechanisms. The full version of the CRI v2 was obtained from <http://mcm.leeds.ac.uk/CRI> while the original reference was the source for all other chemical mechanisms in Table 2.2.

In order to focus on the differences in the representation of VOC degradation between the chemical mechanisms, a number of harmonisations between the chemical mechanisms were implemented. For these harmonisations, the approaches used by the reference chemical mechanism (MCM v3.2) were implemented in the reduced chemical mechanisms. These changes are detailed in Paper I (Chap. 7).

### 2.2.2 Tagging of Chemical Mechanisms

AQ models can be used to allocate the effects of different precursors or emission sources on ozone production. For example, source removal studies perform separate model simulations with and without emissions from a sector to quantify the effect of the sector on ozone production, such as the quantification of megacity emissions on ozone production in Butler and Lawrence (2009). Tagging is another approach where the chemical mechanism includes additional chemical species labelled (tagged) with source information. For example, Emmons et al. (2012) tagged the MOZART-4 chemistry to attribute ozone production to emission sources of  $\text{NO}_x$ .

In Butler et al. (2011), tagged VOC chemistry allows allocation of ozone production to emitted VOCs. Tagging involves labelling every organic degradation product produced during the degradation of a VOC with the name of the VOC. This labelling is repeated for every degradation product until the final degradation products ( $\text{CO}_2$  and  $\text{H}_2\text{O}$ ) are produced, thus every VOC has a separate set of reactions fully describing its degradation. This tagging approach uses  $\text{O}_x$  production as a proxy for  $\text{O}_3$  production and is only valid for  $\text{NO}_x$ -limited and VOC-and- $\text{NO}_x$  sensitive chemistry, not  $\text{NO}_x$ -saturated conditions. The  $\text{O}_x$  family includes  $\text{O}_3$ ,  $\text{NO}_2$ ,  $\text{O}(^1\text{D})$ ,  $\text{O}(^3\text{P})$ ,  $\text{NO}_3$ ,  $\text{N}_2\text{O}_5$  and other species involved in fast production and loss cycles with  $\text{NO}_2$ .

All chemical mechanisms in Table 2.2 were tagged using the approach of Butler et al. (2011). In the first study, the tagging approach was the basis for comparing the representations of VOC degradation chemistry and their effects on ozone production. The second study also used VOC-and-NO<sub>x</sub>-sensitive conditions and the tagged chemical mechanisms were used to determine the sources of differences in ozone production from the solvent sector emission inventories of Table 2.3. Since variable NO<sub>x</sub>-conditions were used in the third study, the tagging approach could not be used in this study. Thus, all model simulations assessing the ozone-temperature relationship with different NO<sub>x</sub> conditions were performed with non-tagged versions of the chemical mechanisms.

## 2.3 Initial and Boundary Conditions

In all simulations of this work, methane (CH<sub>4</sub>) was fixed to 1.75 ppmv, while carbon monoxide (CO) and O<sub>3</sub> were initialised at 200 ppbv and 40 ppbv and then allowed to evolve freely. The initial conditions for NMVOC emissions were held constant until noon of the first day of simulations to simulate a fresh plume of emissions.

### NMVOC Initial Conditions

The initial conditions for NMVOC species differed in each experiment, a brief summary is given below and details are found in the respective publications (Chaps. 7–9). The first study used the initial conditions of the Los Angeles simulation in Butler et al. (2011) to determine the emissions needed for constant mixing ratios of the initial NMVOCs. These emissions were mapped to the appropriate chemical species of each chemical mechanism in Table 2.2 keeping the amount of emitted NMVOC constant between model runs.

The second study used NMVOC emissions specified by the emission inventories for the solvent sector listed in Table 2.3 over a theoretical urban area of 1000 km<sup>2</sup> with total NMVOC emissions of 1000 tons/day. The solvent sector contributes ~43 % by mass of total emissions (EEA, 2011), thus total NMVOC emissions of 430 tons/day were used. Further simulations used emissions from all other sectors (remaining 570 tons/day), while varying the solvent sector NMVOC emissions. Additional simulations included BVOC emissions of isoprene and monoterpenes, while varying the speciation of NMVOC emissions from the solvent sector.

Table 2.3: Solvent sector emission inventories compared in this work.

<b>Speciation</b>	<b>Comment</b>	<b>Reference</b>
TNO	European average	Builtjes et al. (2002)
IPCC	Model Specific	Ehhalt et al. (2001)
EMEP	Model Specific	Simpson et al. (2012)
DE94	Country Specific	Friedrich et al. (2002)
GR95	Country Specific	Sidiropoulos and Tsilingiridis (2007)
GR05	Country Specific	Sidiropoulos and Tsilingiridis (2007)
UK98	Country Specific	Goodwin (2000)
UK08	Country Specific	Murrells et al. (2010)

The NMVOC emissions of the solvent sector were assigned to MCM v3.2 species based on the speciations of each emission inventory. Model simulations were repeated using MOZART-4 and RADM2 to investigate whether changing the chemical mechanism affected the differences in ozone concentrations between the solvent sector emission inventories.

The final study looked at the ozone-temperature relationship over central Europe and used the emissions of NMVOC from the Benelux (Belgium, Netherlands and Luxembourg) region. The TNO\_MACCIII emissions for the year 2011 were used as anthropogenic NMVOC emissions and mapped to MCM v3.2 species. Temperature-independent emissions of biogenic species (isoprene and monoterpenes) were taken from the EMEP speciation (Simpson et al., 2012). Simulations using temperature-dependent emissions of isoprene used the MEGAN2.1 algorithm (Guenther et al., 2012). All simulations were repeated using the CRI v2, MOZART-4, RADM2 and CB05 chemical mechanisms.

### **NO<sub>x</sub> Initial Conditions**

NO<sub>x</sub> conditions generating VOC-and-NO<sub>x</sub> sensitive chemistry were used in the first two studies. This was achieved by emitting the amount of NO required to balance the source of radicals at each time step. On the other hand, the final study assessed the relationship between ozone and temperature with different NO<sub>x</sub> conditions. For these simulations, a constant source of NO emissions was systematically varied between  $5.0 \times 10^9$  and  $1.5 \times 10^{12}$  molecules (NO) cm<sup>-2</sup> s<sup>-1</sup> at each temperature used in this study (15 – 40 °C).

## Boundary Conditions

No chemical boundary conditions were used in the first two studies, as the experiments considered a contained box. In the final study, MECCA included a diurnal profile of the PBL with vertical mixing into the free troposphere using the PBL heights from the BAERLIN2014 campaign (Bonn et al., 2016). The boundary conditions for the free troposphere mixing ratios for O<sub>3</sub>, CH<sub>4</sub> and CO were set to 50 ppbv, 1.8 ppmv and 116 ppbv respectively. These mixing ratios were taken from the 700 hPa height using the MATCH-MPIC chemical weather forecast data (<http://cwf.iass-potsdam.de/>) from March 21st, 2014.



# Chapter 3

## Presentation of Papers

This chapter outlines the main findings in each scientific paper published as part of this thesis. These publications are found in Chaps. 7–9. Chapter 4 discusses the results of the individual papers in the context of the thesis and my contribution to each paper is described in the Appendix to this thesis.

### **3.1 Paper I: A Comparison of Chemical Mechanisms using Tagged Ozone Production Potential (TOPP) Analysis**

Published: J. Coates and T. M. Butler. A comparison of chemical mechanisms using tagged ozone production potential (TOPP) analysis. *Atmospheric Chemistry and Physics*, 15(15):8795–8808, 2015.

This paper compared the effects of VOC degradation represented by different chemical mechanisms on ozone production. Table 2.2 lists the chemical mechanisms compared in this study with the detailed MCM v3.2 chemical mechanism being the reference chemical mechanism. This chemical mechanism comparison used the tagging approach described in Sect. 2.2.2 to obtain insights into the influences of the simplified representations of VOC degradation by chemical mechanisms on ozone production.

A comparison of the time series of ozone mixing ratios on the first two days of simulations showed that they were generally lower using the reduced chemical mechanisms than using the MCM v3.2. The difference in peak ozone on the first day between all chemical mechanisms was 21 ppbv when including the outlier RACM chemical mechanism and 8 ppbv when not including RACM. The representation of the degradation of aromatic VOC in RACM led to lower ozone mixing ratios than all other chemical mechanisms.

The VOC degradation described in CRI v2, a lumped-intermediate chemical mechanism, produced the most similar amounts of  $O_x$  to the MCM v3.2 for each VOC. On the other hand, the VOC degradation in all other reduced chemical mechanisms led to differences in  $O_x$  production with the largest differences occurring after the first day of simulations. The degradation of aromatic VOC in the reduced chemical mechanisms led to the largest differences in  $O_x$  production from the MCM v3.2.

Many VOCs were broken down into smaller-sized degradation products faster on the first day in reduced chemical mechanisms than the MCM v3.2. The faster breakdown of VOC led to lower amounts of larger-sized degradation products that may further degrade and produce  $O_x$ . Thus, many VOCs in reduced chemical mechanisms produced a lower peak of  $O_x$  than the MCM v3.2 leading to lower ozone mixing ratios from the reduced chemical mechanisms compared to the MCM v3.2.

Reactive VOC, such as alkenes and aromatic VOC, produced peak  $O_x$  on the first day of simulations. Alkenes produced similar amounts of  $O_x$  on the first day between chemical mechanisms with differences in  $O_x$  production arising when mechanism species represented individual VOC. Large inter-mechanism differences in  $O_x$  production resulted from the degradation of aromatic VOC on the first day due to the faster breakdown of the mechanism species representing aromatic VOC in reduced chemical mechanisms. The less-reactive alkanes produced peak  $O_x$  on the second day of simulations with peak  $O_x$  lower in each reduced chemical mechanism than the MCM v3.2 due to the faster breakdown of alkanes into smaller sized degradation products on the first day by the reduced chemical mechanisms. The reduced chemical mechanisms generally produced lower ozone than the MCM v3.2 which could lead to an underprediction of ozone production when using 3D models.

## 3.2 Paper II: Variation of the NMVOC Speciation in the Solvent Sector and the Sensitivity of Modelled Tropospheric Ozone

Published: E. von Schneidemesser, J. Coates, H. D. van der Gon, A. Visschedijk, and T. Butler. Variation of the NMVOC speciation in the solvent sector and the sensitivity of modelled tropospheric ozone. *Atmospheric Environment*, 135:59 – 72, 2016.

The second publication compared ozone production using different emission inventories (EIs) of NMVOC emissions for the solvent sector. The MCM v3.2, MOZART-4 and RADM2 chemical mechanisms were used to ascertain whether the representation of tropospheric chemistry affected the differences in ozone production when using the different solvent sector EIs. Simulations using the tagged approach were performed to allocate  $O_x$  production to the emitted NMVOC specified by each EI.

A maximum difference in peak ozone mixing ratios ranged between 11 ppbv and 15 ppbv with different EIs using a single chemical mechanism. When using the same EI, a maximum difference of 7 ppbv in peak ozone mixing ratios was determined between simulations with different chemical mechanisms.

A lower maximum difference in peak ozone (6 – 9 ppbv) was produced from simulations using emissions from all other non-solvent emission sectors while varying the emissions from the solvent sector with each chemical mechanism. Including emissions from biogenic sources further reduced the maximum differences in peak ozone mixing ratios (5 – 8 ppbv) with each chemical mechanism.

Reactive VOCs, such as alkenes and aromatics, contributed the most to  $O_x$  production on the first day. While less-reactive VOCs, such as alkanes and oxygenated VOC, contributed the most to the cumulative  $O_x$  production after seven days of simulations.

A positive correlation was determined between  $O_x$  production and the specified contribution of alkane species by the EI. While a negative correlation was determined between cumulative  $O_x$  production and the contribution of oxygenated species specified by the EIs. No correlation was found between the specification of aromatic species by EIs and  $O_x$  production and as not all solvent sector EIs specify alkene emissions no correlation was calculated between specified alkene emissions and  $O_x$  production.

The results of this study showed that ozone production was influenced by both the choice of chemical mechanism and EI, indicating that updating EI speciations would be appropriate for the wider AQ modelling community to capture changing emission speciations. However, before updating the speciation of EIs, the sensitivity of ozone production to the speciation of an EI should be tested using more realistic 3D models.

### 3.3 Paper III: The Influence of Temperature on Ozone Production under varying $\text{NO}_x$ Conditions – A Modelling Study

Submitted: J. Coates, K. A. Mar, N. Ojha, and T. M. Butler. The influence of temperature on ozone production under varying  $\text{NO}_x$  conditions – a modelling study. *Atmospheric Chemistry and Physics Discussions*, Submitted, 2016.

The final publication considered the ozone-temperature relationship with different  $\text{NO}_x$  conditions simulated by a box model. A series of box model simulations varying temperature and  $\text{NO}_x$  conditions was performed using NMVOC emissions representative of central Europe. Simulations were performed first using a temperature-independent source of isoprene emissions followed by simulations using a temperature-dependent source of isoprene emissions. All simulations were repeated using the MCM v3.2, CRI v2, MOZART-4, RADM2 and CB05 chemical mechanisms.

Each chemical mechanism produced a non-linear relationship between ozone, temperature and  $\text{NO}_x$ . This non-linear relationship was similar to that previously determined by observational studies. With each chemical mechanism, the absolute increase in ozone with temperature was slightly higher for temperature-dependent chemistry than the increase in ozone with temperature due to isoprene emissions. The largest increases in ozone mixing ratios with temperature were obtained with moderate  $\text{NO}_x$  conditions and the lowest increase in ozone mixing ratios was achieved with low  $\text{NO}_x$  conditions.

The total  $\text{O}_x$  production normalised by the total loss rate of emitted NMVOC was roughly constant with temperature showing that the production of  $\text{O}_x$  with temperature was controlled by the loss rate of VOCs. Net production of normalised  $\text{O}_x$  increased with temperature in all  $\text{NO}_x$  conditions due the temperature-dependent chemistry of  $\text{RO}_2\text{NO}_2$  species. At higher temperatures, the equilibrium of  $\text{RO}_2\text{NO}_2$  (R19) shifts towards decomposition to  $\text{RO}_2$  and  $\text{NO}_2$ , thus at higher temperatures more  $\text{RO}_2$  is available to produce  $\text{O}_x$  via (R18).

The box model results were also compared to observational data and output from the WRF-Chem model. The rate of increase of ozone with temperature from the box model was about half the rate of increase of ozone with temperature using observational and WRF-Chem output. Observational data and the output of 3D models such as WRF-Chem include additional influences on ozone such as stagnation where low wind speeds lead to the accumulation of reactants promoting ozone production. Box model simulations without mixing were performed to approximate stagnant conditions which enhanced the rate of increase in ozone with temperature compared with the box model simulations including mixing. These results indicated that the modelled relationship between ozone, temperature and  $\text{NO}_x$  was more sensitive to mixing than the choice of chemical mechanism.



# Chapter 4

## Overall Discussion and Conclusions

The research questions of Sect. 1.5 were addressed by the box modelling studies of Chap. 3. These questions are answered in this chapter. In each study, the near-explicit MCM v3.2 was the reference chemical mechanism and model simulations were repeated using reduced chemical mechanisms typically used by modelling groups for regional and global studies.

The first study compared the effects of different simplification techniques used by chemical mechanisms on ozone production. The reduced chemical mechanisms used in the comparison were developed through lumping VOC degradation intermediates (CRI v2), aggregating emitted NMVOCs into lumped molecules (MOZART-4, RADM2, RACM, RACM2) and expressing the emitted NMVOCs by lumped-structure species (CBM-IV, CB05). Out of these three simplification techniques, the lumped-intermediate approach produced the most similar amounts of ozone from each VOC to the MCM v3.2, while the lumped-molecule and lumped-structure approaches generally produced less ozone than the MCM v3.2 from the degradation of the VOC. Thus, the technique of lumping intermediate species rather than lumping emitted VOCs appears promising for representing ozone production in future chemical mechanisms.

The second objective of the first study was to determine the processes responsible for the differences in ozone production using the different reduced chemical mechanisms. The largest differences in ozone production from the reduced chemical mechanisms versus the MCM v3.2 were obtained for VOC represented by lumped mechanism species rather than those with VOC explicitly represented. In particular,

the representation of aromatic VOC consistently produced lower ozone in all the reduced chemical mechanisms. These differences in ozone production from aromatic VOC are not surprising as the degradation of aromatic VOC is an area of uncertainty (Atkinson and Arey, 2003). Even the detailed degradation chemistry of aromatic VOC in the MCM v3.2 was unable to reproduce the results from chamber experiments (Bloss et al., 2005).

Another process leading to lower ozone production from VOC degradation than the MCM v3.2 was the faster breakdown of emitted VOCs into smaller sized degradation products by lumped-molecule and lumped-structure chemical mechanisms. In particular, the faster breakdown of alkanes in lumped-molecule and lumped-structure chemical mechanisms led to a lower peak of ozone production than the MCM v3.2. As alkanes are less-reactive VOC, they are more likely to be transported downwind of emission sources affecting ozone production in rural areas. Thus, underestimating the ozone production from alkanes may impact simulated ozone levels of rural areas.

The second study looked at the influence of varying the speciation of NMVOC emissions from the solvent sector on ozone production. In box model experiments using the MCM v3.2, differences in ozone production resulted from the different speciations of NMVOC emissions. Ozone production on the first day was influenced by the amounts of alkenes and aromatic VOC specified by the solvent sector emission inventory (EI), while the contribution of alkanes and oxygenated VOC by the solvent sector EI determined ozone production at the end of the simulations.

Similar differences in ozone production were obtained when repeating the box model simulations using reduced chemical mechanisms (MOZART-4, RADM2). Thus, although the emissions of NMVOC were represented by fewer species in the reduced chemical mechanisms than the MCM v3.2, the differences in ozone production were not dampened by reducing the complexity of the chemical mechanism.

This study was designed as a scoping study to determine whether updating the speciation of an EI influenced model predictions of ozone levels. Given the results of this study, further modelling studies using different atmospheric conditions and more complex models are warranted to obtain a complete picture of how varying the speciation of NMVOC emissions influences modelled ozone levels.

The final study modelled the relationship between ozone, temperature and  $\text{NO}_x$  using central European conditions. In order to verify whether temperature-dependent increases in reaction rates or isoprene emissions from nature are more important for the increase in ozone with temperature, separate simulations

using a temperature-independent and temperature-dependent source of isoprene emissions were performed. From these simulations, the absolute increase in ozone with temperature due to faster reaction rates was slightly higher than the increase in ozone with temperature due to increased isoprene emissions with temperature regardless of  $\text{NO}_x$  conditions. This result was somewhat surprising as studies (e.g. Racherla and Adams (2008), Doherty et al. (2013)) attributed the increase of ozone with temperature to increased isoprene emissions from vegetation. These studies also acknowledged the effects of temperature-dependent chemistry on ozone production with temperature, further showing that both temperature-dependent chemistry and isoprene emissions are important for the increase of ozone with temperature.

The increase in ozone with temperature in all  $\text{NO}_x$  conditions was principally due to the faster loss rates of the emitted VOCs with temperature. As expected, peroxy nitrate ( $\text{RO}_2\text{NO}_2$ ) chemistry also played a role in the increase of ozone production with temperature with increased  $\text{RO}_2\text{NO}_2$  decomposition at higher temperatures leading to more  $\text{RO}_2$  available to produce ozone. Thus, the initial oxidation of emitted VOC and  $\text{RO}_2\text{NO}_2$  chemistry are critical to modelling the relationship between ozone, temperature and  $\text{NO}_x$ .

Simulations were performed using reduced chemical mechanisms (CRI v2, RADM2, MOZART-4, CB05) to determine whether the relationship between ozone, temperature and  $\text{NO}_x$  differed between representations of atmospheric chemistry. Each chemical mechanism reproduced the non-linear relationship between ozone, temperature and  $\text{NO}_x$  with the choice of chemical mechanism not significantly changing this relationship. The rate of increase of ozone with temperature was found to be more sensitive to the amount of mixing than the choice of chemical mechanism when comparing the box model simulations to observational and 3D model output.

Overall, the representation of detailed atmospheric chemistry influenced ozone production as in each of the studies differences between ozone levels were obtained when repeating model simulations with different chemical mechanisms. Thus, the choice of chemical mechanism is important for AQ modelling studies predicting future ozone levels. The representation of emitted NMVOC by the different chemical mechanisms was critical leading to differences in ozone production in each study. The secondary degradation processes of  $\text{RO}_2\text{NO}_2$  chemistry and the rate of breakdown of emitted NMVOC by reduced chemical mechanisms also had implications for ozone production.



# Chapter 5

## Outlook

Although ozone pollution is a major problem in Europe, there is currently no legally binding limit value for ozone. The EU Directive 2008/50/EG sets a target value for human health requiring the mean eight hourly ozone concentration not to exceed  $120 \mu\text{g m}^{-3}$  (= 60 ppbv) on more than 25 calendar days per year. The same EU Directive also sets an AOT40 target value for the exposure of vegetation to ozone of less than  $18,000 \mu\text{g m}^{-3} \cdot \text{h}$ . AOT40 is the sum of the differences between the mean hourly ozone values above  $80 \mu\text{g m}^{-3}$  (= 40 ppbv) and the value of  $80 \mu\text{g m}^{-3}$  between 8 am and 8 pm from May to July.

The EU has laws regulating the emissions of ozone precursors ( $\text{NO}_x$  and VOC). While these laws have reduced the emissions of both  $\text{NO}_x$  and VOC over Europe, the target value for ozone is regularly exceeded throughout Europe. The non-linear relationship between ozone,  $\text{NO}_x$  and VOC as well as intercontinental transport of ozone and its precursors impact the response of ozone pollution despite reductions in precursor emissions. The European Environmental Agency (EEA) recommends further mitigation efforts on the local, regional and global scales to reduce ambient ozone levels.

Setting a legally binding limit value for ambient ozone over Europe should inspire mitigation strategies at the local and regional scale in a bid to meet this limit. Meeting a limit value requires assessing different mitigation approaches and here AQ modelling will be a vital tool in determining the efficacy of a mitigation strategy for reducing ambient ozone. Thus, research aiming to improve model performance would also aid in increasing the confidence of AQ predictions from models, an asset for judging different mitigation strategies.

The detailed process studies performed as part of this work were designed to ultimately improve model performance increasing the confidence of the predictions of AQ models for mitigation strategies. A number of recommendations to the AQ modelling community are listed below based on these studies. AQ modelling groups should use up-to-date chemical mechanisms to incorporate the findings and recommendations from the chemical kinetics community as well as updated representations of emitted VOC and their secondary degradation. This is undoubtedly more work for a modelling group as further work such as testing the model with a new chemical mechanism and translating emissions into the new chemical species would need to be performed. However, as shown in the first study, updated versions of the same chemical mechanism produced more similar amounts of ozone to the near-explicit MCM v3.2 chemical mechanism. Thus, using an updated chemical mechanism should increase the confidence of the modelled ozone production from the degradation of emitted VOCs.

As the lumped-intermediate chemical mechanism produced the most similar amounts of ozone to the MCM v3.2, the approach of using a highly detailed chemical mechanism and lumping the degradation products appears promising for developing future chemical mechanisms. This approach did not break down the emitted VOC into smaller degradation products as fast as the lumped-molecule and lumped-structure chemical mechanisms, which was the main cause for the lower ozone production using these chemical mechanisms compared to the MCM v3.2. Lumped-intermediate chemical mechanisms include more chemical species than lumped-molecule and lumped-structure chemical mechanisms making their use less appealing from a computational efficiency perspective. However, gains in computational speed with modern computing centres might reduce this concern and facilitate the use of more complex chemical mechanisms as part of 3D models.

One aspect of future mitigation strategies could be to substitute the emissions of a more-reactive NMVOC, with a less-reactive NMVOC thus changing the NMVOC speciation profile from emission sectors. Such mitigation strategies require updating emission inventories and assessing how the change in speciation could influence ambient ozone levels. The results of the second study indicate that ozone production close to emission sources would be reduced using such mitigation strategies, but ozone production downwind may increase.

A warmer climate is predicted in the future as a result of climate change and this may affect ozone production chemistry in future emission scenarios. The influence of meteorological variables on ozone production is extremely important with the third study demonstrating an increase in ozone production with temperature. A

deeper understanding of the effects of meteorology on ozone production is required to ensure that mitigation strategies are robust enough to still reduce ambient ozone in the future.

The increase of ozone with temperature was determined by the faster oxidation of the emitted NMVOC, further emphasising the importance of adequately representing both the speciation and initial degradation of emitted NMVOC. The ozone-temperature relationship was sensitive to atmospheric mixing with less atmospheric mixing allowing the secondary degradation of NMVOC to proceed further than situations with enhanced atmospheric mixing. This highlights the importance of representing the secondary degradation of NMVOC by the chemical mechanism used by an AQ model.

The results from the detailed process studies performed in this work were all performed using a box model and further work using 3D models is required to verify how additional processes, such as regional transport, also influence ozone production under these conditions. The use of a box model was ideal for the scope of the studies of this thesis allowing a deeper insight into the chemical processes requiring a sharper focus than when using more realistic 3D models. The recommendations of this thesis along with testing the sensitivity of ozone production within 3D models would aid in constructing effective mitigation strategies that would meet the EU regulations for ozone pollution.



# Chapter 6

## Summary and Zusammenfassung

### 6.1 Summary

Tropospheric ozone is a short-lived climate forcing pollutant that is hazardous to human health and impacts deleteriously on vegetation. Ozone is not emitted directly into the troposphere but formed from the photochemical reactions of VOCs and  $\text{NO}_x$  with meteorological conditions strongly influencing ozone production. This thesis assessed the chemical mechanisms of ozone production chemistry represented within air quality models by determining the influence of VOC degradation, the speciation of VOC emissions and temperature on modelled ozone production. In order to focus on the impacts of the representation of tropospheric chemistry on ozone production, all modelling experiments in this work used a box model. The highly-detailed MCM v3.2 chemical mechanism was used as a reference and the model simulations were then repeated using reduced chemical mechanisms typically used by regional and global models.

The effects of different simplification approaches used by chemical mechanisms on ozone production were determined by comparing the ozone produced during VOC degradation between different chemical mechanisms. The lumped-intermediate (CRI v2) chemical mechanism produced the most similar amounts of ozone to the MCM v3.2 from the degradation of each emitted VOC. On the other hand, VOC degradation described by lumped-molecule (MOZART-4, RADM2, RACM and RACM2) and lumped-structure (CBM-IV and CB05) chemical mechanisms generally produced less ozone than the MCM v3.2. The lower ozone production from VOC degradation in the lumped-molecule and lumped-structure chemical mechanisms was caused by a faster breakdown of the emitted VOC into smaller sized degradation products.

The influence of the speciation of VOC emissions by an emission inventory on ozone production was established by comparing the ozone produced from different emission inventories of the solvent sector. In these experiments, both the different emission inventories of VOC emissions and chemical mechanisms (MCM v3.2, MOZART-4, RADM2) led to differences in peak ozone mixing ratios and ozone production. These results indicated a sensitivity of ozone production to both the choice of chemical mechanism and emission inventory speciation. The ozone production on the first day was influenced by the specified contributions of alkene and aromatic VOC. Emission inventories specifying larger amounts of alkane emissions produced greater amounts of ozone at the end of simulations than those specifying a larger contribution of emissions of oxygenated VOC.

The final study of this work considered the relationship between ozone, temperature and  $\text{NO}_x$ . The increase of ozone with temperature due to temperature-dependent chemistry was slightly larger than the increase of ozone with temperature due to temperature-dependent isoprene emissions in all  $\text{NO}_x$ -conditions. A non-linear relationship between ozone, temperature and  $\text{NO}_x$  was obtained with each chemical mechanism used in this study (MCM v3.2, CRI v2, MOZART-4, RADM2 and CB05). With each chemical mechanism, the temperature-dependent chemistry of VOC oxidation and peroxy nitrates, such as PANs, caused the increase in ozone production with temperature.

The detailed process studies of this work will help improve model performance and the confidence in predictions of future ozone levels from air quality modelling studies. In particular, this work has advanced the previous literature in this field by illustrating the chemical processes represented within chemical mechanisms having the greatest influence on simulated ozone production. The representation of VOC degradation and secondary processes, such as the rate of breakdown of the emitted VOCs and peroxy nitrate chemistry by a chemical mechanism, are particularly important processes for the predictions of ozone levels with different mitigation strategies.

## 6.2 Zusammenfassung

Troposphärisches Ozon ist ein kurzlebiger klimawirksamer Schadstoff, der für die menschliche Gesundheit gefährlich ist und sich auf schädliche Weise auf die Vegetation auswirkt. Ozon wird nicht direkt in die Troposphäre emittiert, sondern entsteht aus den photochemischen Reaktionen von flüchtigen

organischen Verbindungen (VOCs) und  $\text{NO}_x$ , wobei meteorologische Bedingungen die Ozonproduktion stark beeinflussen. In der vorliegenden Arbeit wurden verschiedene Chemiemechanismen zur Berechnung der Ozonproduktion in Atmosphären-Chemie-Modellen in Bezug auf den Einfluß des VOC-Abbaus, des Anteils verschiedener VOC-Komponenten an den VOC-Gesamtemissionen („VOC Speciation“) und der Temperatur auf die modellierte Ozonproduktion untersucht. Um detaillierte Prozessstudien mit einem Fokus auf die Repräsentativität der Auswirkung troposphärischer Chemie auf die Ozonproduktion in den Chemiemechanismen durchzuführen, wurden in dieser Arbeit Modellexperimente mit einem Box-Modell durchgeführt. Als Referenz wurde zunächst der sehr detaillierte Chemiemechanismus MCM v3.2 in Modellsimulationen verwendet. Diese Simulationen wurden dann unter der Verwendung von reduzierten Chemiemechanismen, welche typischerweise von regionalen und globalen Modellen verwendet werden, wiederholt.

Um die Auswirkungen der verschiedenen Vereinfachungsansätze, die in den Chemiemechanismen bezüglich der Ozonproduktion verwendet werden, auf die Ozonproduktion zu bestimmen, wurde die durch die verschiedenen Chemiemechanismen simulierte Ozonproduktion während des VOC-Abbaus verglichen. Der Chemiemechanismus CRI v2 mit zusammengefassten Zwischenprodukten („lumped-intermediate“) hatte dabei im Vergleich zu MCM v3.2 die vergleichbarste Ozonmenge aus dem Abbau jedes emittierten VOC erzeugt. Der VOC-Abbau, welcher in den Chemiemechanismen mit zusammengefassten Molekülen („lumped-molecule“) (MOZART-4, RADM2, RACM and RACM2) und zusammengefassten Strukturen („lumped-structure“) (CBM-IV and CB05) beschrieben ist, produzierte jedoch gemeinhin weniger Ozon als MCM v3.2. Die geringere Ozonproduktion während des VOC-Abbaus in den „lumped-molecule“ und „lumped-structure“ Chemiemechanismen wurde durch ein schnellerer Zerfall des emittierten VOC in kleinere Abbauprodukte verursacht.

Der Einfluss der „VOC Speciation“ von VOC-Emissionen durch ein Emissionsinventar wurde durch einen Vergleich des aus verschiedenen Emissionsinventaren des Lösungsmittelsektors produzierten Ozons festgestellt. In diesen Experimenten führte die Verwendung unterschiedlicher VOC-Emissionsinventare und Chemiemechanismen (MCM v3.2, MOZART-4, RADM2) zu Unterschieden bei den Spitzenwerten der Ozonmischungsverhältnisse sowie der Ozonproduktion. Diese Ergebnisse zeigten eine Abhängigkeit der Ozonproduktion sowohl von der Wahl des Chemiemechanismus als auch von den „VOC Speciation“ in den Emissionsinventaren. Am ersten Tag wurde die Ozonproduktion von den spezifizierten Beiträgen von Alken und aromatischen VOC beeinflusst. Die Emissionsinventare mit größere Mengen an Alkanemissionen

erzeugten höhere Mengen an Ozon am Ende der Simulation, im Vergleich zu denen, die einen größeren Beitrag des Ausstoßes von oxygeniertem VOC definierten.

Die letzte Studie dieser Arbeit betrachtete die Beziehung zwischen Ozon, Temperatur und  $\text{NO}_x$ . Der Anstieg des Ozons mit der Temperatur aufgrund der temperaturabhängigen Chemie war geringfügig größer als der Anstieg des Ozons mit der Temperatur aufgrund der temperaturabhängigen Isoprenemissionen unter allen  $\text{NO}_x$ -Bedingungen. Ein nicht-linearer Zusammenhang zwischen Ozon, Temperatur und  $\text{NO}_x$  wurde mit jedem in dieser Studie verwendeten Chemiemechanismus (MCM v3.2, CRI v2, MOZART-4, RADM2 und CB05) aufgezeigt. Bei jedem Chemiemechanismus kam es aufgrund der temperaturabhängigen Chemie von VOC-Abbau und Peroxynitrat, wie z. B. PANs, zu einem Anstieg der Ozonproduktion mit der Temperatur.

Die detaillierten Prozessstudien dieser Arbeit werden dazu beitragen, die Güte von Modellen und das Vertrauen in die Prognosen zukünftiger Ozonwerte von Studien mit Atmosphären-Chemie-Modellen zu verbessern. Insbesondere hat diese Arbeit die bestehende Literatur in diesem Fachgebiet befördert, in dem sie diejenigen Chemieprozesse bewertet hat, welche in den Chemiemechanismen den größten Einfluss auf die Ozonproduktion hat. Die Darstellung des VOC-Abbaus und sekundärer Prozesse, wie der Zerfallgeschwindigkeit von emittierten VOCs sowie der Peroxynitratchemie durch einen Chemiemechanismus, sind besonders wichtige Prozesse für die Vorhersage der Ozonwerte unter Anwendung von unterschiedlichen Minderungsstrategien.

# References

- J. Abbatt, C. George, M. Melamed, P. Monks, S. Pandis, and Y. Rudich. New directions: Fundamentals of atmospheric chemistry: Keeping a three-legged stool balanced. *Atmospheric Environment*, 84:390 – 391, 2014.
- A. Archibald, M. Jenkin, and D. Shallcross. An isoprene mechanism intercomparison. *Atmospheric Environment*, 44(40):5356 – 5364, 2010.
- R. Atkinson. Atmospheric chemistry of VOCs and NO<sub>x</sub>. *Atmospheric Environment*, 34(12-14):2063–2101, 2000.
- R. Atkinson and J. Arey. Atmospheric Degradation of Volatile Organic Compounds. *Chemical Reviews*, 103:4605–4638, 2003.
- A. Baklanov, K. Schlünzen, P. Suppan, J. Baldasano, D. Brunner, S. Aksoyoglu, G. Carmichael, J. Douros, J. Flemming, R. Forkel, S. Galmarini, M. Gauss, G. Grell, M. Hirtl, S. Joffre, O. Jorba, E. Kaas, M. Kaasik, G. Kallos, X. Kong, U. Korsholm, A. Kurganskiy, J. Kushta, U. Lohmann, A. Mahura, A. Manders-Groot, A. Maurizi, N. Moussiopoulos, S. T. Rao, N. Savage, C. Seigneur, R. S. Sokhi, E. Solazzo, S. Solomos, B. Sørensen, G. Tsegas, E. Vignati, B. Vogel, and Y. Zhang. Online coupled regional meteorology chemistry models in Europe: current status and prospects. *Atmospheric Chemistry and Physics*, 14(1):317–398, 2014.
- C. Bloss, V. Wagner, M. E. Jenkin, R. Vollamer, W. J. Bloss, J. D. Lee, D. E. Heard, K. Wirtz, M. Martin-Reviejo, G. Rea, J. C. Wenger, and M. J. Pilling. Development of a detailed chemical mechanism (MCMv3.1) for the atmospheric oxidation of aromatic hydrocarbons. *Atmospheric Chemistry and Physics*, 5:641–664, 2005.
- B. Bonn, E. von Schneidemesser, D. Andrich, J. Quedenau, H. Gerwig, A. Lüdecke, J. Kura, A. Pietsch, C. Ehlers, D. Klemp, C. Kofahl, R. Nothard, A. Kerschbaumer, W. Junkermann, R. Grote, T. Pohl, K. Weber, B. Lode, P. Schönberger, G. Churkina, T. M. Butler, and M. G. Lawrence. BAERLIN2014 - The influence of land surface types on and the horizontal heterogeneity of air pollutant levels in Berlin. *Atmospheric Chemistry and Physics Discussions*, 2016:1–62, 2016.

- A. Boynard, A. Borbon, T. Leonardis, B. Barletta, S. Meinardi, D. R. Blake, and N. Locoge. Spatial and seasonal variability of measured anthropogenic non-methane hydrocarbons in urban atmospheres: Implication on emission ratios. *Atmospheric Environment*, 82(0):258–267, 2014.
- P. Builtjes, M. Loon, M. Schaap, S. Teeuwisse, A. Visschedijk, and J. Bloos. The development of an emission data base over Europe and further contributions of TNO-MEP. Technical report, TNO Environment, 2002.
- T. Butler, M. Lawrence, D. Taraborrelli, and J. Lelieveld. Multi-day ozone production potential of volatile organic compounds calculated with a tagging approach. *Atmospheric Environment*, 45(24):4082 – 4090, 2011.
- T. M. Butler and M. G. Lawrence. The influence of megacities on global atmospheric chemistry: a modelling study. *Environmental Chemistry*, 6:219–225, 2009.
- L. Camalier, W. Cox, and P. Dolwick. The effects of meteorology on ozone in urban areas and their use in assessing ozone trends. *Atmospheric Environment*, 41(33):7127 – 7137, 2007.
- W. P. Carter. Development of ozone reactivity scales for volatile organic compounds. *Air & Waste*, 44(7):881–899, 1994.
- W. P. L. Carter. Development of a Database for Chemical Mechanism Assignments for Volatile Organic Emissions. *Journal of the Air & Waste Management Association*, 65(10), 2015.
- J. Coates and T. M. Butler. A comparison of chemical mechanisms using tagged ozone production potential (TOPP) analysis. *Atmospheric Chemistry and Physics*, 15(15):8795–8808, 2015.
- J. Coates, K. A. Mar, N. Ojha, and T. M. Butler. The influence of temperature on ozone production under varying  $\text{NO}_x$  conditions – a modelling study. *Atmospheric Chemistry and Physics Discussions*, Submitted, 2016.
- I. Coll, C. Rousseau, B. Barletta, S. Meinardi, and D. R. Blake. Evaluation of an urban NMHC emission inventory by measurements and impact on CTM results. *Atmospheric Environment*, 44(31):3843 – 3855, 2010.
- A. C. Comrie. Comparing neural networks and regression models for ozone forecasting. *Journal of the Air & Waste Management Association*, 47(6):653–663, 1997.
- G. Curci, M. Beekmann, R. Vautard, G. Smiatek, R. Steinbrecher, J. Theloke, and R. Friedrich. Modelling study of the impact of isoprene and terpene biogenic

emissions on European ozone levels. *Atmospheric Environment*, 43(7):1444 – 1455, 2009.

V. Damian, A. Sandu, M. Damian, F. Potra, and G. R. Carmichael. The kinetic preprocessor KPP-a software environment for solving chemical kinetics. *Computers & Chemical Engineering*, 26(11):1567 – 1579, 2002.

J. P. Dawson, P. J. Adams, and S. N. Pandis. Sensitivity of ozone to summertime climate in the eastern USA: A modeling case study . *Atmospheric Environment*, 41(7):1494 – 1511, 2007.

H. Denier van der Gon, C. Hendriks, J. Kuenen, A. Segers, and A. Visschedijk. Description of current temporal emission patterns and sensitivity of predicted AQ for temporal emission patterns. Technical Report EU FP7 MACC report: D\_D-EMIS\_1.3, TNO, 2011.

R. M. Doherty, O. Wild, D. T. Shindell, G. Zeng, I. A. MacKenzie, W. J. Collins, A. M. Fiore, D. S. Stevenson, F. J. Dentener, M. G. Schultz, P. Hess, R. G. Derwent, and T. J. Keating. Impacts of climate change on surface ozone and intercontinental ozone pollution: A multi-model study. *Journal of Geophysical Research: Atmospheres*, 118(9):3744–3763, 2013.

C. Dueñas, M. Fernández, S. Cañete, J. Carretero, and E. Liger. Assessment of ozone variations and meteorological effects in an urban area in the Mediterranean Coast. *Science of The Total Environment*, 299(1–3):97 – 113, 2002.

EEA. Air quality in Europe - 2011 report. Technical Report 12/2011, European Environmental Agency, 2011.

EEA. Air quality in Europe - 2013 report. Technical Report 9/2013, European Environmental Agency, 2013.

EEA. Air quality in Europe - 2015 report. Technical Report 5/2015, European Environmental Agency, 2015.

Ehhalt, D., Prather, M., Dentener, F., Derwent, R., Dlugokencky, E., Holland, E., Isaksen, I., Katima, J., Kirchhoff, V., Matson, P., Midgley, P., Wang, and M. Climate Change 2001: The Scientific Basis. Contribution of Working Group I to the Third Assessment Report of the Intergovernmental Panel on Climate Change. Technical report, IPCC, 2001.

K. M. Emmerson and M. J. Evans. Comparison of tropospheric gas-phase chemistry schemes for use within global models. *Atmospheric Chemistry and Physics*, 9(5): 1831–1845, 2009.

- L. K. Emmons, S. Walters, P. G. Hess, J.-F. Lamarque, G. G. Pfister, D. Fillmore, C. Granier, A. Guenther, D. Kinnison, T. Laepple, J. Orlando, X. Tie, G. Tyndall, C. Wiedinmyer, S. L. Baughcum, and S. Kloster. Description and evaluation of the Model for Ozone and Related chemical Tracers, version 4 (MOZART-4). *Geoscientific Model Development*, 3(1):43–67, 2010.
- L. K. Emmons, P. G. Hess, J.-F. Lamarque, and G. G. Pfister. Tagged ozone mechanism for moztart-4, cam-chem and other chemical transport models. *Geoscientific Model Development*, 5(6):1531–1542, 2012.
- V. Eyring, J.-F. Lamarque, P. Hess, F. Arfeuille, K. Bowman, M. P. Chipperfield, B. Duncan, A. Fiore, A. Gettelman, M. A. Giorgetta, C. Granier, M. Hegglin, D. Kinnison, M. Kunze, U. Langematz, B. Luo, R. Martin, K. Matthes, P. A. Newman, T. Peter, A. Robock, T. Ryerson, A. Saiz-Lopez, R. Salawitch, M. Schultz, T. G. Shepherd, D. Shindell, J. Staehelin, S. Tegtmeier, L. Thomason, S. Tilmes, J.-P. Vernier, D. W. Waugh, , and P. J. Young. Overview of IGAC/SPARC Chemistry-Climate Model Initiative (CCMI) Community Simulations in Support of Upcoming Ozone and Climate Assessments. *SPARC Newsletter*, 40:48–66, 2013.
- R. Friedrich, B. Wickert, P. Blank, S. Emeis, W. Engewald, D. Hassel, H. Hoffmann, H. Michael, A. Obermeier, K. Schäfer, T. Schmitz, A. Sedlmaier, M. Stockhause, J. Theloke, and F.-J. Weber. Development of Emission Models and Improvement of Emission Data for Germany. *Journal of Atmospheric Chemistry*, 42(1):179–206, 2002.
- M. W. Gery, G. Z. Whitten, J. P. Killus, and M. C. Dodge. A photochemical kinetics mechanism for urban and regional scale computer modeling. *Journal of Geophysical Research*, 94(D10):12,925–12,956, 1989.
- W. S. Goliff, W. R. Stockwell, and C. V. Lawson. The regional atmospheric chemistry mechanism, version 2. *Atmospheric Environment*, 68:174 – 185, 2013.
- J. Goodwin. UK Emissions of Air Pollutants 1970 to 1998. Technical report, DEFRA, 2000.
- G. Grell, S. Peckham, R. Schmitz, S. McKeen, G. Frost, W. Skamarock, and B. Eder. Fully coupled "online" chemistry within the WRF model. *Atmospheric Environment*, 39(37):6957–6975, 2005.
- S. Grice, J. Stedman, A. Kent, M. Hobson, J. Norris, J. Abbott, and S. Cooke. Recent trends and projections of primary NO<sub>2</sub> emissions in Europe. *Atmospheric Environment*, 43(13):2154 – 2167, 2009.

A. Guenther, T. Karl, P. Harley, C. Wiedinmyer, P. I. Palmer, and C. Geron. Estimates of global terrestrial isoprene emissions using MEGAN (Model of Emissions of Gases and Aerosols from Nature). *Atmospheric Chemistry and Physics*, 6(11): 3181–3210, 2006.

A. B. Guenther, X. Jiang, C. L. Heald, T. Sakulyanontvittaya, T. Duhl, L. K. Emmons, and X. Wang. The Model of Emissions of Gases and Aerosols from Nature version 2.1 (MEGAN2.1): an extended and updated framework for modeling biogenic emissions. *Geoscientific Model Development*, 5(6):1471–1492, 2012.

D. W. Gunz and M. R. Hoffmann. Atmospheric chemistry of peroxides: a review. *Atmospheric Environment. Part A. General Topics*, 24(7):1601 – 1633, 1990.

M. Hallquist, J. C. Wenger, U. Baltensperger, Y. Rudich, D. Simpson, M. Claeys, J. Dommen, N. M. Donahue, C. George, A. H. Goldstein, J. F. Hamilton, H. Herrmann, T. Hoffmann, Y. Iinuma, M. Jang, M. E. Jenkin, J. L. Jimenez, A. Kiendler-Scharr, W. Maenhaut, G. McFiggans, T. F. Mentel, A. Monod, A. S. H. Prévôt, J. H. Seinfeld, J. D. Surratt, R. Szmigielski, and J. Wildt. The formation, properties and impact of secondary organic aerosol: current and emerging issues. *Atmospheric Chemistry and Physics*, 9(14):5155–5236, 2009.

D. A. Hauglustaine, G. P. Brasseur, S. Walters, P. J. Rasch, J.-F. Müller, L. K. Emmons, and M. A. Carroll. MOZART, a global chemical transport model for ozone and related chemical tracers 2. Model results and evaluation. *Journal of Geophysical Research*, 103(D21):28,291–28,335, 1998.

IARC. Outdoor air pollution a leading environmental cause of cancer deaths. [https://www.iarc.fr/en/media-centre/iarcnews/pdf/pr221\\_E.pdf](https://www.iarc.fr/en/media-centre/iarcnews/pdf/pr221_E.pdf), 2013. [Online; accessed 31-December-2015].

D. J. Jacob and D. A. Winner. Effect of climate change on air quality. *Atmospheric Environment*, 43(1):51 – 63, 2009. Atmospheric Environment - Fifty Years of Endeavour.

M. Jenkin, L. Watson, S. Utembe, and D. Shallcross. A Common Representative Intermediates (CRI) mechanism for VOC degradation. Part 1: Gas phase mechanism development. *Atmospheric Environment*, 42(31):7185 – 7195, 2008.

M. E. Jenkin and K. C. Clemitshaw. Ozone and other secondary photochemical pollutants: Chemical processes governing their formation in the planetary boundary layer. *Atmospheric Environment*, 34(16):2499–2527, 2000.

- M. E. Jenkin, S. M. Saunders, and M. J. Pilling. The tropospheric degradation of volatile organic compounds: a protocol for mechanism development. *Atmospheric Environment*, 31(1):81 – 104, 1997.
- M. E. Jenkin, S. M. Saunders, V. Wagner, and M. J. Pilling. Protocol for the development of the Master Chemical Mechanism, MCM v3 (Part B): tropospheric degradation of aromatic volatile organic compounds. *Atmospheric Chemistry and Physics*, 3(1):181–193, 2003.
- T. R. Karl and K. E. Trenberth. Modern global climate change. *Science*, 302(5651):1719–1723, 2003.
- S. Kirschke, P. Bousquet, P. Ciais, M. Saunois, J. G. Canadell, E. J. Dlugokencky, P. Bergamaschi, D. Bergmann, D. R. Blake, L. Bruhwiler, P. Cameron-Smith, S. Castaldi, F. Chevallier, L. Feng, A. Fraser, M. Heimann, E. L. Hodson, S. Houweling, B. Josse, P. J. Fraser, P. B. Krummel, J.-F. Lamarque, R. L. Langenfelds, C. Le Quere, V. Naik, S. O’Doherty, P. I. Palmer, I. Pison, D. Plummer, B. Poulter, R. G. Prinn, M. Rigby, B. Ringeval, M. Santini, M. Schmidt, D. T. Shindell, I. J. Simpson, R. Spahni, L. P. Steele, S. A. Strode, K. Sudo, S. Szopa, G. R. van der Werf, A. Voulgarakis, M. van Weele, R. F. Weiss, J. E. Williams, and G. Zeng. Three decades of global methane sources and sinks. *Nature Geoscience*, 6(10):813–823, 2013.
- L. I. Kleinman. Low and high NO<sub>x</sub> tropospheric photochemistry. *Journal of Geophysical Research*, 99(D8):16,831–16,838, 1994.
- P. E. Korsog and G. T. Wolff. An examination of urban ozone trends in the Northeastern U.S. (1973–1983) using a robust statistical method. *Atmospheric Environment. Part B. Urban Atmosphere*, 25(1):47 – 57, 1991.
- D. Kubistin, H. Harder, M. Martinez, M. Rudolf, R. Sander, H. Bozem, G. Eerdeken, H. Fischer, C. Gurk, T. Klüpfel, R. Königstedt, U. Parchatka, C. L. Schiller, A. Stickler, D. Taraborrelli, J. Williams, and J. Lelieveld. Hydroxyl radicals in the tropical troposphere over the Suriname rainforest: comparison of measurements with the box model MECCA. *Atmospheric Chemistry and Physics*, 10(19):9705–9728, 2010.
- J. J. P. Kuenen, A. J. H. Visschedijk, M. Jozwicka, and H. A. C. Denier van der Gon. TNO-MACC\_II emission inventory; a multi-year (2003–2009) consistent high-resolution european emission inventory for air quality modelling. *Atmospheric Chemistry and Physics*, 14(20):10963–10976, 2014.

- M. Kuhn, P. Builtjes, D. Poppe, D. Simpson, W. Stockwell, Y. Andersson-Skoïld, A. Baart, M. Das, F. Fiedler, Ø. Hov, F. Kirchner, P. Makar, J. Milford, M. Roemer, R. Ruhnke, A. Strand, B. Vogel, and H. Vogel. Intercomparison of the gas-phase chemistry in several chemistry and transport models. *Atmospheric Environment*, 32(4):693 – 709, 1998.
- J.-F. Lamarque, T. C. Bond, V. Eyring, C. Granier, A. Heil, Z. Klimont, D. Lee, C. Liou, A. Mieville, B. Owen, M. G. Schultz, D. Shindell, S. J. Smith, E. Stehfest, J. Van Aardenne, O. R. Cooper, M. Kainuma, N. Mahowald, J. R. McConnell, V. Naik, K. Riahi, and D. P. van Vuuren. Historical (1850–2000) gridded anthropogenic and biomass burning emissions of reactive gases and aerosols: methodology and application. *Atmospheric Chemistry and Physics*, 10(15):7017–7039, 2010.
- J. Lelieveld and F. J. Dentener. What controls tropospheric ozone? *Journal of Geophysical Research: Atmospheres*, 105(D3):3531–3551, 2000.
- A. S. M. Lourens, T. M. Butler, J. P. Beukes, P. G. van Zyl, G. D. Fourie, and M. G. Lawrence. Investigating atmospheric photochemistry in the Johannesburg-Pretoria megacity using a box model. *South African Journal of Science*, 112(1/2), 2016.
- P. S. Monks. A review of the observations and origins of the spring ozone maximum. *Atmospheric Environment*, 34(21):3545 – 3561, 2000.
- P. S. Monks. Gas-phase radical chemistry in the troposphere. *Chem. Soc. Rev.*, 34: 376–395, 2005.
- K. Murazaki and P. Hess. How does climate change contribute to surface ozone change over the united states? *Journal of Geophysical Research: Atmospheres*, 111(D5), 2006. D05301.
- T. P. Murrells, N.R.P., G. Thistlethwaite, A. Wagner, Y. Li, T.B., J. Norris, C. Walker, R. A. Stewart, I. Tsagatakis, R. Whiting, C.C., S. Okamura, M. Peirce, S. Sneddon, J. Webb, J.T., J. MacCarthy, S. Choudrie, and N. Brophy. UK Emissions of Air Pollutants 1970 to 2008. Technical report, DEFRA, Didcot, UK, 2010.
- J. Olivier, J. Berdowski, J. Bakker, A. Visschedijk, and J. Bloos. Applications of EDGAR. Including a description of EDGAR 3.0: reference database with trend data for 1970–1995. Technical Report RIVM report No. 773301 001/NOP report no. 410200 051, RIVM, 2001.
- N. Otero, J. Sillmann, J. L. Schnell, H. W. Rust, and T. Butler. Synoptic and meteorological drivers of extreme ozone concentrations over europe. *Environmental Research Letters*, 11(2):024005, 2016.

- S. A. Penkett and K. A. Brice. The spring maximum of photo-oxidants in the Northern Hemisphere troposphere. *Nature*, 319:655–657, 1986.
- S. E. Pusede, D. R. Gentner, P. J. Wooldridge, E. C. Browne, A. W. Rollins, K.-E. Min, A. R. Russell, J. Thomas, L. Zhang, W. H. Brune, S. B. Henry, J. P. DiGangi, F. N. Keutsch, S. A. Harrold, J. A. Thornton, M. R. Beaver, J. M. St. Clair, P. O. Wennberg, J. Sanders, X. Ren, T. C. VandenBoer, M. Z. Markovic, A. Guha, R. Weber, A. H. Goldstein, and R. C. Cohen. On the temperature dependence of organic reactivity, nitrogen oxides, ozone production, and the impact of emission controls in San Joaquin Valley, California. *Atmospheric Chemistry and Physics*, 14(7):3373–3395, 2014.
- S. E. Pusede, A. L. Steiner, and R. C. Cohen. Temperature and Recent Trends in the Chemistry of Continental Surface Ozone. *Chemical Reviews*, 115(10):3898–3918, 2015.
- P. N. Racherla and P. J. Adams. The response of surface ozone to climate change over the eastern united states. *Atmospheric Chemistry and Physics*, 8(4):871–885, 2008.
- A. Rickard, J. Young, M. J. Pilling, M. E. Jenkin, S. Pascoe, and S. M. Saunders. The Master Chemical Mechanism Version MCM v3.2. <http://mcm.leeds.ac.uk/MCMv3.2/>, 2015. [Online; accessed 25-March-2015].
- J. I. Rubin, A. J. Kean, R. A. Harley, D. B. Millet, and A. H. Goldstein. Temperature dependence of volatile organic compound evaporative emissions from motor vehicles. *Journal of Geophysical Research: Atmospheres*, 111(D3), 2006. D03305.
- A. Russell and R. Dennis. NARSTO critical review of photochemical models and modeling. *Atmospheric Environment*, 34(12–14):2283 – 2324, 2000.
- R. Sander, A. Kerkweg, P. Jöckel, and J. Lelieveld. Technical note: The new comprehensive atmospheric chemistry module mecca. *Atmospheric Chemistry and Physics*, 5(2):445–450, 2005.
- S. M. Saunders, M. E. Jenkin, R. G. Derwent, and M. J. Pilling. Protocol for the development of the Master Chemical Mechanism, MCM v3 (Part A): tropospheric degradation of non-aromatic volatile organic compounds. *Atmospheric Chemistry and Physics*, 3(1):161–180, 2003.
- J. H. Seinfeld and S. N. Pandis. *Atmospheric Chemistry and Physics: From Air Pollution to Climate Change*. John Wiley & Sons Inc, New York, second edition, 2006.

- C. Sidiropoulos and G. Tsilingiridis. Composition changes of NMVOC emissions from solvent use in Greece for the period 1990-2005. *Fresenius Environmental Bulletin*, 16(9):1108–1112, 2007.
- S. Sillman and P. J. Samson. Impact of temperature on oxidant photochemistry in urban, polluted rural and remote environments. *Journal of Geophysical Research: Atmospheres*, 100(D6):11497–11508, 1995.
- D. Simpson, A. Benedictow, H. Berge, R. Bergström, L. D. Emberson, H. Fagerli, C. R. Flechard, G. D. Hayman, M. Gauss, J. E. Jonson, M. E. Jenkin, A. Nyíri, C. Richter, V. S. Semeena, S. Tsyro, J.-P. Tuovinen, Á. Valdebenito, and P. Wind. The EMEP MSC-W chemical transport model – technical description. *Atmospheric Chemistry and Physics*, 12(16):7825–7865, 2012.
- W. R. Stockwell, P. Middleton, J. S. Chang, and X. Tang. The second generation regional acid deposition model chemical mechanism for regional air quality modeling. *Journal of Geophysical Research: Atmospheres*, 95(D10):16343–16367, 1990.
- W. R. Stockwell, F. Kirchner, M. Kuhn, and S. Seefeld. A new mechanism for regional atmospheric chemistry modeling. *Journal of Geophysical Research: Atmospheres*, 102(D22):25847–25879, 1997.
- W. R. Stockwell, C. V. Lawson, E. Saunders, and W. S. Goliff. A review of tropospheric atmospheric chemistry and gas-phase chemical mechanisms for air quality modeling. *Atmosphere*, 3(1):1, 2012.
- S. Syri, M. Amann, W. Schöpp, and C. Heyes. Estimating long-term population exposure to ozone in urban areas of Europe. *Environmental Pollution*, 113(1):59 – 69, 2001.
- E. von Schneidmesser, P. S. Monks, V. Gros, J. Gauduin, and O. Sanchez. How important is biogenic isoprene in an urban environment? a study in london and paris. *Geophysical Research Letters*, 38(19), 2011. L19804.
- E. von Schneidmesser, P. S. Monks, J. D. Allan, L. Bruhwiler, P. Forster, D. Fowler, A. Lauer, W. T. Morgan, P. Paasonen, M. Righi, K. Sindelarova, and M. A. Sutton. Chemistry and the Linkages between Air Quality and Climate Change. *Chemical Reviews*, 2015. PMID: 25926133.
- E. von Schneidmesser, J. Coates, H. D. van der Gon, A. Visschedijk, and T. Butler. Variation of the NMVOC speciation in the solvent sector and the sensitivity of modelled tropospheric ozone. *Atmospheric Environment*, 135:59 – 72, 2016.

A. Voulgarakis, V. Naik, J.-F. Lamarque, D. T. Shindell, P. J. Young, M. J. Prather, O. Wild, R. D. Field, D. Bergmann, P. Cameron-Smith, I. Cionni, W. J. Collins, S. B. Dalsøren, R. M. Doherty, V. Eyring, G. Faluvegi, G. A. Folberth, L. W. Horowitz, B. Josse, I. A. MacKenzie, T. Nagashima, D. A. Plummer, M. Righi, S. T. Rumbold, D. S. Stevenson, S. A. Strode, K. Sudo, S. Szopa, and G. Zeng. Analysis of present day and future OH and methane lifetime in the ACCMIP simulations. *Atmospheric Chemistry and Physics*, 13(5):2563–2587, 2013.

World Meteorological Organisation. Scientific Assessment of Ozone Depletion: 2010. Technical Report 516 pp., World Meteorological Organisation, Geneva, Switzerland, March 2011.

G. Yarwood, S. Rao, M. Yocke, and G. Z. Whitten. Updates to the Carbon Bond Chemical Mechanism: CB05. Technical report, U. S Environmental Protection Agency, 2005.

P. J. Young, A. T. Archibald, K. W. Bowman, J.-F. Lamarque, V. Naik, D. S. Stevenson, S. Tilmes, A. Voulgarakis, O. Wild, D. Bergmann, P. Cameron-Smith, I. Cionni, W. J. Collins, S. B. Dalsøren, R. M. Doherty, V. Eyring, G. Faluvegi, L. W. Horowitz, B. Josse, Y. H. Lee, I. A. MacKenzie, T. Nagashima, D. A. Plummer, M. Righi, S. T. Rumbold, R. B. Skeie, D. T. Shindell, S. A. Strode, K. Sudo, S. Szopa, and G. Zeng. Pre-industrial to end 21st century projections of tropospheric ozone from the Atmospheric Chemistry and Climate Model Intercomparison Project (ACCMIP). *Atmospheric Chemistry and Physics*, 13(4):2063–2090, 2013.

## Chapter 7

**Paper I: A comparison of chemical mechanisms using tagged ozone production potential (TOPP) analysis**





# A comparison of chemical mechanisms using tagged ozone production potential (TOPP) analysis

J. Coates and T. M. Butler

Institute for Advanced Sustainability Studies, Potsdam, Germany

Correspondence to: J. Coates (jane.coates@iass-potsdam.de)

Received: 10 April 2015 – Published in Atmos. Chem. Phys. Discuss.: 29 April 2015

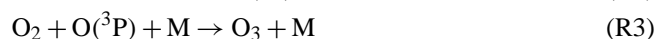
Revised: 23 July 2015 – Accepted: 24 July 2015 – Published: 10 August 2015

**Abstract.** Ground-level ozone is a secondary pollutant produced photochemically from reactions of  $\text{NO}_x$  with peroxy radicals produced during volatile organic compound (VOC) degradation. Chemical transport models use simplified representations of this complex gas-phase chemistry to predict  $\text{O}_3$  levels and inform emission control strategies. Accurate representation of  $\text{O}_3$  production chemistry is vital for effective prediction. In this study, VOC degradation chemistry in simplified mechanisms is compared to that in the near-explicit Master Chemical Mechanism (MCM) using a box model and by “tagging” all organic degradation products over multi-day runs, thus calculating the tagged ozone production potential (TOPP) for a selection of VOCs representative of urban air masses. Simplified mechanisms that aggregate VOC degradation products instead of aggregating emitted VOCs produce comparable amounts of  $\text{O}_3$  from VOC degradation to the MCM. First-day TOPP values are similar across mechanisms for most VOCs, with larger discrepancies arising over the course of the model run. Aromatic and unsaturated aliphatic VOCs have the largest inter-mechanism differences on the first day, while alkanes show largest differences on the second day. Simplified mechanisms break VOCs down into smaller-sized degradation products on the first day faster than the MCM, impacting the total amount of  $\text{O}_3$  produced on subsequent days due to secondary chemistry.

gen oxides ( $\text{NO}_x = \text{NO} + \text{NO}_2$ ) in the presence of sunlight (Atkinson, 2000).

Background  $\text{O}_3$  concentrations have increased during the last several decades due to the increase of overall global anthropogenic emissions of  $\text{O}_3$  precursors (HTAP, 2010). Despite decreases in emissions of  $\text{O}_3$  precursors over Europe since 1990, EEA (2014) reports that 98 % of Europe’s urban population are exposed to levels exceeding the WHO air quality guideline of  $100 \mu\text{g m}^{-3}$  over an 8 h mean. These exceedances result from local and regional  $\text{O}_3$  precursor gas emissions, their intercontinental transport and the non-linear relationship of  $\text{O}_3$  concentrations to  $\text{NO}_x$  and VOC levels (EEA, 2014).

Effective strategies for emission reductions rely on accurate predictions of  $\text{O}_3$  concentrations using chemical transport models (CTMs). These predictions require adequate representation of gas-phase chemistry in the chemical mechanism used by the CTM. For reasons of computational efficiency, the chemical mechanisms used by global and regional CTMs must be simpler than the nearly explicit mechanisms which can be used in box modelling studies. This study compares the impacts of different simplification approaches of chemical mechanisms on  $\text{O}_3$  production chemistry focusing on the role of VOC degradation products.



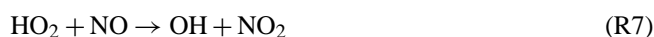
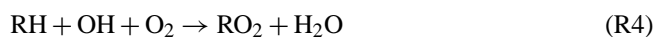
The photochemical cycle (Reactions R1–R3) rapidly produces and destroys  $\text{O}_3$ .  $\text{NO}$  and  $\text{NO}_2$  reach a near-steady state via Reactions (R1) and (R2) which is disturbed in two cases. Firstly, via  $\text{O}_3$  removal (deposition or Reaction R1 during night-time and near large  $\text{NO}$  sources) and secondly,

## 1 Introduction

Ground-level ozone ( $\text{O}_3$ ) is both an air pollutant and a climate forcer that is detrimental to human health and crop growth (Stevenson et al., 2013).  $\text{O}_3$  is produced from the reactions of volatile organic compounds (VOCs) and nitro-

when O<sub>3</sub> is produced through VOC–NO<sub>x</sub> chemistry (Sillman, 1999).

VOCs (RH) are mainly oxidised in the troposphere by the hydroxyl radical (OH) forming peroxy radicals (RO<sub>2</sub>) in the presence of O<sub>2</sub>. For example, Reaction (R4) describes the OH oxidation of alkanes proceeding through abstraction of an H from the alkane. In high-NO<sub>x</sub> conditions, typical of urban environments, RO<sub>2</sub> react with NO (Reaction R5) to form alkoxy radicals (RO), which react quickly with O<sub>2</sub> (Reaction R6) producing a hydroperoxy radical (HO<sub>2</sub>) and a carbonyl species (R'CHO). The secondary chemistry of these first-generation carbon-containing oxidation products is analogous to the sequence of Reactions (R4–R6), producing further HO<sub>2</sub> and RO<sub>2</sub> radicals. Subsequent-generation oxidation products can continue to react, producing HO<sub>2</sub> and RO<sub>2</sub> until they have been completely oxidised to CO<sub>2</sub> and H<sub>2</sub>O. Both RO<sub>2</sub> and HO<sub>2</sub> react with NO to produce NO<sub>2</sub> (Reactions R5 and R7) leading to O<sub>3</sub> production via Reactions (R2) and (R3). Thus, the amount of O<sub>3</sub> produced from VOC degradation is related to the number of NO to NO<sub>2</sub> conversions by RO<sub>2</sub> and HO<sub>2</sub> radicals formed during VOC degradation (Atkinson, 2000).



Three atmospheric regimes with respect to O<sub>3</sub> production can be defined (Jenkin and Clemitshaw, 2000). In the NO<sub>x</sub>-sensitive regime, VOC concentrations are much higher than those of NO<sub>x</sub>, and O<sub>3</sub> production depends on NO<sub>x</sub> concentrations. On the other hand, when NO<sub>x</sub> concentrations are much higher than those of VOCs (VOC-sensitive regime), VOC concentrations determine the amount of O<sub>3</sub> produced. Finally, the NO<sub>x</sub>–VOC-sensitive regime produces maximal O<sub>3</sub> and is controlled by both VOC and NO<sub>x</sub> concentrations.

These atmospheric regimes remove radicals through distinct mechanisms (Kleinman, 1991). In the NO<sub>x</sub>-sensitive regime, radical concentrations are high relative to NO<sub>x</sub> leading to radical removal by radical combination (Reaction R8) and bimolecular destruction (Reaction R9) (Kleinman, 1994).



However, in the VOC-sensitive regime, radicals are removed by reacting with NO<sub>2</sub> leading to nitric acid (HNO<sub>3</sub>) (Reaction R10) and PAN species (Reaction R11).



The NO<sub>x</sub>–VOC-sensitive regime has no dominant radical removal mechanism as radical and NO<sub>x</sub> amounts are compara-

ble. This chemistry results in O<sub>3</sub> concentrations being a non-linear function of NO<sub>x</sub> and VOC concentrations.

Individual VOCs impact O<sub>3</sub> production differently through their diverse reaction rates and degradation pathways. These impacts can be quantified using ozone production potentials (OPPs), which can be calculated through incremental reactivity (IR) studies using photochemical models. In IR studies, VOC concentrations are changed by a known increment and the change in O<sub>3</sub> production is compared to that of a standard VOC mixture. Examples of IR scales are the maximum incremental reactivity (MIR) and maximum ozone incremental reactivity (MOIR) scales in Carter (1994), as well as the photochemical ozone creation potential (POCP) scale of Derwent et al. (1996, 1998). The MIR, MOIR and POCP scales were calculated under different NO<sub>x</sub> conditions, thus calculating OPPs in different atmospheric regimes.

Butler et al. (2011) calculate the maximum potential of a number of VOCs to produce O<sub>3</sub> by using NO<sub>x</sub> conditions inducing NO<sub>x</sub>–VOC-sensitive chemistry over multi-day scenarios using a “tagging” approach – the tagged ozone production potential (TOPP). Tagging involves labelling all organic degradation products produced during VOC degradation with the name of the emitted VOCs. Tagging enables the attribution of O<sub>3</sub> production from VOC degradation products back to the emitted VOCs, thus providing detailed insight into VOC degradation chemistry. Butler et al. (2011), using a near-explicit chemical mechanism, showed that some VOCs, such as alkanes, produce maximum O<sub>3</sub> on the second day of the model run; in contrast to unsaturated aliphatic and aromatic VOCs which produce maximum O<sub>3</sub> on the first day. In this study, the tagging approach of Butler et al. (2011) is applied to several chemical mechanisms of reduced complexity, using conditions of maximum O<sub>3</sub> production (NO<sub>x</sub>–VOC-sensitive regime), to compare the effects of different representations of VOC degradation chemistry on O<sub>3</sub> production in the different chemical mechanisms.

A near-explicit mechanism, such as the Master Chemical Mechanism (MCM) (Jenkin et al., 2003; Saunders et al., 2003; Bloss et al., 2005), includes detailed degradation chemistry making the MCM ideal as a reference for comparing chemical mechanisms. Reduced mechanisms generally take two approaches to simplifying the representation of VOC degradation chemistry: lumped-structure approaches and lumped-molecule approaches (Dodge, 2000).

Lumped-structure mechanisms speciate VOCs by the carbon bonds of the emitted VOCs (e.g. the Carbon Bond mechanisms, CBM-IV (Gery et al., 1989) and CB05 (Yarwood et al., 2005)). Lumped-molecule mechanisms represent VOCs explicitly or by aggregating (lumping) many VOCs into a single mechanism species. Mechanism species may lump VOCs by functionality (MOdel for Ozone and Related chemical Tracers, MOZART-4, Emmons et al., 2010) or OH reactivity (Regional Acid Deposition Model, RADM2 (Stockwell et al., 1990), Regional Atmospheric Chemistry

Mechanism, RACM (Stockwell et al., 1997) and RACM2 (Goliff et al., 2013)). The Common Representative Intermediates mechanism (CRI) lumps the degradation products of VOCs rather than the emitted VOCs (Jenkin et al., 2008).

Many comparison studies of chemical mechanisms consider modelled time series of O<sub>3</sub> concentrations over varying VOC and NO<sub>x</sub> concentrations. Examples are Dunker et al. (1984), Kuhn et al. (1998) and Emmerson and Evans (2009). The largest discrepancies between the time series of O<sub>3</sub> concentrations in different mechanisms from these studies arise when modelling urban rather than rural conditions and are attributed to the treatment of radical production, organic nitrate and night-time chemistry. Emmerson and Evans (2009) also compare the inorganic gas-phase chemistry of different chemical mechanisms; differences in inorganic chemistry arise from inconsistencies between IUPAC and JPL reaction rate constants.

Mechanisms have also been compared using OPP scales. OPPs are a useful comparison tool as they relate O<sub>3</sub> production to a single value. Derwent et al. (2010) compared the near-explicit MCM v3.1 and SAPRC-07 mechanisms using first-day POCP values calculated under VOC-sensitive conditions. The POCP values were comparable between the mechanisms. Butler et al. (2011) compared first-day TOPP values to the corresponding published MIR, MOIR and POCP values. TOPP values were most comparable to MOIR and POCP values due to the similarity of the chemical regimes used in their calculation.

In this study, we compare TOPP values of VOCs using a number of mechanisms to those calculated with the MCM v3.2, under standardised conditions which maximise O<sub>3</sub> production. Differences in O<sub>3</sub> production are explained by the differing treatments of secondary VOC degradation in these mechanisms.

## 2 Methodology

### 2.1 Chemical mechanisms

The nine chemical mechanisms compared in this study are outlined in Table 1 with a brief summary below. We used a subset of each chemical mechanism containing all the reactions needed to fully describe the degradation of the VOCs in Table 2. The reduced mechanisms in this study were chosen as they are commonly used in 3-D models and apply different approaches to representing secondary VOC chemistry. The recent review by Baklanov et al. (2014) shows that each chemical mechanism used in this study are actively used by modelling groups.

The MCM (Jenkin et al., 1997, 2003; Saunders et al., 2003; Bloss et al., 2005; Rickard et al., 2015) is a near-explicit mechanism which describes the degradation of 125 primary VOCs. The MCM v3.2 is the reference mechanism in this study due to its level of detail (16 349 organic reac-

tions). Despite this level of detail, the MCM had difficulties in reproducing the results of chamber study experiments involving aromatic VOCs (Bloss et al., 2005).

The CRI (Jenkin et al., 2008) is a reduced chemical mechanism with 1145 organic reactions describing the oxidation of the same primary VOCs as the MCM v3.1 (12 691 organic reactions). VOC degradation in the CRI is simplified by lumping the degradation products of many VOCs into mechanism species whose overall O<sub>3</sub> production reflects that of the MCM v3.1. The CRI v2 is available in more than one reduced variant, described in Watson et al. (2008). We used a subset of the full version of the CRI v2 (<http://mcm.leeds.ac.uk/CRI>). Differences in O<sub>3</sub> production between the CRI v2 and MCM v3.2 may be due to changes in the MCM versions rather than the CRI reduction techniques, hence the MCM v3.1 is also included in this study.

MOZART-4 represents global tropospheric and stratospheric chemistry (Emmons et al., 2010). Explicit species exist for methane, ethane, propane, ethene, propene, isoprene and  $\alpha$ -pinene. All other VOCs are represented by lumped species determined by the functionality of the VOCs. Tropospheric chemistry is described by 145 organic reactions in MOZART-4.

RADM2 (Stockwell et al., 1990) describes regional-scale atmospheric chemistry using 145 organic reactions with explicit species representing methane, ethane, ethene and isoprene. All other VOCs are assigned to lumped species based on OH reactivity and molecular weight. RADM2 was updated to RACM (Stockwell et al., 1997) with more explicit and lumped species representing VOCs as well as revised chemistry (193 organic reactions). RACM2 is the updated RACM version (Goliff et al., 2013) with substantial updates to the chemistry, including more lumped and explicit species representing emitted VOCs (315 organic reactions).

CBM-IV (Gery et al., 1989) uses 46 organic reactions to simulate polluted urban conditions and represents ethene, formaldehyde and isoprene explicitly while all other emitted VOCs are lumped by their carbon bond types. All primary VOCs were assigned to lumped species in CBM-IV as described in Hogo and Gery (1989). For example, the mechanism species PAR represents the C–C bond. Pentane, having five carbon atoms, is represented as 5 PAR. A pentane mixing ratio of 1200 pptv is assigned to 6000 (= 1200 × 5) pptv of PAR in CBM-IV. CBM-IV was updated to CB05 (Yarwood et al., 2005) by including further explicit species representing methane, ethane and acetaldehyde, and has 99 organic reactions. Other updates include revised allocation of primary VOCs and updated rate constants.

### 2.2 Model set-up

The modelling approach and set-up follows the original TOPP study of Butler et al. (2011). The approach is summarised here; further details can be found in the Supplement and in Butler et al. (2011). We use the MECCA box model,

**Table 1.** The chemical mechanisms used in the study are shown here. MCM v3.2 is the reference mechanism. The number of organic species and reactions needed to fully oxidise the VOCs in Table 2 for each mechanism are also included.

Chemical mechanism	Number of organic species	Number of organic reactions	Type of lumping	Reference	Recent study
MCM v3.2	1884	5621	No lumping	Rickard et al. (2015)	Koss et al. (2015)
MCM v3.1	1677	4862	No lumping	Jenkin et al. (1997) Saunders et al. (2003) Jenkin et al. (2003) Bloss et al. (2005)	Lidster et al. (2014)
CRI v2	189	559	Lumped intermediates	Jenkin et al. (2008)	Derwent et al. (2015)
MOZART-4	61	135	Lumped molecule	Emmons et al. (2010)	Hou et al. (2015)
RADM2	42	105	Lumped molecule	Stockwell et al. (1990)	Li et al. (2014)
RACM	51	152	Lumped molecule	Stockwell et al. (1997)	Ahmadov et al. (2015)
RACM2	92	244	Lumped molecule	Goliff et al. (2013)	Goliff et al. (2015)
CBM-IV	19	47	Lumped structure	Gery et al. (1989)	Foster et al. (2014)
CB05	33	86	Lumped structure	Yarwood et al. (2005)	Dunker et al. (2015)

originally described by Sander et al. (2005), and as subsequently modified by Butler et al. (2011) to include MCM chemistry. In this study, the model is run under conditions representative of 34° N at the equinox (broadly representative of the city of Los Angeles, USA).

Maximum O<sub>3</sub> production is achieved in each model run by balancing the chemical source of radicals and NO<sub>x</sub> at each time step by emitting the appropriate amount of NO. These NO<sub>x</sub> conditions induce NO<sub>x</sub>–VOC-sensitive chemistry. Ambient NO<sub>x</sub> conditions are not required as this study calculates the maximum potential of VOCs to produce O<sub>3</sub>. Future work should verify the extent to which the maximum potential of VOCs to produce O<sub>3</sub> is reached under ambient NO<sub>x</sub> conditions.

VOCs typical of Los Angeles and their initial mixing ratios are taken from Baker et al. (2008), listed in Table 2. Following Butler et al. (2011), the associated emissions required to keep the initial mixing ratios of each VOC constant until noon of the first day were determined for the MCM v3.2. These emissions are subsequently used for each mechanism, ensuring the amount of each VOC emitted was the same in every model run. Methane (CH<sub>4</sub>) was fixed at 1.8 ppmv while CO and O<sub>3</sub> were initialised at 200 and 40 ppbv and then allowed to evolve freely.

The VOCs used in this study are assigned to mechanism species following the recommendations from the literature of each mechanism (Table 1), the representation of each VOC in the mechanisms is found in Table 2. Emissions of lumped species are weighted by the carbon number of the mechanism species ensuring the total amount of emitted reactive carbon was the same in each model run.

The MECCA box model is based upon the Kinetic Pre-Processor (KPP) (Damian et al., 2002). Hence, all chemical mechanisms were adapted into modularised KPP format. The inorganic gas-phase chemistry described in the MCM v3.2 was used in each run to remove any differences between

treatments of inorganic chemistry in each mechanism. Thus, differences between the O<sub>3</sub> produced by the mechanisms are due to the treatment of organic degradation chemistry.

The MCM v3.2 approach to photolysis, dry deposition of VOC oxidation intermediates and RO<sub>2</sub>–RO<sub>2</sub> reactions was used for each mechanism; details of these adaptations can be found in the Supplement. Some mechanisms include reactions which are only important in the stratosphere or free troposphere. For example, PAN photolysis is only important in the free troposphere (Harwood et al., 2003) and was removed from MOZART-4, RACM2 and CB05 for the purpose of the study, as this study considers processes occurring within the planetary boundary layer.

### 2.3 Tagged ozone production potential (TOPP)

This section summarises the tagging approach described in Butler et al. (2011) which is applied in this study.

#### 2.3.1 O<sub>x</sub> family and tagging approach

O<sub>3</sub> production and loss is dominated by rapid photochemical cycles, such as Reactions (R1)–(R3). The effects of rapid production and loss cycles can be removed by using chemical families that include rapidly inter-converting species. In this study, we define the O<sub>x</sub> family to include O<sub>3</sub>, O(<sup>3</sup>P), O(<sup>1</sup>D), NO<sub>2</sub> and other species involved in fast cycling with NO<sub>2</sub>, such as HO<sub>2</sub>NO<sub>2</sub> and PAN species. Thus, production of O<sub>x</sub> can be used as a proxy for production of O<sub>3</sub>.

The tagging approach follows the degradation of emitted VOCs through all possible pathways by labelling every organic degradation product with the name of the emitted VOCs. Thus, each emitted VOC effectively has its own set of degradation reactions. Butler et al. (2011) showed that O<sub>x</sub> production can be attributed to the VOCs by following the tags of each VOC.

**Table 2.** Non-methane volatile organic compounds (NMVOCs) present in Los Angeles. Mixing ratios are taken from Baker et al. (2008) and their representation in each chemical mechanism. The representation of the VOCs in each mechanism is based upon the recommendations of the literature for each mechanism (Table 1).

NMVOCs	Mixing ratio (pptv)	MCM v3.1, v3.2, CRI v2	MOZART-4	RADM2	RACM	RACM2	CBM-IV	CB05
Alkanes								
Ethane	6610	C2H6	C2H6	ETH	ETH	ETH	0.4 PAR	ETHA
Propane	6050	C3H8	C3H8	HC3	HC3	HC3	1.5 PAR	1.5 PAR
Butane	2340	NC4H10	BIGALK	HC3	HC3	HC3	4 PAR	4 PAR
2-Methylpropane	1240	IC4H10	BIGALK	HC3	HC3	HC3	4 PAR	4 PAR
Pentane	1200	NC5H12	BIGALK	HC5	HC5	HC5	5 PAR	5 PAR
2-Methylbutane	2790	IC5H12	BIGALK	HC5	HC5	HC5	5 PAR	5 PAR
Hexane	390	NC6H14	BIGALK	HC5	HC5	HC5	6 PAR	6 PAR
Heptane	160	NC7H16	BIGALK	HC5	HC5	HC5	7 PAR	7 PAR
Octane	80	NC8H18	BIGALK	HC8	HC8	HC8	8 PAR	8 PAR
Alkenes								
Ethene	2430	C2H4	C2H4	OL2	ETE	ETE	ETH	ETH
Propene	490	C3H6	C3H6	OLT	OLT	OLT	OLE + PAR	OLE + PAR
Butene	65	BUT1ENE	BIGENE	OLT	OLT	OLT	OLE + 2 PAR	OLE + 2 PAR
2-Methylpropene	130	MEPROPENE	BIGENE	OLI	OLI	OLI	PAR + FORM + ALD2	FORM + 3 PAR
Isoprene	270	C5H8	ISOP	ISO	ISO	ISO	ISOP	ISOP
Aromatics								
Benzene	480	BENZENE	TOLUENE	TOL	TOL	BEN	PAR	PAR
Toluene	1380	TOLUENE	TOLUENE	TOL	TOL	TOL	TOL	TOL
m-Xylene	410	MXYL	TOLUENE	XYL	XYL	XYM	XYL	XYL
p-Xylene	210	PXYL	TOLUENE	XYL	XYL	XYP	XYL	XYL
o-Xylene	200	OXYL	TOLUENE	XYL	XYL	XYO	XYL	XYL
Ethylbenzene	210	EBENZ	TOLUENE	TOL	TOL	TOL	TOL + PAR	TOL + PAR

$O_x$  production from lumped-mechanism species are re-assigned to the VOCs of Table 2 by scaling the  $O_x$  production of the mechanism species by the fractional contribution of each represented VOC. For example, TOL in RACM2 represents toluene and ethylbenzene with fractional contributions of 0.87 and 0.13 to TOL emissions. Scaling the  $O_x$  production from TOL by these factors gives the  $O_x$  production from toluene and ethylbenzene in RACM2.

Many reduced mechanisms use an operator species as a surrogate for  $RO_2$  during VOC degradation enabling these mechanisms to produce  $O_x$  while minimising the number of  $RO_2$  species represented.  $O_x$  production from operator species is assigned as  $O_x$  production from the organic degradation species producing the operator. This allocation technique is also used to assign  $O_x$  production from  $HO_2$  via Reaction (R7).

### 2.3.2 Definition of TOPP

Attributing  $O_x$  production to individual VOCs using the tagging approach is the basis for calculating the TOPP of a VOC, which is defined as the number of  $O_x$  molecules produced per emitted molecule of VOC. The TOPP value of

a VOC that is not represented explicitly in a chemical mechanism is calculated by multiplying the TOPP value of the mechanism species representing the VOCs by the ratio of the carbon numbers of the VOCs to the mechanism species. For example, CB05 represents hexane as 6 PAR, so the TOPP value of hexane in the CB05 is 6 times the TOPP of PAR. MOZART-4 represents hexane with the five carbon species BIGALK. Thus, hexane emissions are represented molecule for molecule as  $\frac{6}{5}$  of the equivalent number of molecules of BIGALK, and the TOPP value of hexane in MOZART-4 is calculated by multiplying the TOPP value of BIGALK by  $\frac{6}{5}$ .

## 3 Results

### 3.1 Ozone time series and $O_x$ production budgets

Figure 1 shows the time series of  $O_3$  mixing ratios obtained with each mechanism. There is an 8 ppbv difference in  $O_3$  mixing ratios on the first day between RADM2, which has the highest  $O_3$ , and RACM2, which has the lowest  $O_3$  mixing ratios when not considering the outlier time series of RACM. The difference between RADM2 and RACM, the low outlier, was 21 ppbv on the first day. The  $O_3$  mixing ratios in

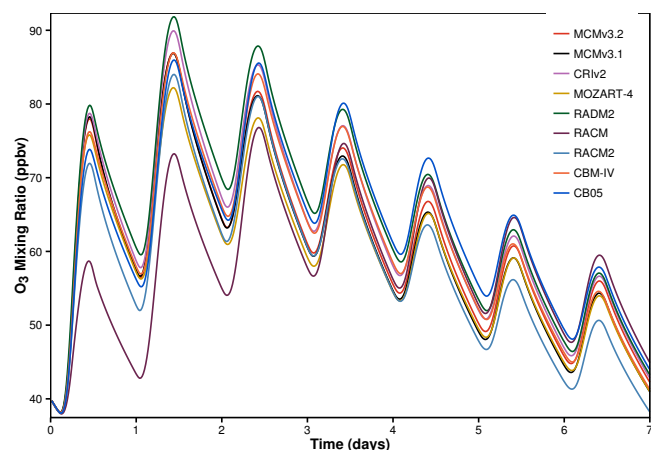


**Figure 1.** Time series of  $O_3$  mixing ratios obtained using each mechanism.

the CRI v2 are larger than those in the MCM v3.1, which is similar to the results in Jenkin et al. (2008) where the  $O_3$  mixing ratios of the CRI v2 and MCM v3.1 are compared over a 5-day period.

The  $O_3$  mixing ratios in Fig. 1 are influenced by the approaches used in developing the chemical mechanisms and not a function of the explicitness of the chemical mechanism. For example, the  $O_3$  mixing ratios obtained using the Carbon Bond mechanisms (CBM-IV and CB05) compare well with the MCM despite both Carbon Bond mechanisms having  $\sim 1\%$  of the number of reactions in the MCM v3.2. Also, the  $O_3$  mixing ratios from RACM2 and RADM2 show similar absolute differences from that of the MCM despite RACM2 having more than double the number of reactions of RADM2.

The day-time  $O_x$  production budgets allocated to individual VOCs for each mechanism are shown in Fig. 2. The relationships between  $O_3$  mixing ratios in Fig. 1 are mirrored in Fig. 2 where mechanisms producing high amounts of  $O_x$  also have high  $O_3$  mixing ratios. The conditions in the box model lead to a daily maximum of OH that increases with each day leading to an increase on each day in both the reaction rate of the OH oxidation of  $CH_4$  and the daily contribution of  $CH_4$  to  $O_x$  production.

The first-day mixing ratios of  $O_3$  in RACM are lower than other mechanisms due to a lack of  $O_x$  production from aromatic VOCs on the first day in RACM (Fig. 2). Aromatic degradation chemistry in RACM results in net loss of  $O_x$  on the first day, described later in Sect. 3.2.1.

RADM2 is the only reduced mechanism that produces higher  $O_3$  mixing ratios than the more detailed mechanisms (MCM v3.2, MCM v3.1 and CRI v2). Higher mixing ratios of  $O_3$  in RADM2 are produced due to increased  $O_x$  production from propane compared to the MCM v3.2; on the first day, the  $O_x$  production from propane in RADM2 is triple that of the MCM v3.2 (Fig. 2). Propane is represented as HC3 in

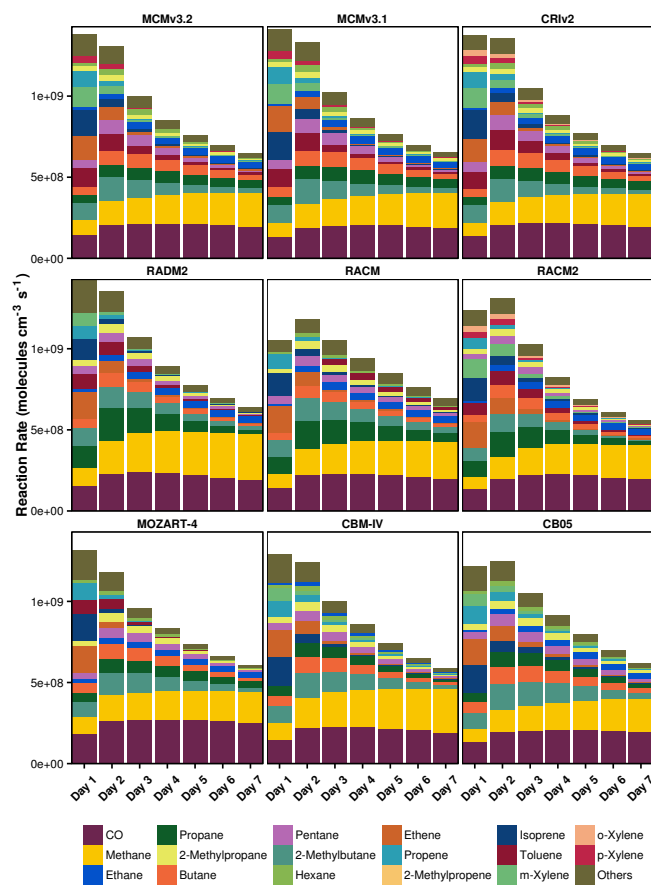


**Figure 2.** Day-time  $O_x$  production budgets in each mechanism allocated to individual VOCs.

RADM2 (Stockwell et al., 1990) and the degradation of HC3 has a lower yield of the less-reactive ketones compared to the MCM. The further degradation of ketones hinders  $O_x$  production due to the low OH reactivity and photolysis rate of ketones. Secondary degradation of HC3 proceeds through the degradation of acetaldehyde ( $CH_3CHO$ ) propagating  $O_x$  production through the reactions of  $CH_3CO_3$  and  $CH_3O_2$  with NO. Thus, the lower ketone yields lead to increased  $O_x$  production from propane degradation in RADM2 compared to the MCM v3.2.

### 3.2 Time-dependent $O_x$ production

Time series of daily TOPP values for each VOC are presented in Fig. 3 and the cumulative TOPP values at the end of the model run obtained for each VOC using each of the mechanisms, normalised by the number of atoms of C in each VOC are presented in Table 3. In the MCM and CRI v2, the cumulative TOPP values obtained for each VOC show that by the end of the model run, larger alkanes have produced more  $O_x$  per unit of reactive C than alkenes or aromatic VOCs. By the end of the runs using the lumped-structure mechanisms (CBM-IV and CB05), alkanes produce similar

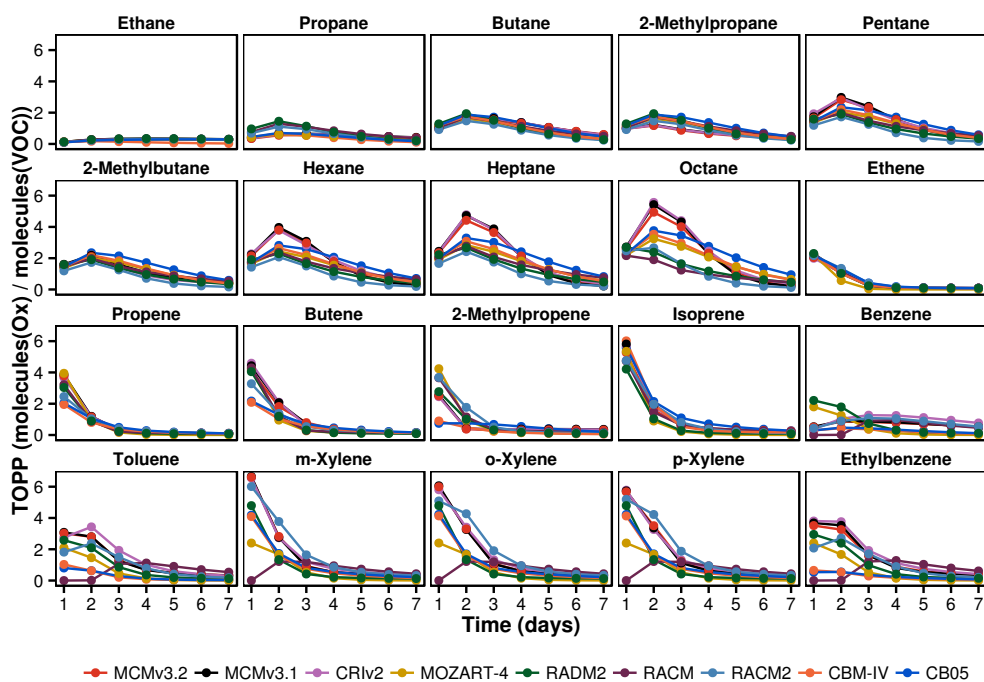


**Figure 3.** TOPP value time series using each mechanism for each VOC.

**Table 3.** Cumulative TOPP values at the end of the model run for all VOCs with each mechanism, normalised by the number of C atoms in each VOC.

NMVOCS	MCM v3.2	MCM v3.1	CRI v2	MOZART-4	RADM2	RACM	RACM2	CBM-IV	CB05
Alkanes									
Ethane	0.9	1.0	0.9	0.9	1.0	1.0	0.9	0.3	0.9
Propane	1.1	1.2	1.2	1.1	1.8	1.8	1.4	0.9	1.0
Butane	2.0	2.0	2.0	1.7	1.8	1.8	1.4	1.7	2.1
2-Methylpropane	1.3	1.3	1.3	1.7	1.8	1.8	1.4	1.7	2.1
Pentane	2.1	2.1	2.2	1.7	1.5	1.6	1.1	1.7	2.1
2-Methylbutane	1.6	1.6	1.5	1.7	1.5	1.6	1.1	1.7	2.1
Hexane	2.1	2.1	2.2	1.7	1.5	1.6	1.1	1.7	2.1
Heptane	2.0	2.1	2.2	1.7	1.5	1.6	1.1	1.7	2.1
Octane	2.0	2.0	2.2	1.7	1.2	1.0	1.0	1.7	2.1
Alkenes									
Ethene	1.9	1.9	1.9	1.4	2.0	2.0	2.2	1.9	2.2
Propene	1.9	2.0	1.9	1.7	1.5	1.6	1.5	1.2	1.4
Butene	1.9	2.0	2.0	1.5	1.5	1.6	1.5	0.8	0.9
2-Methylpropene	1.1	1.2	1.2	1.5	1.1	1.5	1.6	0.5	0.5
Isoprene	1.8	1.8	1.8	1.3	1.2	1.6	1.7	1.9	2.1
Aromatics									
Benzene	0.8	0.8	1.1	0.6	0.9	0.6	0.9	0.3	0.3
Toluene	1.3	1.3	1.5	0.6	0.9	0.6	1.0	0.3	0.3
m-Xylene	1.5	1.5	1.6	0.6	0.9	0.6	1.7	0.9	1.0
p-Xylene	1.5	1.5	1.6	0.6	0.9	0.6	1.7	0.9	1.0
o-Xylene	1.5	1.5	1.6	0.6	0.9	0.6	1.7	0.9	1.0
Ethylbenzene	1.3	1.4	1.5	0.6	0.9	0.6	1.0	0.2	0.3

amounts of  $O_x$  per reactive C, while aromatic VOCs and some alkenes produce less  $O_x$  per reactive C than the MCM. However, in lumped-molecule mechanisms (MOZART-4, RADM2, RACM, RACM2), practically all VOCs produce less  $O_x$  per reactive C than the MCM by the end of the run. This lower efficiency of  $O_x$  production from many individual VOCs in lumped-molecule and lumped-structure mechanisms would lead to an underestimation of  $O_3$  levels downwind of an emission source, and a smaller contribution to background  $O_3$  when using lumped-molecule and lumped-structure mechanisms.

The lumped-intermediate mechanism (CRI v2) produces the most similar  $O_x$  to the MCM v3.2 for each VOC, seen in Fig. 3 and Table 3. Higher variability in the time-dependent  $O_x$  production is evident for VOCs represented by lumped-mechanism species. For example, 2-methylpropene, represented in the reduced mechanisms by a variety of lumped species, has a higher spread in time-dependent  $O_x$  production than ethene, which is explicitly represented in each mechanism.

In general, the largest differences in  $O_x$  produced by aromatic and alkene species are on the first day of the simulations, while the largest inter-mechanism differences in  $O_x$  produced by alkanes are on the second and third days of the simulations. The reasons for these differences in behaviour will be explored in Sect. 3.2.1, which examines differences in first day  $O_x$  production between the chemical mechanisms, and Sect. 3.2.2, which examines the differences in  $O_x$  production on subsequent days.

### 3.2.1 First-day ozone production

The first-day TOPP values of each VOC from each mechanism, representing  $O_3$  production from freshly emitted VOCs near their source region, are compared to those obtained with the MCM v3.2 in Fig. 4. The root mean square error (RMSE) of all first-day TOPP values in each mechanism relative to those in the MCM v3.2 are also included in Fig. 4. The RMSE value of the CRI v2 shows that first-day  $O_x$  production from practically all the individual VOC matches that in the MCM v3.2. All other reduced mechanisms have much larger RMSE values indicating that the first-day  $O_x$  production from the majority of the VOCs differs from that in the MCM v3.2.

The reduced complexity of reduced mechanisms means that aromatic VOCs are typically represented by one or two mechanism species leading to differences in  $O_x$  production of the actual VOCs compared to the MCM v3.2. For example, all aromatic VOCs in MOZART-4 are represented as toluene, thus less-reactive aromatic VOCs, such as benzene, produce higher  $O_x$  whilst more-reactive aromatic VOCs, such as the xylenes, produce less  $O_x$  in MOZART-4 than the MCM v3.2. RACM2 includes explicit species representing benzene, toluene and each xylene resulting in  $O_x$  production

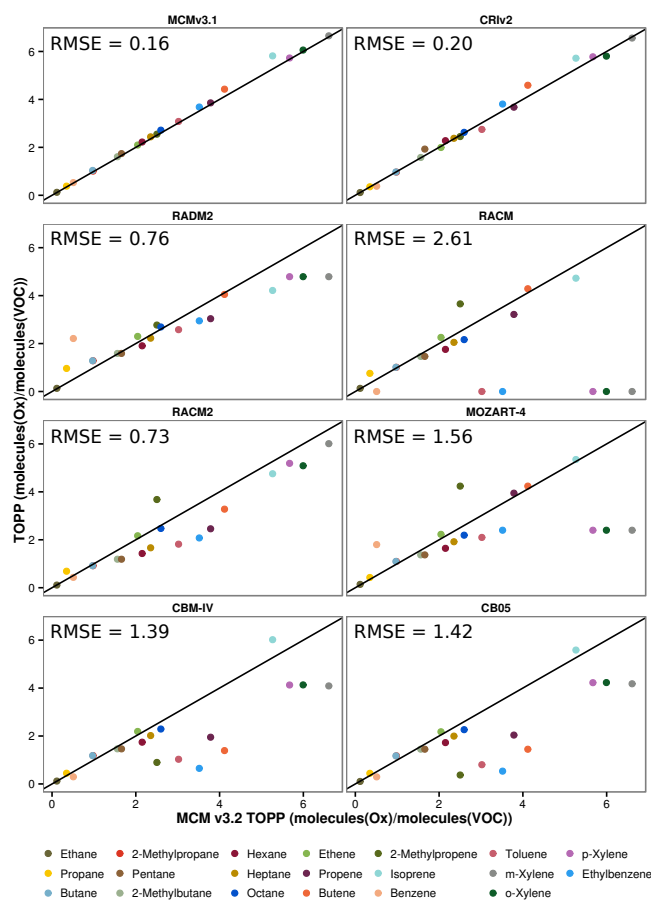


**Figure 4.** The first-day TOPP values for each VOC calculated using MCM v3.2 and the corresponding values in each mechanism. The root mean square error (RMSE) of each set of TOPP values is also displayed. The black line is the 1 : 1 line.

that is the most similar to the MCM v3.2 than other reduced mechanisms.

Figure 3 shows a high spread in  $O_x$  production from aromatic VOCs on the first day indicating that aromatic degradation is treated differently between mechanisms. Toluene degradation is examined in more detail by comparing the reactions contributing to  $O_x$  production and loss in each mechanism, shown in Fig. 5. These reactions are determined by following the “toluene” tags in the tagged version of each mechanism.

Toluene degradation in RACM includes several reactions consuming  $O_x$  that are not present in the MCM, resulting in net loss of  $O_x$  on the first 2 days. Ozonolysis of the cresol OH adduct mechanism species, ADDC, contributes significantly to  $O_x$  loss in RACM. This reaction was included in RACM due to improved cresol product yields when comparing RACM predictions with experimental data (Stockwell et al., 1997). Other mechanisms that include cresol OH adduct species do not include ozonolysis and these reactions are not included in the updated RACM2.

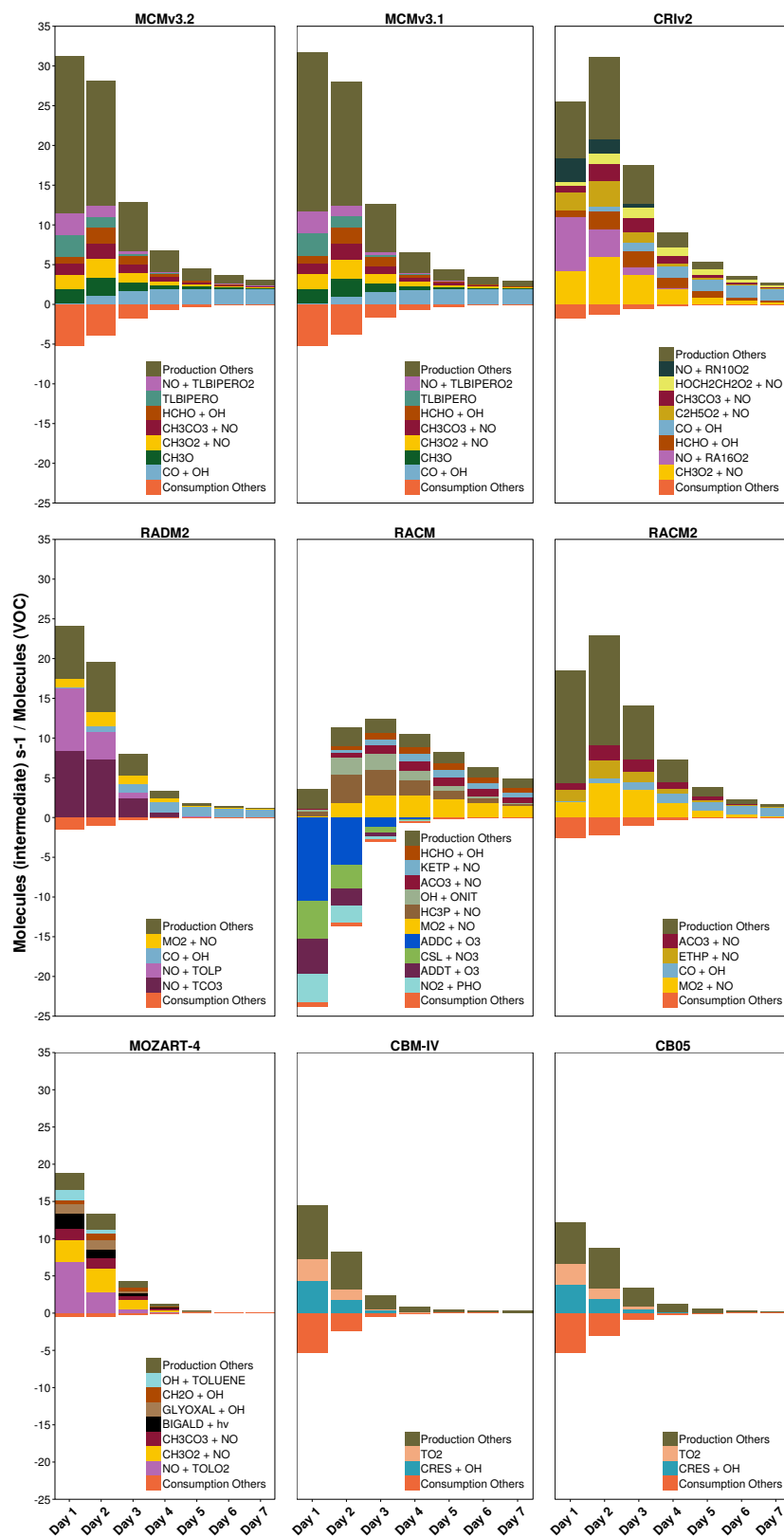


**Figure 5.** Day-time  $O_x$  production and loss budgets allocated to the responsible reactions during toluene degradation in all mechanisms. These reactions are presented using the species defined in each mechanism in Table 1.

The total  $O_x$  produced on the first day during toluene degradation in each reduced mechanism is less than that in the MCM v3.2 (Fig. 5). Less  $O_x$  is produced in all reduced mechanisms due to a faster breakdown of the VOCs into smaller fragments than the MCM, described later in Sect. 3.3. Moreover, in CBM-IV and CB05, less  $O_x$  is produced during toluene degradation as reactions of the toluene degradation products  $CH_3O_2$  and CO do not contribute to the  $O_x$  production budgets, which is not the case in any other mechanism (Fig. 5).

Maximum  $O_x$  production from toluene degradation in CRI v2 and RACM2 is reached on the second day in contrast to the MCM v3.2 which produces peak  $O_x$  on the first day. The second-day maximum of  $O_x$  production in CRI v2 and RACM2 from toluene degradation results from more efficient production of unsaturated dicarbonyls than the MCM v3.2. The degradation of unsaturated dicarbonyls produces peroxy radicals such as  $C_2H_5O_2$  which promote  $O_x$  production via reactions with NO.

Unsaturated aliphatic VOCs generally produce similar amounts of  $O_x$  between mechanisms, especially explicitly represented VOCs, such as ethene and isoprene. On the other hand, unsaturated aliphatic VOCs that are not explicitly represented produce differing amounts of  $O_x$  between mechanisms (Fig. 3). For example, the  $O_x$  produced during 2-methylpropene degradation varies between mechanisms; differing rate constants of initial oxidation reactions and non-realistic secondary chemistry lead to these differences; further details are found in the Supplement.

Non-explicit representations of aromatic and unsaturated aliphatic VOCs coupled with differing degradation chemistry and a faster breakdown into smaller-size degradation products results in different  $O_x$  production in lumped-molecule and lumped-structure mechanisms compared to the MCM v3.2.

### 3.2.2 Ozone production on subsequent days

Alkane degradation in CRI v2 and both MCMs produces a second-day maximum in  $O_x$  that increases with alkane carbon number (Fig. 3). The increase in  $O_x$  production on the second day is reproduced for each alkane by the reduced mechanisms, except octane in RADM2, RACM and RACM2. However, larger alkanes produce less  $O_x$  than the MCM on the second day in all lumped-molecule and lumped-structure mechanisms.

The lumped-molecule mechanisms (MOZART-4, RADM2, RACM and RACM2) represent many alkanes by mechanism species which may lead to unrepresentative secondary chemistry for alkane degradation. For example, 3 times more  $O_x$  is produced during the degradation of propane in RADM2 than the MCM v3.2 on the first day (Fig. 2). Propane is represented in RADM2 by the mechanism species HC3 which also represents other classes of VOCs, such as alcohols. The secondary chemistry of HC3 is

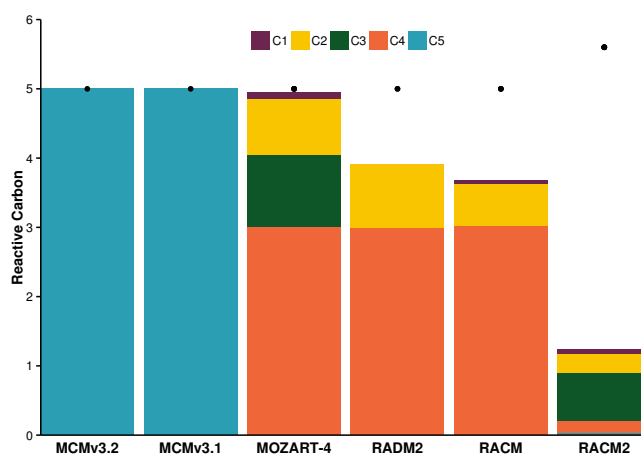


**Figure 6.** The distribution of reactive carbon in the products of the reaction between NO and the pentyl peroxy radical in lumped-molecule mechanisms compared to the MCM. The black dot represents the reactive carbon of the pentyl peroxy radical.

tailored to produce  $O_x$  from these different VOCs and differs from alkane degradation in the MCM v3.2 by producing less ketones in RADM2.

As will be shown in Sect. 3.3, another feature of reduced mechanisms is that the breakdown of emitted VOCs into smaller-sized degradation products is faster than the MCM. Alkanes are broken down quicker in CBM-IV, CB05, RADM2, RACM and RACM2 through a higher rate of reactive carbon loss than the MCM v3.2 (shown for pentane and octane in Fig. 8); reactive carbon is lost through reactions not conserving carbon. Despite many degradation reactions of alkanes in MOZART-4 almost conserving carbon, the organic products have less reactive carbon than the organic reactant also speeding up the breakdown of the alkane compared to the MCM v3.2.

For example, Fig. 6 shows the distribution of reactive carbon in the reactants and products from the reaction of NO with the pentyl peroxy radical in both MCMs and each lumped-molecule mechanism. In all the lumped-molecule mechanisms, the individual organic products have less reactive carbon than the organic reactant. Moreover, in RADM2, RACM and RACM2, this reaction does not conserve reactive carbon leading to faster loss rates of reactive carbon.

The faster breakdown of alkanes in lumped-molecule and lumped-structure mechanisms on the first day limits the amount of  $O_x$  produced on the second day, as less of the larger-sized degradation products are available for further degradation and  $O_x$  production.

### 3.3 Treatment of degradation products

The time-dependent  $O_x$  production of the different VOCs in Fig. 3 results from the varying rates at which VOCs break up into smaller fragments (Butler et al., 2011). Varying breakdown rates of the same VOCs between mechanisms could

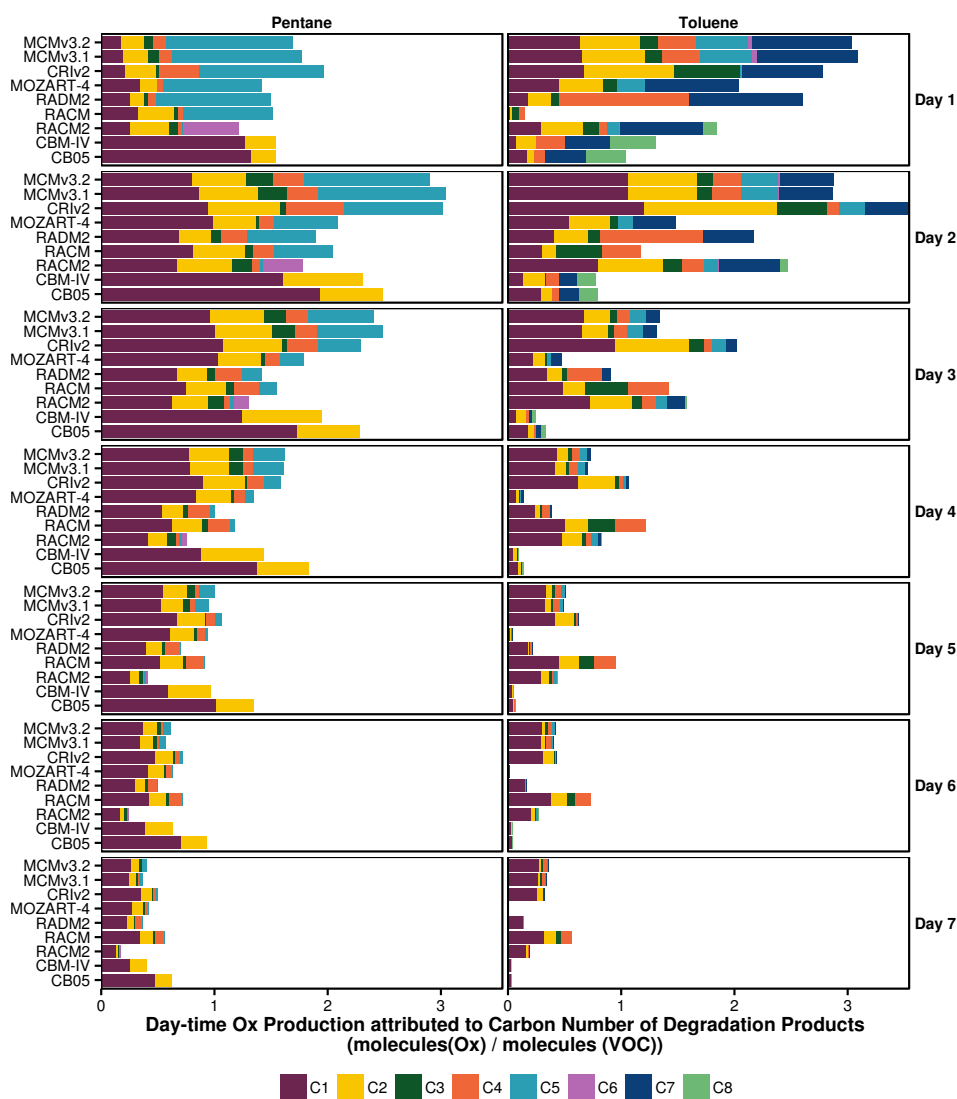


**Figure 7.** Day-time  $O_x$  production during pentane and toluene degradation is attributed to the number of carbon atoms of the degradation products for each mechanism.

explain the different time-dependent  $O_x$  production between mechanisms. The breakdown of pentane and toluene between mechanisms is compared in Fig. 7 by allocating the  $O_x$  production to the number of carbon atoms in the degradation products responsible for  $O_x$  production on each day of the model run in each mechanism. Some mechanism species in RADM2, RACM and RACM2 have fractional carbon numbers (Stockwell et al., 1990, 1997; Goliff et al., 2013) and  $O_x$  production from these species was reassigned as  $O_x$  production of the nearest integral carbon number.

The degradation of pentane, a five-carbon VOC, on the first day in the MCM v3.2 produces up to 50 % more  $O_x$  from degradation products also having five carbon atoms than any reduced mechanism. Moreover, the contribution of the degradation products having five carbon atoms in the MCM v3.2 is consistently higher throughout the model run than in re-

duced mechanisms (Fig. 7). Despite producing less total  $O_x$ , reduced mechanisms produce up to double the amount of  $O_x$  from degradation products with one carbon atom than in the MCM v3.2. The lower contribution of larger degradation products indicates that pentane is generally broken down faster in reduced mechanisms, consistent with the specific example shown for the breakdown of the pentyl peroxy radical in Fig. 6.

The rate of change in reactive carbon during pentane, octane and toluene degradation was determined by multiplying the rate of each reaction occurring during pentane, octane and toluene degradation by its net change in carbon, shown in Fig. 8. Pentane is broken down faster in CBM-IV, CB05, RADM2, RACM and RACM2 by losing reactive carbon more quickly than the MCM v3.2. MOZART-4 also breaks pentane down into smaller-sized products quicker

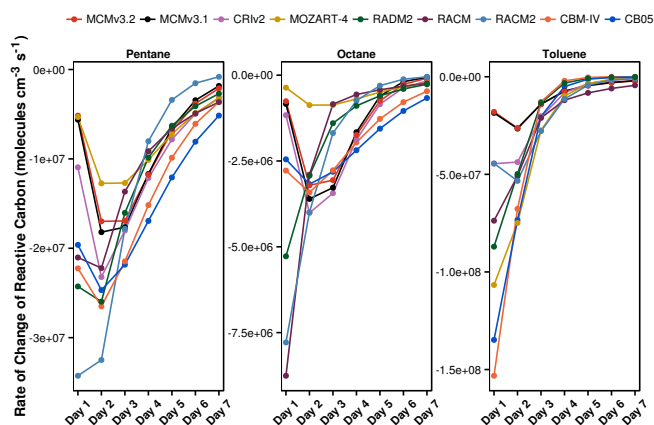


**Figure 8.** Daily rate of change in reactive carbon during pentane, octane and toluene degradation. Octane is represented by the five carbon species, BIGALK, in MOZART-4.

than the MCM v3.2 as reactions during pentane degradation in MOZART-4 have organic products whose carbon number is less than the organic reactant, described in Sect. 3.2.2. The faster breakdown of pentane on the first day limits the amount of reactive carbon available to produce further  $O_x$  on subsequent days leading to lower  $O_x$  production after the first day in reduced mechanisms.

Figure 3 showed that octane degradation produces peak  $O_x$  on the first day in RADM2, RACM and RACM2 in contrast to all other mechanisms where peak  $O_x$  is produced on the second day. Octane degradation in RADM2, RACM and RACM2 loses reactive carbon much faster than any other mechanism on the first day so that there are not enough degradation products available to produce peak  $O_x$  on the second day (Fig. 8). This loss of reactive carbon during alkane degradation leads to the lower accumulated ozone production from these VOCs shown in Table 3.

As seen in Fig. 3,  $O_x$  produced during toluene degradation has a high spread between the mechanisms. Figure 7 shows differing distributions of the sizes of the degradation products that produce  $O_x$ . All reduced mechanisms omit  $O_x$  production from at least one degradation fragment size which produces  $O_x$  in the MCM v3.2, indicating that toluene is also broken down more quickly in the reduced mechanisms than the more explicit mechanisms. For example, toluene degradation in RACM2 does not produce  $O_x$  from degradation products with six carbons, as is the case in the MCM v3.2. Figure 8 shows that all reduced mechanisms lose reactive carbon during toluene degradation faster than the MCM v3.2. Thus, the degradation of aromatic VOCs in reduced mechanisms are unable to produce similar amounts of  $O_x$  as the explicit mechanisms.

## 4 Conclusions

Tagged ozone production potentials (TOPPs) were used to compare  $O_x$  production during VOC degradation in reduced chemical mechanisms to the near-explicit MCM v3.2. First-day mixing ratios of  $O_3$  are similar to the MCM v3.2 for most mechanisms; the  $O_3$  mixing ratios in RACM were much lower than the MCM v3.2 due to a lack of  $O_x$  production from the degradation of aromatic VOCs. Thus, RACM may not be the appropriate chemical mechanism when simulating atmospheric conditions having a large fraction of aromatic VOCs.

The lumped-intermediate mechanism, CRI v2, produces the most similar amounts of  $O_x$  to the MCM v3.2 for each VOC. The largest differences between  $O_x$  production in CRI v2 and MCM v3.2 were obtained for aromatic VOCs; however, overall these differences were much lower than any other reduced mechanism. Thus, when developing chemical mechanisms, the technique of using lumped-intermediate species whose degradation are based upon more detailed mechanism should be considered.

Many VOCs are broken down into smaller-sized degradation products faster on the first day in reduced mechanisms than the MCM v3.2 leading to lower amounts of larger-sized degradation products that can further degrade and produce  $O_x$ . Thus, many VOCs in reduced mechanisms produce a lower maximum of  $O_x$  and lower total  $O_x$  per reactive C by the end of the run than the MCM v3.2. This lower  $O_x$  production from many VOCs in reduced mechanisms leads to lower  $O_3$  mixing ratios compared to the MCM v3.2.

Alkanes produce maximum  $O_3$  on the second day of simulations and this maximum is lower in reduced mechanisms than the MCM v3.2 due to the faster breakdown of alkanes into smaller-sized degradation products on the first day. The lower maximum in  $O_3$  production during alkane degradation in reduced mechanisms leads to an underestimation of the  $O_3$  levels downwind of VOC emissions and an underestimation of the VOC contribution to tropospheric background  $O_3$  when using reduced mechanisms in regional or global modelling studies.

This study has determined the maximum potential of VOCs represented in reduced mechanisms to produce  $O_3$ ; this potential may not be reached as ambient  $NO_x$  conditions may not induce  $NO_x$ -VOC-sensitive chemistry. Moreover, the maximum potential of VOCs to produce  $O_3$  may not be reached when using these reduced mechanisms in 3-D models due to the influence of additional processes, such as mixing and meteorology. Future work shall examine the extent to which the maximum potential of VOCs to produce  $O_3$  in reduced chemical mechanisms is reached using ambient  $NO_x$  conditions and including processes found in 3-D models.

**The Supplement related to this article is available online at doi:10.5194/acp-15-8795-2015-supplement.**

*Acknowledgements.* The authors would like to thank Mike Jenkin and William Stockwell for their helpful reviews, as well as Mark Lawrence and Peter J. H. Builtjes for valuable discussions during the preparation of this manuscript.

Edited by: R. Harley

## References

- Ahmadov, R., McKeen, S., Trainer, M., Banta, R., Brewer, A., Brown, S., Edwards, P. M., de Gouw, J. A., Frost, G. J., Gilman, J., Helmig, D., Johnson, B., Karion, A., Koss, A., Langford, A., Lerner, B., Olson, J., Oltmans, S., Peischl, J., Pétron, G., Pichugina, Y., Roberts, J. M., Ryerson, T., Schnell, R., Senff, C., Sweeney, C., Thompson, C., Veres, P. R., Warneke, C., Wild, R., Williams, E. J., Yuan, B., and Zamora, R.: Understanding high wintertime ozone pollution events in an oil- and natural gas-producing region of the western US, *Atmos. Chem. Phys.*, 15, 411–429, doi:10.5194/acp-15-411-2015, 2015.
- Atkinson, R.: Atmospheric chemistry of VOCs and NO<sub>x</sub>, *Atmos. Environ.*, 34, 2063–2101, 2000.
- Baker, A. K., Beyersdorf, A. J., Doezema, L. A., Katzenstein, A., Meinardi, S., Simpson, I. J., Blake, D. R., and Rowland, F. S.: Measurements of nonmethane hydrocarbons in 28 United States cities, *Atmos. Environ.*, 42, 170–182, 2008.
- Baklanov, A., Schlünzen, K., Suppan, P., Baldasano, J., Brunner, D., Aksoyoglu, S., Carmichael, G., Douros, J., Flemming, J., Forkel, R., Galmarini, S., Gauss, M., Grell, G., Hirtl, M., Joffre, S., Jorba, O., Kaas, E., Kaasik, M., Kallos, G., Kong, X., Korsholm, U., Kurganskiy, A., Kushta, J., Lohmann, U., Mahura, A., Manders-Groot, A., Maurizi, A., Moussiopoulos, N., Rao, S. T., Savage, N., Seigneur, C., Sokhi, R. S., Solazzo, E., Solomos, S., Sørensen, B., Tsegas, G., Vignati, E., Vogel, B., and Zhang, Y.: Online coupled regional meteorology chemistry models in Europe: current status and prospects, *Atmos. Chem. Phys.*, 14, 317–398, doi:10.5194/acp-14-317-2014, 2014.
- Bloss, C., Wagner, V., Jenkin, M. E., Volkamer, R., Bloss, W. J., Lee, J. D., Heard, D. E., Wirtz, K., Martin-Reviejo, M., Rea, G., Wenger, J. C., and Pilling, M. J.: Development of a detailed chemical mechanism (MCMv3.1) for the atmospheric oxidation of aromatic hydrocarbons, *Atmos. Chem. Phys.*, 5, 641–664, doi:10.5194/acp-5-641-2005, 2005.
- Butler, T. M., Lawrence, M. G., Taraborrelli, D., and Lelieveld, J.: Multi-day ozone production potential of volatile organic compounds calculated with a tagging approach, *Atmos. Environ.*, 45, 4082–4090, 2011.
- Carter, W. P. L.: Development of ozone reactivity scales for volatile organic compounds, *J. Air Waste Manage.*, 44, 881–899, 1994.
- Damian, V., Sandu, A., Damian, M., Potra, F., and Carmichael, G.: The kinetic preprocessor KPP – a software environment for solving chemical kinetics, *Comput. Chem. Eng.*, 26, 1567–1579, 2002.
- Derwent, R. G., Jenkin, M. E., and Saunders, S. M.: Photochemical ozone creation potentials for a large number of reactive hydrocarbons under European conditions, *Atmos. Environ.*, 30, 181–199, 1996.
- Derwent, R. G., Jenkin, M. E., Saunders, S. M., and Pilling, M. J.: Photochemical ozone creation potentials for organic compounds in Northwest Europe calculated with a master chemical mechanism, *Atmos. Environ.*, 32, 2429–2441, 1998.
- Derwent, R. G., Jenkin, M. E., Pilling, M. J., Carter, W. P. L., and Kaduwela, A.: Reactivity scales as comparative tools for chemical mechanisms, *J. Air Waste Manage.*, 60, 914–924, 2010.
- Derwent, R. G., Utember, S. R., Jenkin, M. E., and Shallcross, D. E.: Tropospheric ozone production regions and the intercontinental origins of surface ozone over Europe, *Atmos. Environ.*, 112, 216–224, 2015.
- Dodge, M.: Chemical oxidant mechanisms for air quality modeling: critical review, *Atmos. Environ.*, 34, 2103–2130, 2000.
- Dunker, A. M., Kumar, S., and Berzins, P. H.: A comparison of chemical mechanisms used in atmospheric models, *Atmos. Environ.*, 18, 311–321, 1984.
- Dunker, A. M., Koo, B., and Yarwood, G.: Source Apportionment of the Anthropogenic Increment to Ozone, Formaldehyde, and Nitrogen Dioxide by the Path- Integral Method in a 3D Model, *Environ. Sci. Technol.*, 49, 6751–6759, 2015.
- EEA: Air quality in Europe – 2014 report, Tech. Rep. 5/2014, European Environmental Agency, Publications Office of the European Union, doi:10.2800/22847, 2014.
- Emmerson, K. M. and Evans, M. J.: Comparison of tropospheric gas-phase chemistry schemes for use within global models, *Atmos. Chem. Phys.*, 9, 1831–1845, doi:10.5194/acp-9-1831-2009, 2009.
- Emmons, L. K., Walters, S., Hess, P. G., Lamarque, J.-F., Pfister, G. G., Fillmore, D., Granier, C., Guenther, A., Kinnison, D., Laepple, T., Orlando, J., Tie, X., Tyndall, G., Wiedinmyer, C., Baughcum, S. L., and Kloster, S.: Description and evaluation of the Model for Ozone and Related chemical Tracers, version 4 (MOZART-4), *Geosci. Model Dev.*, 3, 43–67, doi:10.5194/gmd-3-43-2010, 2010.
- Foster, P. N., Prentice, I. C., Morfopoulos, C., Siddall, M., and van Weele, M.: Isoprene emissions track the seasonal cycle of canopy temperature, not primary production: evidence from remote sensing, *Biogeosciences*, 11, 3437–3451, doi:10.5194/bg-11-3437-2014, 2014.
- Gery, M. W., Whitten, G. Z., Killus, J. P., and Dodge, M. C.: A photochemical kinetics mechanism for urban and regional scale computer modeling, *J. Geophys. Res.*, 94, 12925–12956, 1989.
- Goliff, W. S., Stockwell, W. R., and Lawson, C. V.: The regional atmospheric chemistry mechanism, version 2, *Atmos. Environ.*, 68, 174–185, 2013.
- Goliff, W. S., Luria, M., Blake, D. R., Zielinska, B., Hallar, G., Valente, R. J., Lawson, C. V., and Stockwell, W. R.: Nighttime air quality under desert conditions, *Atmos. Environ.*, 114, 102–111, 2015.
- Harwood, M., Roberts, J., Frost, G., Ravishankara, A., and Burkholder, J.: Photochemical studies of CH<sub>3</sub>C(O)OONO<sub>2</sub> (PAN) and CH<sub>3</sub>CH<sub>2</sub>C(O)OONO<sub>2</sub> (PPN): NO<sub>3</sub> quantum yields, *J. Phys. Chem. A*, 107, 1148–1154, 2003.
- Hogo, H. and Gery, M.: User's guide for executing OZIPM-4 (Ozone Isoleth Plotting with Optional Mechanisms, Version 4) with CBM-IV (Carbon-Bond Mechanisms-IV) or optional mechanisms. Volume 1. Description of the ozone isopleth plotting package. Version 4, Tech. rep., US Environmental Protection Agency, Durham, North Carolina, USA, 1989.
- Hou, X., Zhu, B., Fei, D., and Wang, D.: The impacts of summer monsoons on the ozone budget of the atmospheric boundary

- layer of the Asia-Pacific region, *Sci. Total Environ.*, 502, 641–649, 2015.
- HTAP: Hemispheric Transport of Air Pollution 2010, Part A: Ozone and Particulate Matter, Air Pollution Studies No.17, Geneva, Switzerland, 2010.
- Jenkin, M. E. and Clemitshaw, K. C.: Ozone and other secondary photochemical pollutants: chemical processes governing their formation in the planetary boundary layer, *Atmos. Environ.*, 34, 2499–2527, 2000.
- Jenkin, M. E., Saunders, S. M., and Pilling, M. J.: The tropospheric degradation of volatile organic compounds: a protocol for mechanism development, *Atmos. Environ.*, 31, 81–104, 1997.
- Jenkin, M. E., Saunders, S. M., Wagner, V., and Pilling, M. J.: Protocol for the development of the Master Chemical Mechanism, MCM v3 (Part B): tropospheric degradation of aromatic volatile organic compounds, *Atmos. Chem. Phys.*, 3, 181–193, doi:10.5194/acp-3-181-2003, 2003.
- Jenkin, M. E., Watson, L. A., Utembe, S. R., and Shallcross, D. E.: A Common Representative Intermediates (CRI) mechanism for VOC degradation. Part 1: Gas phase mechanism development, *Atmos. Environ.*, 42, 7185–7195, 2008.
- Kleinman, L. I.: Seasonal dependence of boundary layer peroxide concentration: the low and high NO<sub>x</sub> regimes, *J. Geophys. Res.*, 96, 20721–20733, 1991.
- Kleinman, L. I.: Low and high NO<sub>x</sub> tropospheric photochemistry, *J. Geophys. Res.*, 99, 16831–16838, 1994.
- Koss, A. R., de Gouw, J., Warneke, C., Gilman, J. B., Lerner, B. M., Graus, M., Yuan, B., Edwards, P., Brown, S. S., Wild, R., Roberts, J. M., Bates, T. S., and Quinn, P. K.: Photochemical aging of volatile organic compounds associated with oil and natural gas extraction in the Uintah Basin, UT, during a wintertime ozone formation event, *Atmos. Chem. Phys.*, 15, 5727–5741, doi:10.5194/acp-15-5727-2015, 2015.
- Kuhn, M., Bultjes, P. J. H., Poppe, D., Simpson, D., Stockwell, W. R., Andersson-Sköld, Y., Baart, A., Das, M., Fiedler, F., Hov, Ø., Kirchner, F., Makar, P. A., Milford, J. B., Roemer, M. G. M., Ruhnke, R., Strand, A., Vogel, B., and Vogel, H.: Intercomparison of the gas-phase chemistry in several chemistry and transport models, *Atmos. Environ.*, 32, 693–709, 1998.
- Li, J., Georgescu, M., Hyde, P., Mahalov, A., and Moustouli, M.: Achieving accurate simulations of urban impacts on ozone at high resolution, *Environ. Res. Lett.*, 9, 114019, doi:10.1088/1748-9326/9/11/114019, 2014.
- Lidster, R. T., Hamilton, J. F., Lee, J. D., Lewis, A. C., Hopkins, J. R., Punjabi, S., Rickard, A. R., and Young, J. C.: The impact of monoaromatic hydrocarbons on OH reactivity in the coastal UK boundary layer and free troposphere, *Atmos. Chem. Phys.*, 14, 6677–6693, doi:10.5194/acp-14-6677-2014, 2014.
- Rickard, A., Young, J., Pilling, M., Jenkin, M., Pascoe, S., and Saunders S.: The Master Chemical Mechanism Version MCM v3.2, available at: <http://mcm.leeds.ac.uk/MCMv3.2/>, last access: 15 July 2015.
- Sander, R., Kerkweg, A., Jöckel, P., and Lelieveld, J.: Technical note: The new comprehensive atmospheric chemistry module MECCA, *Atmos. Chem. Phys.*, 5, 445–450, doi:10.5194/acp-5-445-2005, 2005.
- Saunders, S. M., Jenkin, M. E., Derwent, R. G., and Pilling, M. J.: Protocol for the development of the Master Chemical Mechanism, MCM v3 (Part A): tropospheric degradation of non-aromatic volatile organic compounds, *Atmos. Chem. Phys.*, 3, 161–180, doi:10.5194/acp-3-161-2003, 2003.
- Sillman, S.: The relation between ozone, NO<sub>x</sub> and hydrocarbons in urban and polluted rural environments, *Atmos. Environ.*, 33, 1821–1845, 1999.
- Stevenson, D. S., Young, P. J., Naik, V., Lamarque, J.-F., Shindell, D. T., Voulgarakis, A., Skeie, R. B., Dalsoren, S. B., Myhre, G., Berntsen, T. K., Folberth, G. A., Rumbold, S. T., Collins, W. J., MacKenzie, I. A., Doherty, R. M., Zeng, G., van Noije, T. P. C., Strunk, A., Bergmann, D., Cameron-Smith, P., Plummer, D. A., Strode, S. A., Horowitz, L., Lee, Y. H., Szopa, S., Sudo, K., Nagashima, T., Josse, B., Cionni, I., Righi, M., Eyring, V., Conley, A., Bowman, K. W., Wild, O., and Archibald, A.: Tropospheric ozone changes, radiative forcing and attribution to emissions in the Atmospheric Chemistry and Climate Model Intercomparison Project (ACCMIP), *Atmos. Chem. Phys.*, 13, 3063–3085, doi:10.5194/acp-13-3063-2013, 2013.
- Stockwell, W. R., Middleton, P., Chang, J. S., and Tang, X.: The second generation regional acid deposition model chemical mechanism for regional air quality modeling, *J. Geophys. Res.*, 95, 16343–16367, 1990.
- Stockwell, W. R., Kirchner, F., Kuhn, M., and Seefeld, S.: A new mechanism for regional atmospheric chemistry modeling, *J. Geophys. Res.-Atmos.*, 102, 25847–25879, 1997.
- Watson, L. A., Shallcross, D. E., Utembe, S. R., and Jenkin, M. E.: A Common Representative Intermediates (CRI) mechanism for VOC degradation. Part 2: Gas phase mechanism reduction, *Atmos. Environ.*, 42, 7196–7204, 2008.
- Yarwood, G., Rao, S., Yocke, M., and Whitten, G. Z.: Updates to the Carbon Bond Chemical Mechanism: CB05, Tech. rep., US Environmental Protection Agency, Novato, California, USA, 2005.

Supplement of Atmos. Chem. Phys., 15, 8795–8808, 2015  
<http://www.atmos-chem-phys.net/15/8795/2015/>  
doi:10.5194/acp-15-8795-2015-supplement  
© Author(s) 2015. CC Attribution 3.0 License.



Atmospheric  
Chemistry  
and Physics  
Open Access 

*Supplement of*

## **A comparison of chemical mechanisms using tagged ozone production potential (TOPP) analysis**

**J. Coates and T. M. Butler**

*Correspondence to:* J. Coates ([jane.coates@iass-potsdam.de](mailto:jane.coates@iass-potsdam.de))

The copyright of individual parts of the supplement might differ from the CC-BY 3.0 licence.

## S1 Introduction

2 This is the supplementary material to the research paper “A Comparison of Chemical  
Mechanisms using Tagged Ozone Production Potential (TOPP) Analysis” and provides  
4 further information about the methodology as well as additional analysis.

## S2 Mechanism Setup

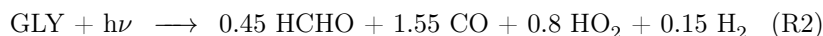
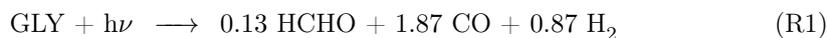
6 All chemical mechanisms were adapted from their original format into the modularised  
KPP (Damian et al., 2002) format for use in the MECCA boxmodel (Sander et al., 2005)  
8 as modified by (Butler et al., 2011).

The MCM v3.2 (Jenkin et al., 1997, 2003; Saunders et al., 2003; Bloss et al., 2005; Rickard  
10 et al., 2015) is the reference mechanism and its approach to dry deposition, photolysis and  
peroxy radical–peroxy radical reactions were applied to all mechanisms.

### 12 S2.1 Photolysis

Photolysis was parameterised as a function of the solar zenith angle following the MCM  
14 approach (Saunders et al., 2003). Species from reduced mechanisms with a direct counterpart  
in the MCM v3.2 were assigned the corresponding MCM v3.2 photolysis rate parameter.  
16 Otherwise, the recommended rate parameter in the mechanism determined the appropriate  
MCM v3.2 photolysis rate parameter. In some cases, the MCM v3.2 photolysis rate  
18 parameter closest in magnitude to that specified by the mechanism was used. For  
example, the organic nitrate species ONIT in RACM2 has a photolysis rate parameter  
20 of  $1.96 \times 10^{-6} \text{ s}^{-1}$  that was compared to the MCM v3.2 organic nitrate photolysis rate  
parameters ( $J_{51} - J_{57}$ ). The rate parameter  $J_{54}$  is the most similar in magnitude and was  
22 assigned as the ONIT photolysis rate parameter in RACM2.

Photolysis reactions of a species in reduced mechanisms were sometimes represented by  
24 more than one MCM v3.2 photolysis reaction. The product yields of the original mechanism  
reactions were preserved using combinations of the MCM v3.2 rate parameters. For example,  
26 glyoxal photolysis described by (R1) and (R2) in RADM2.



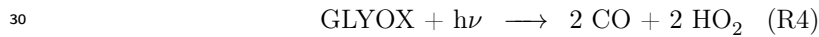
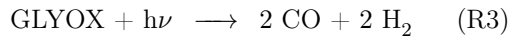
	Rate Parameter	MCM v3.2 Products and Yields
(R1)	0.87 J <sub>31</sub>	1.74 CO + 0.87 H <sub>2</sub>
	0.13 J <sub>32</sub>	0.13 CO + 0.13 HCHO
	0.87 J <sub>31</sub> + 0.13 J <sub>32</sub>	1.87 CO + 0.13 HCHO + 0.87 H <sub>2</sub>
(R2)	0.15 J <sub>31</sub>	0.30 CO + 0.15 H <sub>2</sub>
	0.45 J <sub>32</sub>	0.45 CO + 0.45 HCHO
	0.4 J <sub>33</sub>	0.80 CO + 0.80 HO <sub>2</sub>
	0.15 J <sub>31</sub> + 0.45 J <sub>32</sub> + 0.4 J <sub>33</sub>	1.55 CO + 0.45 HCHO + 0.80 HO <sub>2</sub> + 0.15 H <sub>2</sub>

Table S1: Calculation of glyoxal MCM v3.2 photolysis rate parameters retaining RADM2 glyoxal photolysis product yields.

Mechanism	Reaction	Rate Constant
MCM v3.2	C2H5O2 = C2H5O	$k^*RO2*0.6 \text{ s}^{-1}$
	C2H5O2 = C2H5OH	$k^*RO2*0.2 \text{ s}^{-1}$
	C2H5O2 = CH3CHO	$k^*RO2*0.2 \text{ s}^{-1}$
MOZART-4	C2H5O2 + CH3O2 = 0.7 CH2O + 0.8 CH3CHO + HO2 + 0.3 CH3OH + 0.2 C2H5OH	$2 \times 10^{-13} \text{ cm}^3 \text{ molecules}^{-1} \text{ s}^{-1}$
	C2H5O2 + C2H5O2 = 1.6 CH3CHO + 1.2 HO2 + 0.4 C2H5OH	$6.8 \times 10^{-14} \text{ cm}^3 \text{ molecules}^{-1} \text{ s}^{-1}$
MOZART-4 modified	C2H5O2 = 0.8 CH3CHO + 0.6 HO2 + 0.2 C2H5OH	$2 \times 10^{-13}*RO2 \text{ s}^{-1}$

Table S2: Ethyl peroxy radical (C<sub>2</sub>H<sub>5</sub>O<sub>2</sub>) self and cross organic peroxy reactions in MCM v3.2 and MOZART-4 including rate constants.  $k = 2(6.6 \times 10^{-27} \exp(365/T))^{\frac{1}{2}} \text{ molecules}^{-1} \text{ s}^{-1}$  and RO2 is the sum of all organic peroxy radical mixing ratios.

28 Whereas in the MCM v3.2, (R3), (R4) and (R5) are prescribed for glyoxal photolysis with the rates J<sub>31</sub>, J<sub>32</sub> and J<sub>33</sub>.



The product yields in (R1) were retained using a photolysis rate parameter of  
32  $0.87 J_{31} + 0.13 J_{32}$ , whilst for (R2) the rate  $0.15 J_{31} + 0.45 J_{32} + 0.4 J_{33}$  was used.

Table S1 illustrates the product yield calculations.

Reactants	Products	Rate Constant
MO2 + MO2	0.74 HO2 + 1.37 HCHO + 0.63 MOH	$9.4 \times 10^{-14} \exp(390/T)$ $\text{cm}^3 \text{ molecules}^{-1} \text{ s}^{-1}$
MO2	0.37 HO2 + 0.685 HCHO + 0.315 MOH	$9.4 \times 10^{-14} \exp(390/T) * \text{RO2}$ $\text{s}^{-1}$
ETHP + MO2	HO2 + 0.75 HCHO + 0.75 ACD + 0.25 MOH + 0.25 EOH	$1.18 \times 10^{-13} \exp(158/T)$ $\text{cm}^3 \text{ molecules}^{-1} \text{ s}^{-1}$
ETHP	0.63 HO2 + 0.065 HCHO + 0.75 ACD + 0.25 EOH	$1.18 \times 10^{-13} \exp(158/T) * \text{RO2}$ $\text{s}^{-1}$

Table S3: Dermination of ETHP pseudo-unimolecular reaction and rate constant in RACM2 including rate constants. RO2 is the sum of all organic peroxy radical mixing ratios.

## 34 S2.2 Organic Peroxy Radical Self and Cross Reactions

Reactions of organic peroxy radicals ( $\text{RO}_2$ ) with other organic peroxy radicals are divided  
36 into self ( $\text{RO}_2 + \text{RO}_2$ ) and cross ( $\text{RO}_2 + \text{R}'\text{O}_2$ ) reactions. These reactions are typically  
represented in chemical mechanisms as bimolecular reactions which would cause ambiguities  
38 when implementing the tagging scheme. Namely, which tag to be used for the products  
of reactions between  $\text{RO}_2$  reactants having different tags. The MCM v3.2 approach to  
40 self and cross  $\text{RO}_2$  reactions (each  $\text{RO}_2$  species reacts with the pool of all other  $\text{RO}_2$  at a  
single uniform rate) is used to avoid such ambiguities. The MCM v3.2 approach represents  
42  $\text{RO}_2$ - $\text{RO}_2$  reactions as a pseudo-unimolecular reaction whose rate constant includes a factor  
‘RO2’ which is the sum of the mixing ratios of all organic peroxy radicals (Saunders et al.,  
44 2003).

The pseudo-unimolecular reaction products and their yields were determined by one  
46 of two methods. Firstly, by using the  $\text{RO}_2 + \text{RO}_2$  reaction and halving the product  
yields, demonstrated for the MOZART-4 treatment of the ethyl peroxy radical in Table S2.  
48 Alternatively, the  $\text{RO}_2 + \text{CH}_3\text{O}_2$  reaction was used to determine the products due to  $\text{CH}_3\text{O}_2$   
and these products are then removed.

50 Table S3 demonstrates the steps determining the ETHP pseudo-unimolecular reaction  
in RACM2. First the products due to MO2 ( $\text{CH}_3\text{O}_2$  in RACM2) are determined as outlined  
52 previously using the  $\text{MO2} + \text{MO2}$  reaction. The MO2 product yields are subtracted from  
the  $\text{ETHP} + \text{MO2}$  reaction. Any products having a negative yield are not included in the

54 final pseudo-unimolecular reaction.

The methyl acyl peroxy radical ( $\text{CH}_3\text{C}(\text{O})\text{O}_2$ ) was the exception to the above approach. Although most mechanisms include a  $\text{CH}_3\text{C}(\text{O})\text{O}_2 + \text{CH}_3\text{C}(\text{O})\text{O}_2$  reaction, the  $\text{CH}_3\text{C}(\text{O})\text{O}_2$  pseudo-unimolecular reaction was derived by subtracting the  $\text{CH}_3\text{O}_2$  product yields from the  $\text{CH}_3\text{C}(\text{O})\text{O}_2 + \text{CH}_3\text{O}_2$  reaction. This approach was used as the  $\text{CH}_3\text{C}(\text{O})\text{O}_2 + \text{CH}_3\text{O}_2$  reaction is the most significant reaction for  $\text{CH}_3\text{C}(\text{O})\text{O}_2$ .

60 The rate constant for each pseudo-unimolecular reaction was taken as that of the  $\text{RO}_2 + \text{CH}_3\text{O}_2$  reaction multiplied by an ‘RO2’ factor, which is the sum of the mixing ratios of all organic peroxy radicals. The  $\text{RO}_2 + \text{CH}_3\text{O}_2$  rate constant was chosen as this is the most likely reaction to occur.

64 Model runs using the original and modified approach to the  $\text{RO}_2$ - $\text{RO}_2$  reactions for each mechanism were performed. The resulting  $\text{O}_3$  concentration time series were compared and shown in Figure S1.

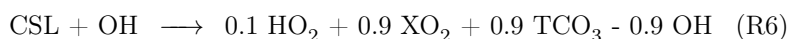
### S2.3 Dry Deposition

68 Dry deposition velocities for individual chemical species are taken from the MCM v3.2. The MCM v3.2 dry deposition velocities of the same chemical functional group were used for mechanism species without direct MCM v3.2 analogues. For example, the dry deposition velocity of PAN-like species in all mechanisms was equivalent to that of the PAN species in the MCM v3.2.

### S2.4 Negative Product Yield Treatment

74 Some mechanisms include reactions where products have a negative yield. These reactions were re-written including an operator species with a positive yield as the analysis tools used in this study do not allow negative product yields. The operator species acts as a sink for the original product by immediately reacting with the original product generating a ‘NULL’ product.

For example, in RADM2 the  $\text{OH} + \text{CSL}$  (cresol) reaction has negative OH yield in (R6) (Stockwell et al., 1990).



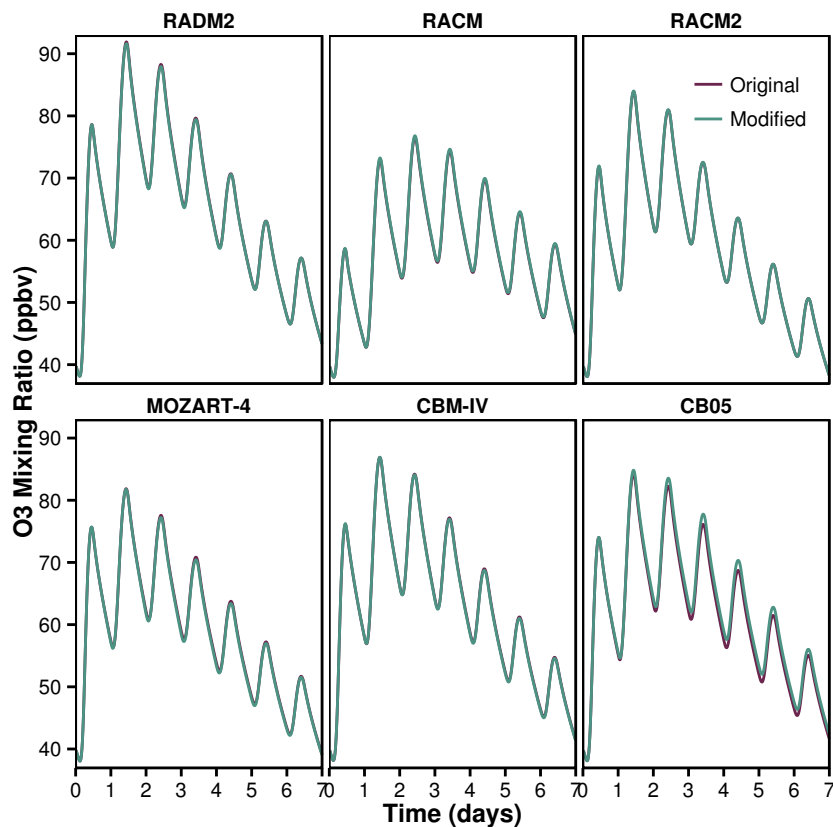
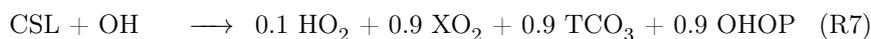


Figure S1:  $O_3$  mixing ratio time series for each reduced mechanism using the original and modified approach to  $RO_2$ - $RO_2$  reactions

82 The negative OH yield was adapted to a positive operator (OHOP) yield in (R7). OHOP  
then reacts immediately with OH giving a ‘NULL’ product with a rate constant of  
84  $8.0 \times 10^{-11} \text{ cm}^3 \text{ s}^{-1}$  (R8). Thus preserving the OH yields from (R6) in RADM2.



### 86 S3 Mapping Emitted NMVOC to Mechanism Species

The emitted NMVOC are typical of Los Angeles as described in Baker et al. (2008). The  
88 MCM v3.2, v3.1 (Jenkin et al., 1997; Saunders et al., 2003; Jenkin et al., 2003) and CRI v2  
(Jenkin et al., 2008) explicitly represent all of these NMVOC.

90 The representation of NMVOC in all other mechanisms required mapping the individual  
NMVOC to specific mechanism species. This mapping followed the recommendations on

92 the literature of the mechanism; Table S4 describes the mechanism species used for mapping  
the initial NMVOC. Table 2 of the main article shows the final mapping of each NMVOC  
94 to each mechanism species.

## S4 Treatment of 2-methylpropene Degradation

96 Figure 4 of the main article shows the first day TOPP values of the VOC obtained in  
each reduced mechanism compared to the MCM v3.2. The first day TOPP values of  
98 2-methylpropene in RACM, RACM2, MOZART-4, CBM-IV and CB05 signify differences  
in its degradation to the MCM v3.2.

100 The variation between RACM, RACM2 and MCM v3.2 arises from differences in the  
ozonolysis rate constant of 2-methylpropene. This rate constant is an order of magnitude  
102 faster in RACM and RACM2 than in MCM v3.2 as the RACM, RACM2 rate constant  
is a weighted mean of the ozonolysis rate constants of each VOC represented as OLI  
104 (Stockwell et al., 1997; Goliff et al., 2013). The faster rate constant promotes increased  
radical production leading to more  $O_x$  in RACM and RACM2 than the MCM v3.2.

106 2-methylpropene is represented as BIGENE in MOZART-4. The degradation of BIGENE  
produces  $CH_3CHO$  through the reaction between NO and the 2-methylpropene peroxy  
108 radical, whereas no  $CH_3CHO$  is produced during 2-methylpropene degradation in the  
MCM v3.2.  $CH_3CHO$  initiates a degradation chain producing  $O_x$  involving  $CH_3CO_3$  and  
110  $CH_3O_2$  leading to more  $O_x$  in MOZART-4 than MCM v3.2.

CBM-IV and CB05 represent 2-methylpropene as a combination of aldehydes and  
112 PAR, the C–C bond (Gery et al., 1989; Yarwood et al., 2005). This representation of  
2-methylpropene does not produce the 2-methylpropene peroxy radical, whose reaction  
114 with NO is the main source of  $O_x$  production in all other mechanisms.

Mechanism	Species	Description	Mechanism	Species	Description
MOZART-4 (Emmons et al., 2010)	C2H6	Ethane	ETH	Ethane	
	C3H8	Propane	HC3	OH rate constant (298 K, 1 atm) less than $3.4 \times 10^{-12}$ $\text{cm}^3 \text{s}^{-1}$	
	BIGALK	Lumped alkanes C >3	HC5	OH rate constant (298 K, 1 atm) between $3.4 \times 10^{-12}$ and $6.8 \times 10^{-12} \text{ cm}^3 \text{ s}^{-1}$	
	C2H4	Ethene	HC8	OH rate constant (298 K, 1 atm) greater than $6.8 \times 10^{-12} \text{ cm}^3 \text{ s}^{-1}$	
	C3H6	Propene	ETE	Ethene	
	BIGENE	Lumped alkenes C >3	OLT	Terminal alkenes	
	ISOP	Isoprene	OLI	Internal alkenes	
	TOLUENE	Lumped aromatics	ISO	Isoprene	
	ETH	Ethane	BEN	Benzene	
	HC3	OH rate constant (298, 1 atm) between $2.7 \times 10^{-13}$ and $3.4 \times 10^{-12}$	TOL	Toluene and less reactive aromatics	
RADM2 (Stockwell et al., 1990)	HC5	OH rate constant (298, 1 atm) between $3.4 \times 10^{-12}$ and $6.8 \times 10^{-12}$	XYM	m-Xylene	
	HC8	OH rate constant (298, 1 atm) greater than $6.8 \times 10^{-12}$	XYO	o-Xylene	
	OL2	Ethene	XYP	p-Xylene	
	OLT	Terminal Alkenes	PAR	Paraffin carbon bond C-C	
	OLI	Internal Alkenes	ETH	Ethene	
	ISO	Isoprene	OLE	Olefinic carbon bond C=C	
	TOL	Toluene and less reactive aromatics	ALD2	High molecular weight aldehydes	
	XYL	Xylene and more reactive aromatics	ISOP	Isoprene	
	ETH	Ethane	TOL	Toluene	
	HC3	OH rate constant (298 K, 1 atm) less than $3.4 \times 10^{-12} \text{ cm}^3 \text{ s}^{-1}$	XYL	Xylene	
RACM (Stockwell et al., 1997)	HC5	OH rate constant (298 K, 1 atm) between $3.4 \times 10^{-12}$ and $6.8 \times 10^{-12} \text{ cm}^3 \text{ s}^{-1}$	FORM	Formaldehyde	
	HC8	OH rate constant (298 K, 1 atm) greater than $6.8 \times 10^{-12}$	ETHA	Ethane	
	ETE	Ethene	PAR	Paraffin carbon bond C-C	
	OLT	Terminal alkenes	OLE	Terminal olefin carbon bond R-C=C	
	OLI	Internal alkenes	FORM	Formaldehyde	
	ISO	Isoprene	ISOP	Isoprene	
	TOL	Toluene and less reactive aromatics	TOL	Toluene and other monoalkyl aromatics	
	XYL	Xylene and more reactive aromatics	XYL	Xylene and other polyalkyl aromatics	

Table S4: Description of primary mechanism species used for mapping emitted NMVOCs.

## References

- 116 Angela K. Baker, Andreas J. Beyersdorf, Lambert A. Doezema, Aaron Katzenstein, Simone  
Meinardi, Isobel J. Simpson, Donald R. Blake, and F. Sherwood Rowland. Measurements  
118 of nonmethane hydrocarbons in 28 United States cities. *Atmospheric Environment*, 42:  
170–182, 2008.
- 120 C. Bloss, V. Wagner, M. E. Jenkin, R. Vollamer, W. J. Bloss, J. D. Lee, D. E. Heard,  
K. Wirtz, M. Martin-Reviejo, G. Rea, J. C. Wenger, and M. J. Pilling. Development  
122 of a detailed chemical mechanism (MCMv3.1) for the atmospheric oxidation of aromatic  
hydrocarbons. *Atmospheric Chemistry and Physics*, 5:641–664, 2005.
- 124 T. M. Butler, M. G. Lawrence, D. Taraborrelli, and J. Lelieveld. Multi-day ozone production  
potential of volatile organic compounds calculated with a tagging approach. *Atmospheric*  
126 *Environment*, 45(24):4082–4090, 2011.
- V. Damian, A. Sandu, M. Damian, F. Potra, and G.R. Carmichael. The kinetic preprocessor  
128 KPP - A software environment for solving chemical kinetics. *Computers and Chemical*  
*Engineering*, 26(11):1567–1579, 2002.
- 130 L. K. Emmons, S. Walters, P. G. Hess, J.-F. Lamarque, G. G. Pfister, D. Fillmore, C. Granier,  
A. Guenther, D. Kinnison, T. Laepple, J. Orlando, X. Tie, G. Tyndall, C. Wiedinmyer,  
132 S. L. Baughcum, and S. Kloster. Description and evaluation of the Model for Ozone and  
Related chemical Tracers, version 4 (MOZART-4). *Geoscientific Model Development*, 3:  
134 43–67, 2010.
- Michael W. Gery, Gary Z. Whitten, James P. Killus, and Marcia C. Dodge. A photochemical  
136 kinetics mechanism for urban and regional scale computer modeling. *Journal of Geophysical*  
*Research*, 94(D10):12,925–12,956, 1989.
- 138 Wendy S. Goliff, William R. Stockwell, and Charlene V. Lawson. The regional atmospheric  
chemistry mechanism, version 2. *Atmospheric Environment*, 68:174–185, 2013.
- 140 M. E. Jenkin, S. M. Saunders, V. Wagner, and M. J. Pilling. Protocol for the development of  
the Master Chemical Mechanism, MCM v3 (Part B): Tropospheric degradation of aromatic  
142 volatile organic compounds. *Atmospheric Chemistry and Physics*, 3(1):181–193, 2003.

- M. E. Jenkin, L. A. Watson, S. R. Utembe, and D. E. Shallcross. A Common Representative  
144 Intermediates (CRI) mechanism for VOC degradation. Part 1: Gas phase mechanism  
development. *Atmospheric Environment*, 42:7185–7195, 2008.
- 146 Michael E. Jenkin, Sandra M. Saunders, and Michael J. Pilling. The tropospheric  
degradation of volatile organic compounds: A protocol for mechanism development.  
148 *Atmospheric Environment*, 31(1):81–104, 1997.
- Andrew Rickard, Jenny Young, and Stephen Pascoe. The Master Chemical Mechanism  
150 Version MCM v3.2. <http://mcm.leeds.ac.uk/MCMv3.2/>, 2015. [Online; accessed  
25-March-2015].
- 152 R. Sander, A. Kerkweg, P. Jöckel, and J. Lelieveld. Technical Note: The new comprehensive  
atmospheric chemistry module MECCA. *Atmospheric Chemistry and Physics*, 5:445–450,  
154 2005.
- S. M. Saunders, M. E. Jenkin, R. G. Derwent, and M. J. Pilling. Protocol for the development  
156 of the Master Chemical Mechanism, MCM v3 (Part A): Tropospheric degradation of  
non-aromatic volatile organic compounds. *Atmospheric Chemistry and Physics*, 3(1):  
158 161–180, 2003.
- William R. Stockwell, Paulete Middleton, Julius S. Chang, and Xiaoyan Tang. The Second  
160 Generation Regional Acid Deposition Model Chemical Mechanism for Regional Air Quality  
Modeling. *Journal of Geophysical Research*, 95(D10):16,343–16,367, 1990.
- 162 William R. Stockwell, Frank Kirchner, Michael Kuhn, and Stephan Seefeld. A new  
mechanism for regional atmospheric chemistry modeling. *Journal of Geophysical Research*  
164 *D: Atmospheres*, 102(22):25,847–25,879, 1997.
- Greg Yarwood, Sunja Rao, Mark Yocke, and Gary Z. Whitten. Updates to the Carbon Bond  
166 Chemical Mechanism: CB05. Technical report, U. S Environmental Protection Agency,  
2005.

## Chapter 8

### **Paper II: Variation of the NMVOC Speciation in the Solvent Sector and the Sensitivity of Modelled Tropospheric Ozone**



This article has been removed due to copyright issues. The original article is found at <http://dx.doi.org/10.1016/j.atmosenv.2016.03.057>.



## Chapter 9

### Paper III: The Influence of Temperature on Ozone Production under varying NO<sub>x</sub> Conditions – a modelling study



1 The Influence of Temperature on Ozone Production under  
2 varying NO<sub>x</sub> Conditions – a modelling study

3 J. Coates<sup>1</sup>, K. Mar<sup>1</sup>, N. Ojha<sup>2</sup> and T. Butler<sup>1</sup>

4 <sup>1</sup>Institute for Advanced Sustainability Studies, Potsdam, Germany

5 <sup>2</sup>Atmospheric Chemistry Department, Max Planck Institute for Chemistry, Mainz,  
6 Germany

7 March 24, 2016

8 **Abstract**

9 Surface ozone is a secondary air pollutant produced during the atmospheric photochemical  
10 degradation of emitted volatile organic compounds (VOCs) in the presence of sunlight and  
11 nitrogen oxides (NO<sub>x</sub>). Temperature directly influences ozone production through speeding  
12 up the rates of the chemical reactions and increasing the emissions of VOCs, such as isoprene,  
13 from vegetation. In this study, we used a box model to examine the non-linear relationship  
14 between ozone, NO<sub>x</sub> and temperature, and compared this to previous observational studies.  
15 Under high-NO<sub>x</sub> conditions, an increase in ozone from 20 °C to 40 °C of up to 20 ppbv  
16 was due to faster reaction rates while increased isoprene emissions added up to a further  
17 11 ppbv of ozone. The increased oxidation rate of emitted VOC with temperature controlled  
18 the rate of O<sub>x</sub> production, the net influence of peroxy nitrates increased net O<sub>x</sub> production  
19 per molecule of emitted VOC oxidised. The rate of increase in ozone mixing ratios with  
20 temperature from our box model simulations was about half the rate of increase in ozone with  
21 temperature observed over central Europe or simulated by a regional chemistry transport  
22 model. Modifying the box model setup to approximate stagnant meteorological conditions  
23 increased the rate of increase of ozone with temperature as the accumulation of oxidants  
24 enhanced ozone production through the increased production of peroxy radicals from the  
25 secondary degradation of emitted VOCs. The box model simulations approximating stagnant  
26 conditions and the maximal ozone production chemical regime reproduced the 2 ppbv increase  
27 in ozone per °C from the observational and regional model data over central Europe. The  
28 simulated ozone-temperature relationship was more sensitive to mixing than the choice of

29 chemical mechanism. Our analysis suggests that reductions in  $\text{NO}_x$  emissions would be  
30 required to offset the additional ozone production due to an increase in temperature in the  
31 future.

## 32 1 Introduction

33 Surface-level ozone ( $\text{O}_3$ ) is a secondary air pollutant formed during the photochemical degradation  
34 of volatile organic compounds (VOCs) in the presence of nitrogen oxides ( $\text{NO}_x \equiv \text{NO} + \text{NO}_2$ ).  
35 Due to the photochemical nature of ozone production, it is strongly influenced by meteorological  
36 variables such as temperature (Jacob and Winner, 2009). Otero et al. (2016) showed that  
37 temperature was a major meteorological driver for summertime ozone in many areas of central  
38 Europe.

39 Temperature primarily influences ozone production in two ways: speeding up the rates of many  
40 chemical reactions, and increasing emissions of VOCs from biogenic sources (BVOCs) (Sillman and  
41 Samson, 1995). While emissions of anthropogenic VOCs (AVOCs) are generally not dependent on  
42 temperature, evaporative emissions of some AVOCs do increase with temperature (Rubin et al.,  
43 2006). The review of Pusede et al. (2015) provides further details of the temperature-dependent  
44 processes impacting ozone production.

45 Regional modelling studies over the US (Sillman and Samson, 1995; Steiner et al., 2006;  
46 Dawson et al., 2007) examined the sensitivity of ozone production during a pollution episode  
47 to increased temperatures. These studies noted that increased temperatures (without changing  
48 VOC or  $\text{NO}_x$ -conditions) led to higher ozone levels, often exceeding local air quality guidelines.  
49 Sillman and Samson (1995) and Dawson et al. (2007) varied the temperature dependence of the  
50 PAN (peroxy acetyl nitrate) decomposition rate during simulations of the eastern US determining  
51 the sensitivity of ozone production with temperature to the PAN decomposition rate. In addition  
52 to the influence of PAN decomposition on ozone production, Steiner et al. (2006) correlated the  
53 increase in ozone mixing ratios with temperature over California to increased mixing ratios of  
54 formaldehyde, a secondary degradation production of many VOCs and an important radical  
55 source. Steiner et al. (2006) also noted increased emissions of BVOCs at higher temperatures in  
56 urban areas with high  $\text{NO}_x$  emissions also increased ozone levels with temperature.

57 Pusede et al. (2014) used an analytical model constrained by observations over the San  
58 Joaquin Valley, California to infer a non-linear relationship between ozone, temperature and  
59  $\text{NO}_x$ , similar to the well-known non-linear relationship of ozone production on  $\text{NO}_x$  and VOC

60 levels (Sillman, 1999). Moreover, Pusede et al. (2014) showed that temperature can be used  
61 as a surrogate for VOC levels when considering the relationship of ozone under different  $\text{NO}_x$   
62 conditions.

63 Environmental chamber studies have also been used to analyse the relationship of ozone with  
64 temperature using a fixed mixture of VOCs. The chamber experiments of Carter et al. (1979)  
65 and Hatakeyama et al. (1991) showed increases in ozone from a VOC mix with temperature.  
66 Both studies compared the concentration time series of ozone and nitrogen-containing compounds  
67 ( $\text{NO}_x$ , PAN,  $\text{HNO}_3$ ) at various temperatures linking the maximum ozone concentration to the  
68 decrease in PAN concentrations at temperatures greater than 303 K.

69 Despite many studies considering the ozone-temperature relationship from an observational  
70 and chamber study perspective, modelling studies focusing on the detailed chemical processes of  
71 the ozone-temperature relationship under different  $\text{NO}_x$  conditions have not been performed (to  
72 our knowledge). The regional modelling studies described previously concentrated on reproducing  
73 ozone levels (using a single chemical mechanism) over regions with known meteorology and  
74  $\text{NO}_x$  conditions then varying the temperature. These modelling studies did not consider the  
75 relationship between ozone,  $\text{NO}_x$  and temperature. The review of Pusede et al. (2015) also  
76 highlights a lack of modelling studies looking at the relationship of ozone with temperature under  
77 different  $\text{NO}_x$  conditions.

78 Comparisons of different chemical mechanisms, such as Emmerson and Evans (2009) and  
79 Coates and Butler (2015), showed that different representations of tropospheric chemistry  
80 influenced ozone production. Neither of these studies examined the ozone-temperature relationship  
81 differences between chemical mechanisms. Furthermore, Rasmussen et al. (2013) acknowledged  
82 that the modelled ozone-temperature relationship may be sensitive to the choice of chemical  
83 mechanism and recommended investigating this sensitivity. Comparing the ozone-temperature  
84 relationship predicted by different chemical mechanisms is potentially important for modelling of  
85 future air quality due to the expected increase in heatwaves (Karl and Trenberth, 2003).

86 In this study, we use an idealised box model to determine how ozone levels vary with  
87 temperature under different  $\text{NO}_x$  conditions. We determine whether faster chemical reaction  
88 rates or increased BVOC emissions have a greater influence on instantaneous ozone production  
89 with higher temperature under different  $\text{NO}_x$  conditions. Furthermore, we compare the  
90 ozone-temperature relationship produced by different chemical mechanisms.

## 91 2 Methodology

### 92 2.1 Model Setup

93 We used the MECCA box model (Sander et al., 2005) to determine the important gas-phase  
94 chemical processes for ozone production under different temperatures and  $\text{NO}_x$  conditions. The  
95 MECCA box model was set up as described in Coates and Butler (2015) and updated to  
96 include vertical mixing with the free troposphere using a diurnal cycle for the PBL height. The  
97 supplementary material includes further details of these updates.

98 Simulations were broadly representative of urban conditions in central Europe and were run  
99 for daylight hours in one full day. Methane was fixed at 1.7 ppmv throughout the model run,  
100 carbon monoxide (CO) and ozone were initialised at 200 ppbv and 40 ppbv and then allowed  
101 to evolve freely throughout the simulation. All VOC emissions were held constant until noon  
102 simulating a plume of freshly-emitted VOC.

103 Separate box model simulations were performed by systematically varying the  
104 temperature between 288 and 313 K (15–40 °C) in steps of 0.5 K. NO emissions were  
105 systematically varied between  $5.0 \times 10^9$  and  $1.5 \times 10^{12}$  molecules(NO)  $\text{cm}^{-2} \text{s}^{-1}$  in steps of  
106  $1 \times 10^{10}$  molecules(NO)  $\text{cm}^{-2} \text{s}^{-1}$  at each temperature step. At 20 °C, these NO emissions  
107 corresponded to peak  $\text{NO}_x$  mixing ratios of 0.02 ppbv and 10 ppbv respectively, this range  
108 of  $\text{NO}_x$  mixing ratios covers the  $\text{NO}_x$  conditions found in pristine and urban conditions (von  
109 Schneidmesser et al., 2015).

110 All simulations were repeated using different chemical mechanisms to investigate whether  
111 the relationship between ozone, temperature and  $\text{NO}_x$  changes using different representations of  
112 ozone production chemistry. The reference chemical mechanism was the near-explicit Master  
113 Chemical Mechanism, MCMv3.2, (Jenkin et al., 1997, 2003; Saunders et al., 2003; Rickard  
114 et al., 2015). The reduced chemical mechanisms in our study were Common Representative  
115 Intermediates, CRIV2 (Jenkin et al., 2008), Model for OZone and Related Chemical Tracers,  
116 MOZART-4 (Emmons et al., 2010), Regional Acid Deposition Model, RADM2 (Stockwell et al.,  
117 1990) and the Carbon Bond Mechanism, CB05 (Yarwood et al., 2005). Coates and Butler (2015)  
118 described the implementation of these chemical mechanisms in MECCA. These reduced chemical  
119 mechanisms were chosen as they are commonly used by modelling groups in 3D regional and  
120 global models (Baklanov et al., 2014).

121 Model runs were repeated using a temperature-dependent and temperature-independent

Table 1: Total AVOC emissions in 2011 in tonnes from each anthropogenic source category assigned from TNO-MACC\_III emission inventory and temperature-independent BVOC emissions in tonnes from Benelux region assigned from EMEP. The allocation of these emissions to MCMv3.2, CRIV2, CB05, MOZART-4 and RADM2 species are found in the supplementary material.

Source Category	Total Emissions	Source Category	Total Emissions
Public Power	13755	Road Transport: Diesel	6727
Residential Combustion	21251	Road Transport: Others	1433
Industry	62648	Road Transport: Evaporation	2327
Fossil Fuel	15542	Non-road Transport	17158
Solvent Use	100826	Waste	1342
Road Transport: Gasoline	24921	BVOC	10702

122 source of BVOC emissions to determine the relative importance of increased emissions of BVOC  
123 and faster reaction rates of chemical processes for the increase of ozone with temperature.  
124 MEGAN2.1 (Guenther et al., 2012) specified the temperature-dependent BVOC emissions of  
125 isoprene, Sect. 2.3 provides further details. As isoprene emissions are the most important source  
126 of BVOC on the global scale (Guenther et al., 2006), we considered only isoprene emissions from  
127 vegetation. Only isoprene emissions were dependent on temperature, all other emissions were  
128 constant in all simulations. In reality, many other BVOC are emitted from varying vegetation  
129 types (Guenther et al., 2006) and increased temperature can also increase AVOC emissions  
130 through increased evaporation (Rubin et al., 2006).

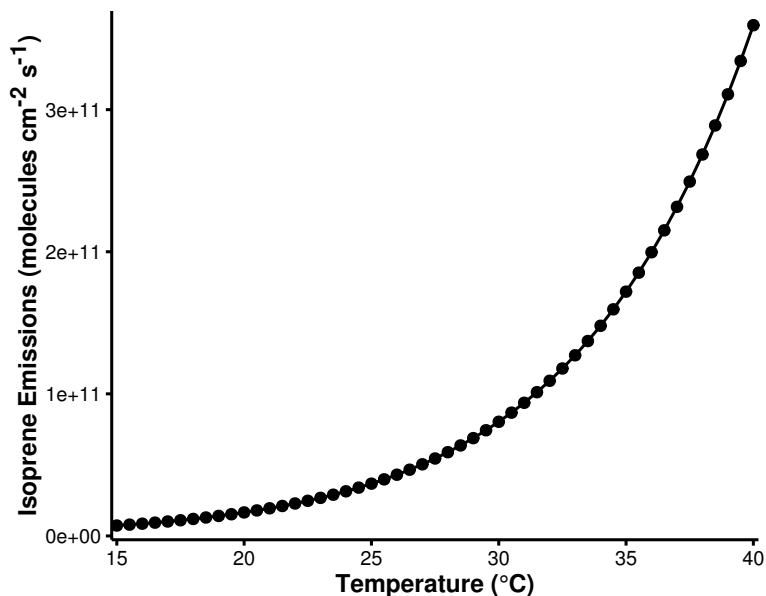
## 131 2.2 VOC Emissions

132 Emissions of urban AVOC over central Europe were taken from the TNO-MACC\_III emission  
133 inventory for the Benelux (Belgium, Netherlands and Luxembourg) region for the year 2011.  
134 TNO-MACC\_III is the updated TNO-MACC\_II emission inventory created using the same  
135 methodology as Kuenen et al. (2014) and based upon improvements to the existing emission  
136 inventory during AQMEII-2 (Pouliot et al., 2015).

137 Temperature-independent emissions of isoprene and monoterpenes from biogenic sources were  
138 calculated as a fraction of the total AVOC emissions from each country in the Benelux region.  
139 This data was obtained from the supplementary data available from the EMEP (European  
140 Monitoring and Evaluation Programme) model (Simpson et al., 2012). Temperature-dependent  
141 emissions of isoprene are described in Sect. 2.3.

142 Table 1 shows the quantity of VOC emissions from each source category and the

Figure 1: The estimated isoprene emissions (molecules isoprene  $\text{cm}^{-2} \text{s}^{-1}$ ) using MEGAN2.1 at each temperature used in the study.



143 temperature-independent BVOC emissions. These AVOC emissions were assigned to chemical  
144 species and groups based on the profiles provided by TNO. The NMVOC emissions were speciated  
145 to MCMv3.2 species as described by von Schneidmesser et al. (2016). For simulations done  
146 with other chemical mechanisms, the VOC emissions represented by the MCMv3.2 were mapped  
147 to the mechanism species representing VOC emissions in each reduced chemical mechanism  
148 based on the recommendations of the source literature and Carter (2015). The VOC emissions  
149 in the reduced chemical mechanisms were weighted by the carbon numbers of the MCMv3.2  
150 species and the emitted mechanism species, thus keeping the amount of emitted reactive carbon  
151 constant between simulations. The supplementary data outlines the primary VOC and calculated  
152 emissions with each chemical mechanism.

### 153 **2.3 Temperature Dependent Isoprene Emissions**

154 Temperature-dependent emissions of isoprene were estimated using the MEGAN2.1 algorithm  
155 for calculating the emissions of VOC from vegetation (Guenther et al., 2012). Emissions from  
156 nature are dependent on many variables including temperature, radiation and age of vegetation  
157 but for the purpose of our study all variables except temperature were held constant.

158 The MEGAN2.1 parameters were chosen to give similar isoprene mixing ratios at 20 °C to  
159 the temperature-independent emissions of isoprene in order to compare the effects of increased  
160 isoprene emissions with temperature. The estimated emissions of isoprene with MEGAN2.1

Table 2: Increase in mean ozone mixing ratio (ppbv) due to chemistry (i.e. faster reaction rates) and temperature-dependent isoprene emissions from 20 °C to 40 °C in the NO<sub>x</sub>-regimes of Fig. 3.

Chemical Mechanism	Source of Difference	Increase in Ozone from 20 °C to 40 °C (ppbv)		
		Low-NO <sub>x</sub>	Maximal-O <sub>3</sub>	High-NO <sub>x</sub>
MCMv3.2	Isoprene Emissions Chemistry	4.6	7.7	10.6
		6.8	12.5	15.2
CRIV2	Isoprene Emissions Chemistry	4.8	7.9	10.8
		6.0	11.1	13.7
MOZART-4	Isoprene Emissions Chemistry	4.1	6.7	10.0
		6.0	10.2	12.3
CB05	Isoprene Emissions Chemistry	4.6	7.4	9.8
		9.3	16.0	19.9
RADM2	Isoprene Emissions Chemistry	3.8	5.7	7.8
		8.6	14.1	17.3

161 using these assumptions are illustrated in Fig. 1 and show the expected exponential increase in  
 162 isoprene emissions with temperature (Guenther et al., 2006).

163 The estimated emissions of isoprene at 20 °C lead to 0.07 ppbv of isoprene in our simulations  
 164 while at 30 °C, the increased emissions of isoprene using MEGAN2.1 estimations lead to 0.35 ppbv  
 165 of isoprene in the model. A measurement campaign over Essen, Germany (Wagner and Kuttler,  
 166 2014) measured 0.1 ppbv of isoprene at temperature 20 °C and 0.3 ppbv of isoprene were measured  
 167 at 30 °C. The similarity of the simulated and observed isoprene mixing ratios indicates that the  
 168 MEGAN2.1 variables chosen for calculating the temperature-dependent emissions of isoprene  
 169 were suitable for simulating urban conditions over central Europe.

## 170 3 Results and Discussion

### 171 3.1 Relationship between Ozone, NO<sub>x</sub> and Temperature

172 Figure 2 depicts the peak mixing ratio from ozone of each simulation as a function of the total NO<sub>x</sub>  
 173 emissions and temperature when using a temperature-independent and temperature-dependent  
 174 source of isoprene emissions for each chemical mechanism. A non-linear relationship of ozone  
 175 mixing ratios with NO<sub>x</sub> and temperature is produced by each chemical mechanism. This  
 176 non-linear relationship is similar to that determined by Pusede et al. (2014) using an analytical  
 177 model constrained to observational measurements over the San Joaquin Valley, California.

178 Higher peak ozone mixing ratios are produced when using a temperature-dependent source  
 179 of isoprene emissions (Fig. 2). The highest mixing ratios of peak ozone are produced at high  
 180 temperatures and moderate emissions of NO<sub>x</sub> regardless of the temperature dependence of  
 181 isoprene emissions. Conversely, the least amount of peak ozone is produced with low emissions of

Figure 2: Contours of peak ozone mixing ratios (ppbv) as a function of the total  $\text{NO}_x$  emissions and temperature for each chemical mechanism using a temperature-dependent and temperature-independent source of isoprene emissions. The contours can be split into three separate regimes: High- $\text{NO}_x$ , Maximal- $\text{O}_3$  and Low- $\text{NO}_x$  indicated in the figure.

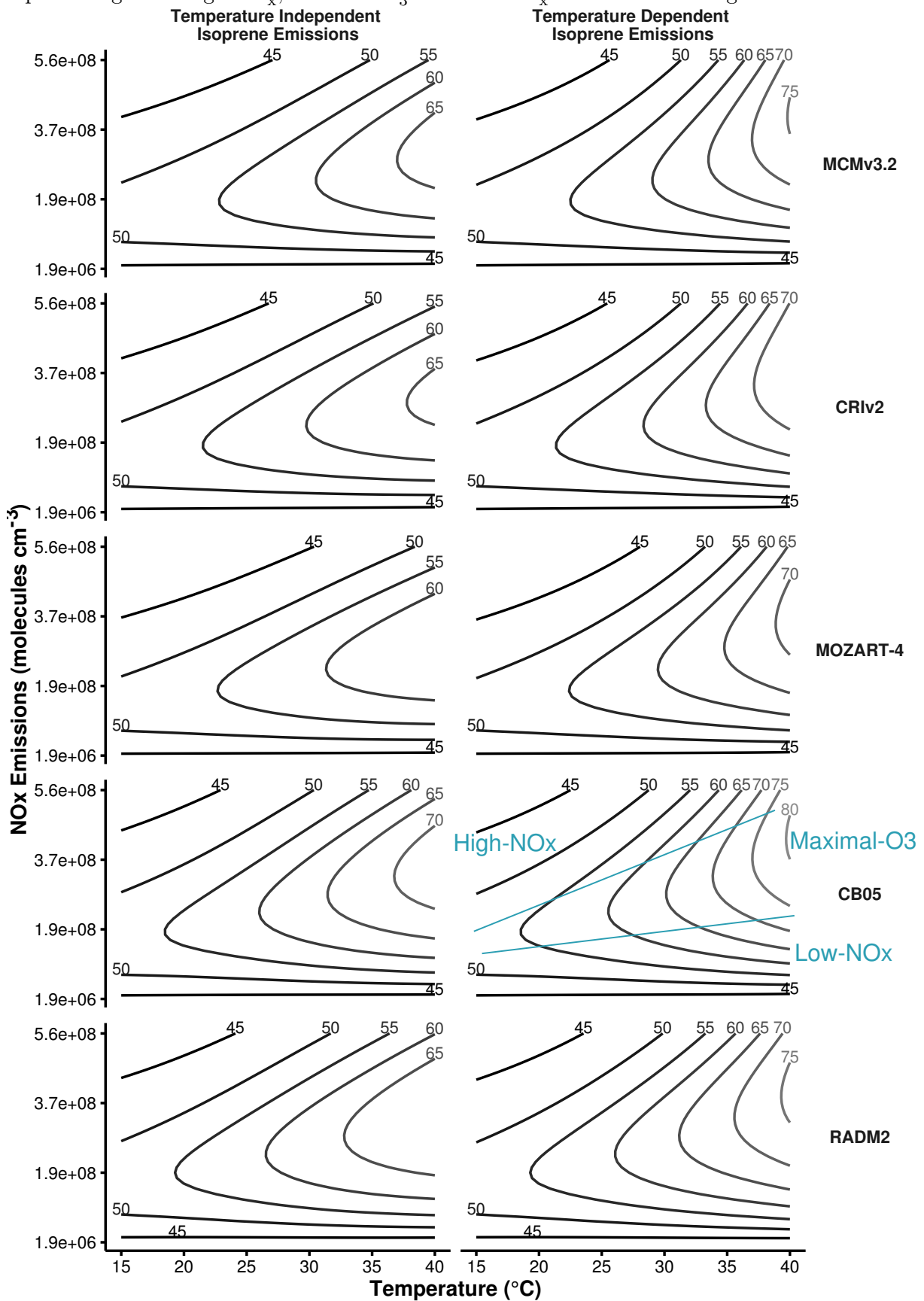
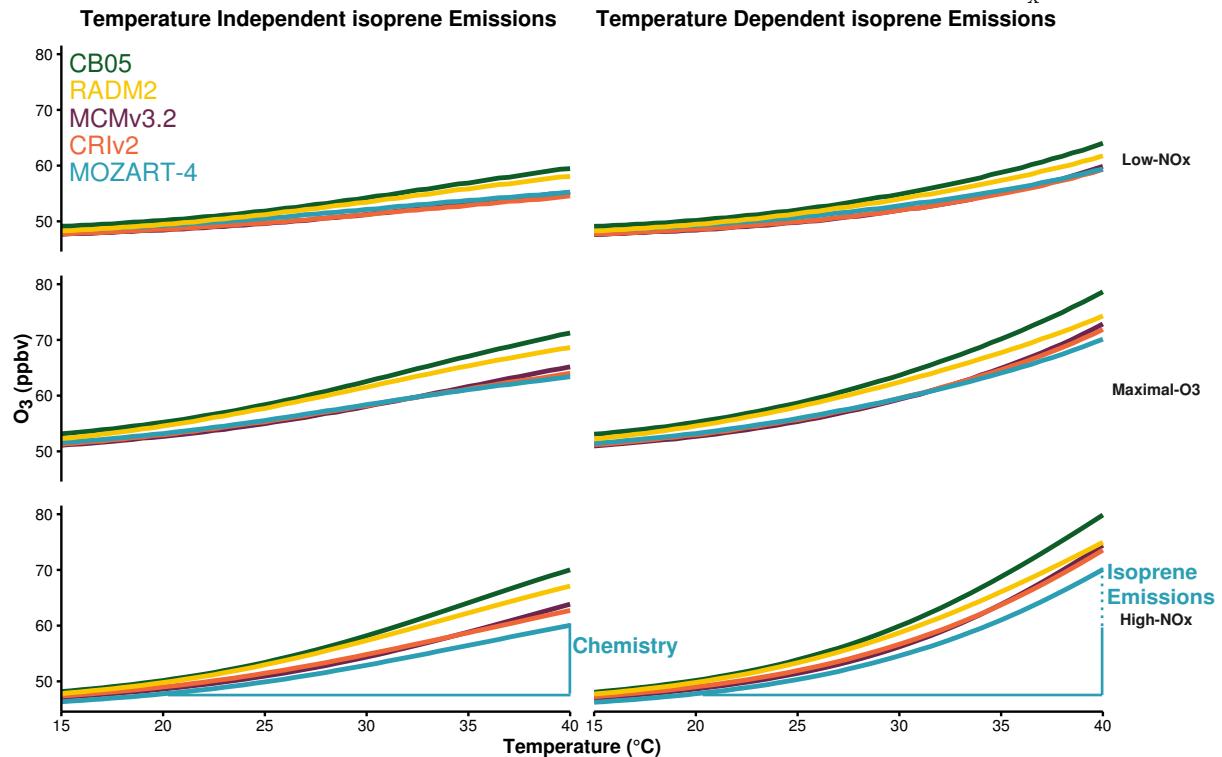


Figure 3: Mean ozone mixing ratios (ppbv) at each temperature after allocation to the different  $\text{NO}_x$ -regimes of Fig. 2. The differences in ozone mixing ratios due to chemistry (solid line) and isoprene emissions (dotted line) are represented graphically for MOZART-4 with High- $\text{NO}_x$  conditions. Table 2 details the differences for each chemical mechanism and  $\text{NO}_x$ -condition.



182  $\text{NO}_x$  over the whole temperature range (15 – 40 °C) when using both a temperature-independent  
 183 and temperature-dependent source of isoprene emissions.

184 The contours of ozone mixing ratios as a function of  $\text{NO}_x$  and temperature can be split into  
 185 three  $\text{NO}_x$  regimes (Low- $\text{NO}_x$ , Maximal- $\text{O}_3$  and High- $\text{NO}_x$ ), similar to the  $\text{NO}_x$  regimes defined  
 186 for the non-linear relationship of ozone with VOC and  $\text{NO}_x$ . The Low- $\text{NO}_x$  regime corresponds  
 187 with regions having little increase in ozone with temperature, also called the  $\text{NO}_x$ -sensitive regime.  
 188 The High- $\text{NO}_x$  (or  $\text{NO}_x$ -saturated) regime is when ozone levels increase rapidly with temperature.  
 189 The contour ridges correspond to regions of maximal ozone production; this is the Maximal- $\text{O}_3$   
 190 regime. Pusede et al. (2014) showed that temperature can be used as a proxy for VOC, thus we  
 191 assigned the ozone mixing ratios from each box model simulation to a  $\text{NO}_x$  regime based on the  
 192  $\text{H}_2\text{O}_2:\text{HNO}_3$  ratio. This ratio was used by Sillman (1995) to designate ozone to  $\text{NO}_x$  regimes  
 193 based on  $\text{NO}_x$  and VOC levels. The Low- $\text{NO}_x$  regime corresponds to  $\text{H}_2\text{O}_2:\text{HNO}_3$  ratios less  
 194 than 0.5, the High- $\text{NO}_x$  regime corresponds to ratios larger than 0.3 and ratios between 0.3 and  
 195 0.5 correspond to the Maximal- $\text{O}_3$  regime.

196 The peak ozone mixing ratio from each simulation was assigned to a  $\text{NO}_x$  regime based on the  
 197  $\text{H}_2\text{O}_2:\text{HNO}_3$  ratio of that simulation. The peak ozone mixing ratios assigned to each  $\text{NO}_x$  regime

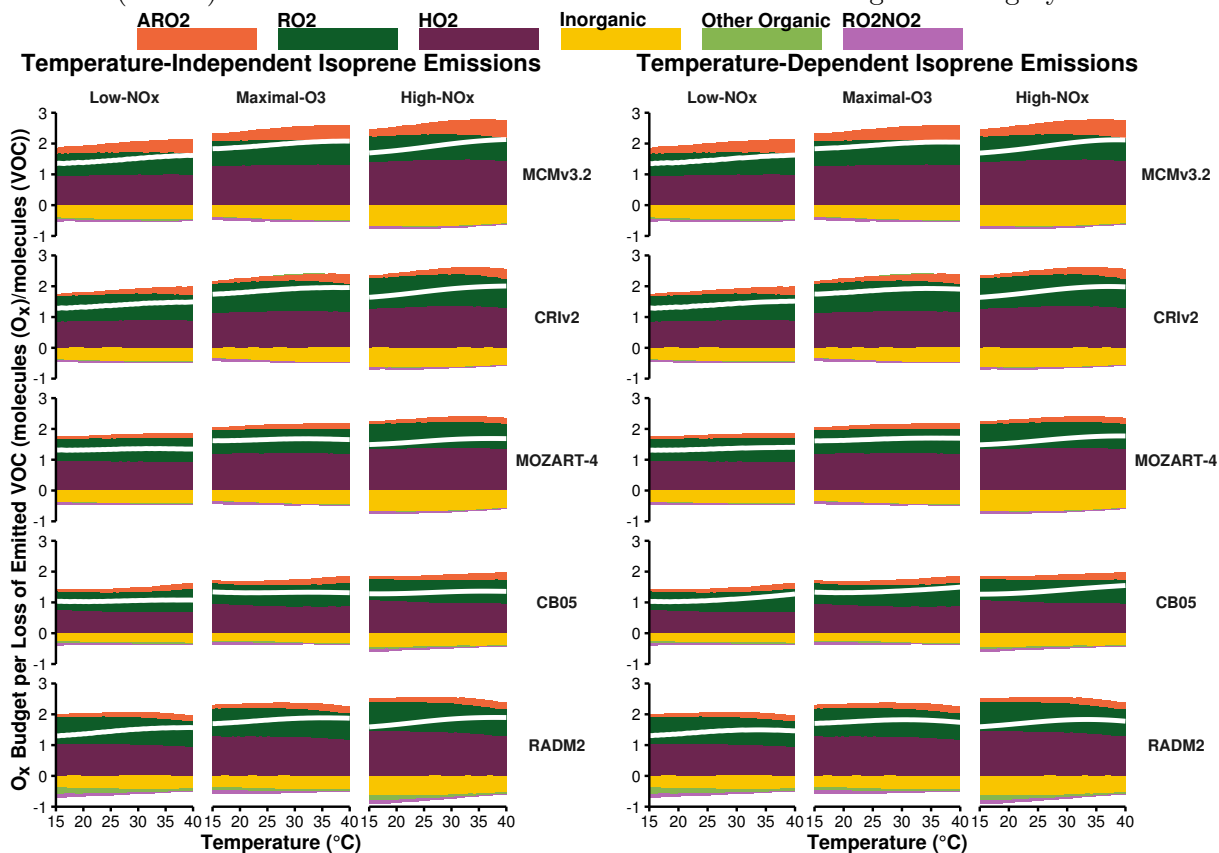
198 at each temperature were averaged, and illustrated in Fig. 3 for each chemical mechanism and each  
199 type of isoprene emissions (temperature independent and temperature dependent). We define  
200 the absolute increase in ozone from 20 °C to 40 °C due to faster reaction rates as the difference  
201 between ozone mixing ratios from 20 °C to 40 °C when using a temperature-independent source  
202 of isoprene emissions. When using a temperature-dependent source of isoprene emissions, the  
203 difference in ozone mixing ratios from 20 °C to 40 °C minus the increase due to faster reaction  
204 rates, gives the absolute increase in ozone mixing ratios from increased isoprene emissions. These  
205 differences are represented graphically in Fig. 3 and summarised in Table 2.

206 Table 2 shows that the absolute increase in ozone with temperature due to chemistry (i.e. faster  
207 reaction rates) is larger than the absolute increase in ozone due to increased isoprene emissions for  
208 each chemical mechanism and each NO<sub>x</sub> regime. In all cases the absolute increase in ozone with  
209 temperature is largest under High-NO<sub>x</sub> conditions and lowest with Low-NO<sub>x</sub> conditions (Fig. 3  
210 and Table 2). The increase in ozone mixing ratio from 20 °C to 40 °C due to faster reaction rates  
211 with High-NO<sub>x</sub> conditions is almost double that with Low-NO<sub>x</sub> conditions. In the Low-NO<sub>x</sub>  
212 regime, the increase of ozone with temperature using the reduced chemical mechanisms (CRIV2,  
213 MOZART-4, CB05 and RADM2) is similar to that from the MCMv3.2. Larger differences occur  
214 in the Maximal-O<sub>3</sub> and High-NO<sub>x</sub> regimes.

215 All reduced chemical mechanisms except RADM2 have similar increases in ozone due to  
216 increased isoprene emissions as the MCMv3.2 (Table 2). RADM2 produces 3 ppbv less ozone  
217 than the MCMv3.2 due to increased isoprene emissions in each NO<sub>x</sub> regime, indicating that this  
218 difference is due the representation of isoprene degradation chemistry in RADM2.

219 Coates and Butler (2015) compared ozone production in different chemical mechanisms to  
220 the MCMv3.2 using the TOPP metric (Tagged Ozone Production Potential) as defined in Butler  
221 et al. (2011) and showed that less ozone is produced per molecule of isoprene emitted using  
222 RADM2 than with MCMv3.2. The degradation of isoprene has been extensively studied and  
223 it is well-known that methyl vinyl ketone (MVK) and methacrolein are signatures of isoprene  
224 degradation (Atkinson, 2000). All chemical mechanisms in our study except RADM2 explicitly  
225 represent MVK and methacrolein (or in the case of CB05, a lumped species representing both  
226 these secondary degradation products). RADM2 does not represent methacrolein and the  
227 mechanism species representing ketones (KET) is a mixture of acetone and methyl ethyl ketone  
228 (MEK) (Stockwell et al., 1990). Thus the secondary degradation of isoprene in RADM2 is  
229 unable to represent the ozone production from the further degradation of the signature secondary

Figure 4: Day-time budgets of  $O_x$  normalised by the total loss rate of emitted VOC in the  $NO_x$ -regimes of Fig. 3. The white line indicates net production or consumption of  $O_x$ . The net contribution of reactions to  $O_x$  budgets are allocated to categories of inorganic reactions, peroxy nitrates (RO2NO2), reactions of NO with HO2, alkyl peroxy radicals (RO2) and acyl peroxy radicals (ARO2). All other reactions are allocated to the ‘Other Organic’ category.



230 degradation products of isoprene, MVK and methacrolein. Updated versions of RADM2, RACM  
 231 (Stockwell et al., 1997) and RACM2 (Goliff et al., 2013), sequentially included methacrolein and  
 232 MVK and with these updates the ozone production from isoprene oxidation approached that of  
 233 the MCMv3.2 (Coates and Butler, 2015).

### 234 3.2 Ozone Production and Consumption Budgets

235 In order to understand the temperature dependence of ozone production directly, we examine  
 236 the modelled day-time production and consumption budgets of  $O_x$  ( $\equiv O_3 + NO_2 + O(^1D) + O$ )  
 237 normalised by the total chemical loss rate of the emitted VOC (Fig. 4). The  $O_x$  budgets are  
 238 assigned to each  $NO_x$  regime for each chemical mechanism and type of isoprene emissions. The  
 239 budgets are allocated to the net contribution of major chemical categories, where ‘HO2’, ‘RO2’,  
 240 ‘ARO2’ represent the reactions of NO with  $HO_2$ , alkyl peroxy radicals and acyl peroxy radicals  
 241 respectively. ‘RO2NO2’ represents the net effects of peroxy nitrates, which remove  $O_x$  when  
 242 produced and are a source of  $O_x$  when they thermally decompose. ‘Inorganic’ is all other inorganic

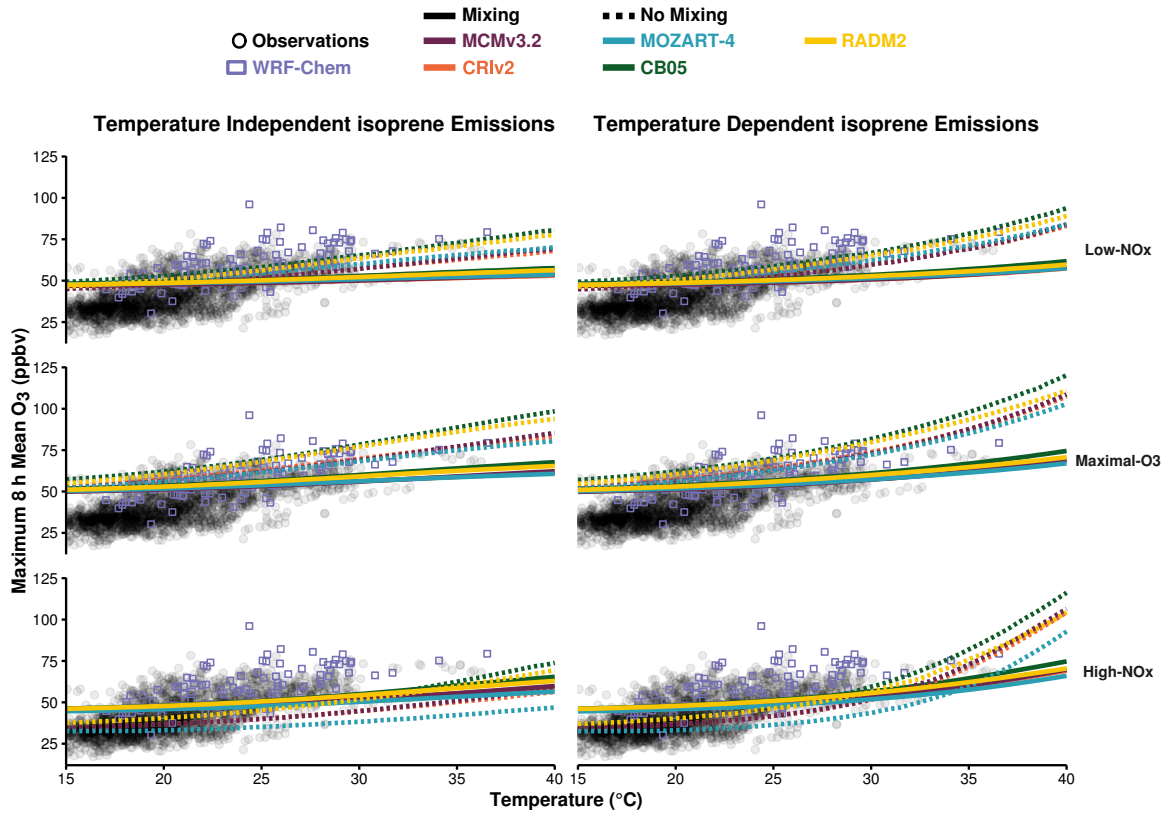
243 contributions to  $O_x$  production and any other remaining organic reactions are included in the  
244 ‘Other Organic’ category. Figure 4 also illustrates the net production or consumption of  $O_x$  in  
245 each case. The ratio of net ozone to net  $O_x$  production was practically constant with temperature  
246 in all cases showing that using  $O_x$  budgets as a proxy for ozone budgets was suitable at each  
247 temperature in our study. The absolute production and consumption budgets of  $O_x$  allocated  
248 to the same source categories as Fig. 4 are included in the supplementary material and further  
249 illustrate the increase in  $O_x$  production with temperature.

250 The net  $O_x$  production efficiency increases from 20 °C to 40 °C by  $\sim 0.25$  molecules of  $O_x$   
251 per molecule of VOC oxidised with each  $NO_x$ -condition and type of isoprene emissions using  
252 the detailed MCMv3.2 chemical mechanism (Fig. 4). A lower increase in normalised net  $O_x$   
253 production efficiency from 20 °C to 40 °C was obtained with the reduced chemical mechanisms  
254 ( $\sim 0.2$  molecules of  $O_x$  per molecule of VOC oxidised with CRIV2, CB05 and RADM2, and  
255  $\sim 0.1$  molecules of  $O_x$  per molecule of VOC oxidised using MOZART-4). The increase in net  
256  $O_x$  production efficiency is due to the increased contribution with temperature of acyl peroxy  
257 radicals (ARO2) reacting with NO and the decreased net contribution with temperature of  
258 RO2NO2 (peroxy nitrates) to the normalised  $O_x$  budgets.

259 The increased contribution of ARO2 to  $O_x$  production with temperature is linked to the  
260 decreased net contribution of RO2NO2 with temperature to  $O_x$  budgets as peroxy nitrates are  
261 produced from the reactions of acyl peroxy radicals with  $NO_2$ . The decomposition rate of peroxy  
262 nitrates is strongly temperature dependent and at higher temperatures the faster decomposition  
263 rate of  $RO_2NO_2$  leads to faster release of acyl peroxy radicals and  $NO_2$ . Thus the equilibrium  
264 of RO2NO2 shifts towards thermal decomposition with increasing temperature leading to the  
265 increased contribution of ARO2 with temperature to  $O_x$  production (Fig. 4). Dawson et al.  
266 (2007) attributed the increase in maximum 8 h ozone mixing ratios with temperature during a  
267 modelling study over the eastern US to the decrease in PAN lifetime with temperature. Steiner  
268 et al. (2006) also recognised that the decrease in PAN lifetime with temperature contributed  
269 to the increase of ozone with temperature concluding that the combined effects of increased  
270 oxidation rates of VOC and faster PAN decomposition increased the production of ozone with  
271 temperature.

272 As the production efficiency of  $O_x$  remains constant with temperature ( $\sim 2$  molecules of  $O_x$   
273 per molecule of VOC oxidised, Fig. 4), the rate of  $O_x$  production is controlled by the oxidation of  
274 VOCs. Faster oxidation of VOCs with temperature speeds up the production of peroxy radicals

Figure 5: MDA8 values of ozone from the box model simulations allocated to the different  $\text{NO}_x$  regimes for each chemical mechanism with mixing (solid lines) and without mixing (dashed lines). The box model ozone-temperature correlation is compared to the summer 2007 observational data (black circles) and WRF-Chem output (purple boxes).



275 increasing ozone production when peroxy radicals react with  $\text{NO}$  to produce  $\text{NO}_2$ . The reactivity  
 276 of VOCs has been linked to ozone production (e.g. Kleinman (2005), Sadanaga et al. (2005))  
 277 and the review of Pusede et al. (2015) acknowledged the importance of organic reactivity and  
 278 radical production to the ozone-temperature relationship. Also, the modelling study of Steiner  
 279 et al. (2006) noted that the increase in initial oxidation rates of VOCs with temperature leads to  
 280 increased formaldehyde concentrations and in turn an increase of ozone as formaldehyde is an  
 281 important source of  $\text{HO}_2$  radicals.

### 282 3.3 Comparison to Observations and 3D Model Simulations

283 This section compares the results from our idealised box model simulations to real-world  
 284 observations and model output from a 3D model. Using the interpolated observations of  
 285 the maximum daily 8 h mean (MDA8) of ozone from Schnell et al. (2015) and the meteorological  
 286 observational data set of the ERA-Interim re-analysis, Otero et al. (2016) showed that over the  
 287 summer (JJA) months, temperature is the main meteorological driver of ozone production over  
 288 many regions of central Europe. Model output from the 3D WRF-Chem regional model using

Table 3: Slopes ( $m_{O_3-T}$ , ppbv per  $^{\circ}C$ ) of the linear fit to MDA8 values of ozone and temperature correlations in Fig. 5, indicating the increase of MDA8 in ppbv of ozone per  $^{\circ}C$ . The slope of the observational data is 2.15 ppbv/ $^{\circ}C$  and the slope of the WRF-Chem output is 2.05 ppbv/ $^{\circ}C$ .

Mechanism	Isoprene Emissions	Low-NO <sub>x</sub>		Maximal-O <sub>3</sub>		High-NO <sub>x</sub>	
		Mixing	No Mixing	Mixing	No Mixing	Mixing	No Mixing
MCMv3.2	Temperature Independent	0.28	1.01	0.51	1.36	0.59	0.96
	Temperature Dependent	0.42	1.48	0.74	2.16	0.93	2.63
CRIV2	Temperature Independent	0.25	0.93	0.47	1.27	0.55	0.88
	Temperature Dependent	0.40	1.44	0.71	2.09	0.90	2.52
MOZART-4	Temperature Independent	0.25	0.97	0.44	1.21	0.49	0.59
	Temperature Dependent	0.38	1.43	0.65	1.98	0.81	2.05
CB05	Temperature Independent	0.39	1.30	0.67	1.72	0.79	1.45
	Temperature Dependent	0.52	1.72	0.89	2.44	1.12	2.94
RADM2	Temperature Independent	0.37	1.31	0.61	1.64	0.70	1.28
	Temperature Dependent	0.48	1.68	0.79	2.22	0.97	2.49

289 MOZART-4 chemistry set-up over the European domain for simulations of the year 2007 from  
 290 Mar et al. (2016) was used to further compare the box model simulations to a model including  
 291 more meteorological processes than our box model.

292 Figure 5 compares the observational and WRF-Chem data from summer 2007 averaged over  
 293 central and eastern Germany, where summertime ozone values are driven by temperature (Otero  
 294 et al., 2016), to the MDA8 values of ozone from the box model simulations for each chemical  
 295 mechanism (solid lines). Despite a high bias in simulated ozone in WRF-Chem, the rate of change  
 296 of ozone with temperature from the WRF-Chem simulations (2.05 ppbv/ $^{\circ}C$ ) is similar to the  
 297 rate of change of ozone with temperature from the observed data (2.15 ppbv/ $^{\circ}C$ ). The differences  
 298 in ozone production between the different chemical mechanisms with the box model are small  
 299 compared to the spread of the observational and WRF-Chem data. A temperature-dependent  
 300 source of isoprene with high-NO<sub>x</sub> conditions produces the highest ozone-temperature slope, but  
 301 is still lower than the observed ozone-temperature slope by a factor of two. In particular, the  
 302 box model simulations over-predict the ozone values at lower temperatures and under-predict  
 303 the ozone values at higher temperatures compared to the observed data.

304 In our simulations, we focused on instantaneous production of ozone from a freshly-emitted  
 305 source of VOC with mixing of clean air from the free troposphere due to a growing boundary  
 306 layer. This box model setup did not consider stagnant atmospheric conditions characterized by  
 307 low wind speeds slowing the transport of ozone and its precursors away from sources. Stagnant  
 308 conditions have been correlated to high-ozone episodes in the summer over eastern US (Jacob  
 309 et al., 1993).

310 In order to investigate the sensitivity of ozone production to mixing, box model simulations

311 were performed without vertical mixing to approximate stagnant conditions that favour  
312 accumulation of secondary VOC oxidation products. The ozone-temperature relationship obtained  
313 with each chemical mechanism, using both a temperature-independent and temperature-dependent  
314 source of isoprene emissions and the different  $\text{NO}_x$  conditions are displayed in Fig. 5 (dotted  
315 lines). Table 3 summarises the slopes ( $m_{\text{O}_3\text{-T}}$ ) of the linear fits of the box model simulations  
316 displayed in Fig. 5 in ppbv of ozone per  $^\circ\text{C}$  determining the rate of increase of ozone with  
317 temperature, for both case: with, and without mixing.

318 For all chemical mechanisms, the rate of increase of ozone with temperature increased in the  
319 box model simulations without mixing. The  $m_{\text{O}_3\text{-T}}$  calculated from the box model simulations  
320 without mixing using a temperature-dependent source of isoprene and with Maximal- $\text{O}_3$  conditions  
321 (ranging between 2.0 and 2.4 ppbv/ $^\circ\text{C}$ ) are very similar to the slopes of the observational and  
322 WRF-Chem results (2.1 and 2.2 ppbv/ $^\circ\text{C}$ , respectively). The differences in  $m_{\text{O}_3\text{-T}}$  when not  
323 including mixing in the box model compared to the differences in  $m_{\text{O}_3\text{-T}}$  between chemical  
324 mechanisms in Table 3 show that the ozone-temperature relationship using our box model setup  
325 is more sensitive to mixing than the choice of chemical mechanism.

326 An analysis similar to that presented in Fig. 4 shows no appreciable difference between the  
327 cases with and without mixing (not shown). The chemical production of  $\text{O}_x$  in each chemical  
328 mechanism normalised by the chemical loss rate of VOC remains unchanged. Furthermore,  
329 the supplementary material includes the absolute production and consumption budgets of  $\text{O}_x$   
330 which also show the increased  $\text{O}_x$  production with temperature for the simulations performed  
331 without mixing. From this we conclude that the increased ozone production seen in the box  
332 model simulations with reduced mixing is due to enhanced OH reactivity from secondary VOC  
333 oxidation products.

## 334 4 Conclusions

335 In this study, we determined the effects of temperature on ozone production using a box  
336 model over a range of temperatures and  $\text{NO}_x$  conditions with a temperature-independent and  
337 temperature-dependent source of isoprene emissions. These simulations were repeated using  
338 reduced chemical mechanism schemes (CRIV2, MOZART-4, CB05 and RADM2) typically used  
339 in 3D models and compared to the near-explicit MCMv3.2 chemical mechanism.

340 Each chemical mechanism produced a non-linear relationship of ozone with temperature

341 and  $\text{NO}_x$  with the most ozone produced at high temperatures and moderate emissions of  $\text{NO}_x$ .  
342 Conversely, lower  $\text{NO}_x$  levels led to a minimal increase of ozone with temperature. Thus air  
343 quality in a future with higher temperatures would benefit from reductions in  $\text{NO}_x$  emissions.

344 Faster reaction rates at higher temperatures were responsible for a greater absolute increase  
345 in ozone than increased isoprene emissions. In our simulations, ozone production was controlled  
346 by the increased rate of VOC oxidation with temperature. The net influence of peroxy nitrates  
347 increased the net production of  $\text{O}_x$  per molecule of emitted VOC oxidised with temperature.

348 The rate of increase of ozone with temperature using observational data over Europe was  
349 twice as high as the rate of increase of ozone with temperature when using the box model.  
350 This was consistent with our box model setup not representing stagnant atmospheric conditions  
351 that are inherently included in observational data and models including meteorology, such as  
352 WRF-Chem. In model simulations without mixing the rate of increase of ozone with temperature  
353 was faster than the simulations including mixing. The simulations without mixing and a maximal  
354 ozone production chemical regime led to very similar rates of increase of ozone with temperature  
355 to the observational and WRF-Chem data. Furthermore, the ozone-temperature relationship  
356 was more sensitive to mixing than the choice of chemical mechanism.

## 357 **Acknowledgements**

358 The authors would like to thank Noelia Otero Felipe for providing the ERA-Interim data.

## 359 **References**

360 R. Atkinson. Atmospheric chemistry of VOCs and  $\text{NO}_x$ . *Atmospheric Environment*, 34(12-14):  
361 2063–2101, 2000.

362 A. Baklanov, K. Schlünzen, P. Suppan, J. Baldasano, D. Brunner, S. Aksoyoglu, G. Carmichael,  
363 J. Douros, J. Flemming, R. Forkel, S. Galmarini, M. Gauss, G. Grell, M. Hirtl, S. Joffre, O. Jorba,  
364 E. Kaas, M. Kaasik, G. Kallos, X. Kong, U. Korsholm, A. Kurganskiy, J. Kushta, U. Lohmann,  
365 A. Mahura, A. Manders-Groot, A. Maurizi, N. Moussiopoulos, S. T. Rao, N. Savage, C. Seigneur,  
366 R. S. Sokhi, E. Solazzo, S. Solomos, B. Sørensen, G. Tsegas, E. Vignati, B. Vogel, and Y. Zhang.  
367 Online coupled regional meteorology chemistry models in Europe: current status and prospects.  
368 *Atmospheric Chemistry and Physics*, 14(1):317–398, 2014.

369 T. Butler, M. Lawrence, D. Taraborrelli, and J. Lelieveld. Multi-day ozone production potential  
370 of volatile organic compounds calculated with a tagging approach. *Atmospheric Environment*, 45  
371 (24):4082 – 4090, 2011.

372 W. P. L. Carter. Development of a Database for Chemical Mechanism Assignments for Volatile  
373 Organic Emissions. *Journal of the Air & Waste Management Association*, 0, 2015.

374 W. P. L. Carter, A. M. Winer, K. R. Darnall, and J. N. P. Jr. Smog chamber studies of temperature  
375 effects in photochemical smog. *Environmental Science & Technology*, 13(9):1094–1100, 1979.

376 J. Coates and T. M. Butler. A comparison of chemical mechanisms using tagged ozone production  
377 potential (TOPP) analysis. *Atmospheric Chemistry and Physics*, 15(15):8795–8808, 2015.

378 J. P. Dawson, P. J. Adams, and S. N. Pandis. Sensitivity of ozone to summertime climate in the  
379 eastern USA: A modeling case study . *Atmospheric Environment*, 41(7):1494 – 1511, 2007.

380 K. M. Emmerson and M. J. Evans. Comparison of tropospheric gas-phase chemistry schemes for  
381 use within global models. *Atmospheric Chemistry and Physics*, 9(5):1831–1845, 2009.

382 L. K. Emmons, S. Walters, P. G. Hess, J.-F. Lamarque, G. G. Pfister, D. Fillmore, C. Granier,  
383 A. Guenther, D. Kinnison, T. Laepple, J. Orlando, X. Tie, G. Tyndall, C. Wiedinmyer, S. L.  
384 Baughcum, and S. Kloster. Description and evaluation of the Model for Ozone and Related  
385 chemical Tracers, version 4 (MOZART-4). *Geoscientific Model Development*, 3(1):43–67, 2010.

386 W. S. Goliff, W. R. Stockwell, and C. V. Lawson. The regional atmospheric chemistry mechanism,  
387 version 2. *Atmospheric Environment*, 68:174 – 185, 2013.

388 A. Guenther, T. Karl, P. Harley, C. Wiedinmyer, P. I. Palmer, and C. Geron. Estimates of global  
389 terrestrial isoprene emissions using MEGAN (Model of Emissions of Gases and Aerosols from  
390 Nature). *Atmospheric Chemistry and Physics*, 6(11):3181–3210, 2006.

391 A. B. Guenther, X. Jiang, C. L. Heald, T. Sakulyanontvittaya, T. Duhl, L. K. Emmons, and  
392 X. Wang. The Model of Emissions of Gases and Aerosols from Nature version 2.1 (MEGAN2.1):  
393 an extended and updated framework for modeling biogenic emissions. *Geoscientific Model  
394 Development*, 5(6):1471–1492, 2012.

395 S. Hatakeyama, H. Akimoto, and N. Washida. Effect of temperature on the formation of  
396 photochemical ozone in a propene-nitrogen oxide (NO<sub>x</sub>)-air-irradiation system. *Environmental  
397 Science & Technology*, 25(11):1884–1890, 1991.

398 D. J. Jacob and D. A. Winner. Effect of climate change on air quality. *Atmospheric Environment*,  
399 43(1):51 – 63, 2009. Atmospheric Environment - Fifty Years of Endeavour.

400 D. J. Jacob, J. A. Logan, G. M. Gardner, R. M. Yevich, C. M. Spivakovsky, S. C. Wofsy,  
401 S. Sillman, and M. J. Prather. Factors regulating ozone over the United States and its export to  
402 the global atmosphere. *Journal of Geophysical Research*, 98(D8), 1993.

403 M. Jenkin, L. Watson, S. Utembe, and D. Shallcross. A Common Representative Intermediates  
404 (CRI) mechanism for VOC degradation. Part 1: Gas phase mechanism development. *Atmospheric*  
405 *Environment*, 42(31):7185 – 7195, 2008.

406 M. E. Jenkin, S. M. Saunders, and M. J. Pilling. The tropospheric degradation of volatile organic  
407 compounds: a protocol for mechanism development. *Atmospheric Environment*, 31(1):81 – 104,  
408 1997.

409 M. E. Jenkin, S. M. Saunders, V. Wagner, and M. J. Pilling. Protocol for the development of the  
410 Master Chemical Mechanism, MCM v3 (Part B): tropospheric degradation of aromatic volatile  
411 organic compounds. *Atmospheric Chemistry and Physics*, 3(1):181–193, 2003.

412 T. R. Karl and K. E. Trenberth. Modern global climate change. *Science*, 302(5651):1719–1723,  
413 2003.

414 L. I. Kleinman. The dependence of tropospheric ozone production rate on ozone precursors.  
415 *Atmospheric Environment*, 39(3):575 – 586, 2005.

416 J. J. P. Kuenen, A. J. H. Visschedijk, M. Jozwicka, and H. A. C. Denier van der Gon.  
417 TNO-MACC\_II emission inventory; a multi-year (2003–2009) consistent high-resolution european  
418 emission inventory for air quality modelling. *Atmospheric Chemistry and Physics*, 14(20):  
419 10963–10976, 2014.

420 K. A. Mar, N. Ojha, A. Pozzer, and T. M. Butler. WRF-Chem Simulations over Europe: Model  
421 Evaluation and Chemical Mechanism Comparison. *In Preparation*, 2016.

422 R. Mészáros, I. G. Zsély, D. Szinyei, C. Vincze, and I. Lagzi. Sensitivity analysis of an ozone  
423 deposition model. *Atmospheric Environment*, 43(3):663 – 672, 2009.

424 N. Otero, J. Sillmann, J. L. Schnell, H. W. Rust, and T. Butler. Synoptic and meteorological  
425 drivers of extreme ozone concentrations over europe. *Environmental Research Letters*, 11(2):  
426 024005, 2016.

427 N. Passant. Speciation of UK emissions of non-methane volatile organic compounds. Technical  
428 report, DEFRA, Oxon, UK., 2002.

429 G. Pouliot, H. A. D. van der Gon, J. Kuenen, J. Zhang, M. D. Moran, and P. A. Makar. Analysis  
430 of the emission inventories and model-ready emission datasets of Europe and North America for  
431 phase 2 of the AQMEII project. *Atmospheric Environment*, 115:345–360, 2015.

432 S. E. Pusede, D. R. Gentner, P. J. Wooldridge, E. C. Browne, A. W. Rollins, K.-E. Min, A. R.  
433 Russell, J. Thomas, L. Zhang, W. H. Brune, S. B. Henry, J. P. DiGangi, F. N. Keutsch, S. A.  
434 Harrold, J. A. Thornton, M. R. Beaver, J. M. St. Clair, P. O. Wennberg, J. Sanders, X. Ren,  
435 T. C. VandenBoer, M. Z. Markovic, A. Guha, R. Weber, A. H. Goldstein, and R. C. Cohen.  
436 On the temperature dependence of organic reactivity, nitrogen oxides, ozone production, and  
437 the impact of emission controls in San Joaquin Valley, California. *Atmospheric Chemistry and*  
438 *Physics*, 14(7):3373–3395, 2014.

439 S. E. Pusede, A. L. Steiner, and R. C. Cohen. Temperature and Recent Trends in the Chemistry  
440 of Continental Surface Ozone. *Chemical Reviews*, 115(10):3898–3918, 2015.

441 D. J. Rasmussen, J. Hu, A. Mahmud, and M. J. Kleeman. The ozone–climate penalty: Past,  
442 present, and future. *Environmental Science & Technology*, 47(24):14258–14266, 2013. PMID:  
443 24187951.

444 A. Rickard, J. Young, M. J. Pilling, M. E. Jenkin, S. Pascoe, and S. M. Saunders. The Master  
445 Chemical Mechanism Version MCM v3.2. <http://mcm.leeds.ac.uk/MCMv3.2/>, 2015. [Online;  
446 accessed 25-March-2015].

447 J. I. Rubin, A. J. Kean, R. A. Harley, D. B. Millet, and A. H. Goldstein. Temperature dependence  
448 of volatile organic compound evaporative emissions from motor vehicles. *Journal of Geophysical*  
449 *Research: Atmospheres*, 111(D3), 2006. D03305.

450 Y. Sadanaga, A. Yoshino, S. Kato, , and Y. Kajii. Measurements of oh reactivity and  
451 photochemical ozone production in the urban atmosphere. *Environmental Science & Technology*,  
452 39(22):8847–8852, 2005. PMID: 16323785.

453 R. Sander, A. Kerkweg, P. Jöckel, and J. Lelieveld. Technical note: The new comprehensive  
454 atmospheric chemistry module mecca. *Atmospheric Chemistry and Physics*, 5(2):445–450, 2005.

455 S. M. Saunders, M. E. Jenkin, R. G. Derwent, and M. J. Pilling. Protocol for the development of  
456 the Master Chemical Mechanism, MCM v3 (Part A): tropospheric degradation of non-aromatic  
457 volatile organic compounds. *Atmospheric Chemistry and Physics*, 3(1):161–180, 2003.

458 J. L. Schnell, M. J. Prather, B. Josse, V. Naik, L. W. Horowitz, P. Cameron-Smith, D. Bergmann,  
459 G. Zeng, D. A. Plummer, K. Sudo, T. Nagashima, D. T. Shindell, G. Faluvegi, and S. A. Strode.  
460 Use of north american and european air quality networks to evaluate global chemistry–climate  
461 modeling of surface ozone. *Atmospheric Chemistry and Physics*, 15(18):10581–10596, 2015.

462 S. Sillman. The use of NO<sub>y</sub>, H<sub>2</sub>O<sub>2</sub>, and HNO<sub>3</sub> as indicators for ozone-NO<sub>x</sub>-hydrocarbon sensitivity  
463 in urban locations. *Journal of Geophysical Research: Atmospheres*, 100(D7):14175–14188, 1995.

464 S. Sillman. The relation between ozone, NO<sub>x</sub> and hydrocarbons in urban and polluted rural  
465 environments. *Atmospheric Environment*, 33(12):1821 – 1845, 1999.

466 S. Sillman and P. J. Samson. Impact of temperature on oxidant photochemistry in urban,  
467 polluted rural and remote environments. *Journal of Geophysical Research: Atmospheres*, 100  
468 (D6):11497–11508, 1995.

469 D. Simpson, A. Benedictow, H. Berge, R. Bergström, L. D. Emberson, H. Fagerli, C. R. Flechard,  
470 G. D. Hayman, M. Gauss, J. E. Jonson, M. E. Jenkin, A. Nyíri, C. Richter, V. S. Semeena,  
471 S. Tsyro, J.-P. Tuovinen, Á. Valdebenito, and P. Wind. The EMEP MSC-W chemical transport  
472 model – technical description. *Atmospheric Chemistry and Physics*, 12(16):7825–7865, 2012.

473 A. L. Steiner, S. Tonse, R. C. Cohen, A. H. Goldstein, and R. A. Harley. Influence of future  
474 climate and emissions on regional air quality in California. *Journal of Geophysical Research:*  
475 *Atmospheres*, 111(D18), 2006. D18303.

476 W. R. Stockwell, P. Middleton, J. S. Chang, and X. Tang. The second generation regional acid  
477 deposition model chemical mechanism for regional air quality modeling. *Journal of Geophysical*  
478 *Research: Atmospheres*, 95(D10):16343–16367, 1990.

479 W. R. Stockwell, F. Kirchner, M. Kuhn, and S. Seefeld. A new mechanism for regional atmospheric  
480 chemistry modeling. *Journal of Geophysical Research: Atmospheres*, 102(D22):25847–25879,  
481 1997.

482 E. von Schneidmesser, P. S. Monks, J. D. Allan, L. Bruhwiler, P. Forster, D. Fowler, A. Lauer,

483 W. T. Morgan, P. Paasonen, M. Righi, K. Sindelarova, and M. A. Sutton. Chemistry and the  
484 Linkages between Air Quality and Climate Change. *Chemical Reviews*, 2015. PMID: 25926133.

485 E. von Schneidmesser, J. Coates, A. J. H. Visschedijk, H. A. C. Denier van der Gon, and T. M.  
486 Butler. Variation of the NMVOC speciation in the solvent sector and the sensitivity of modelled  
487 tropospheric ozone. *Atmospheric Environment*, Submitted for Publication, 2016.

488 P. Wagner and W. Kuttler. Biogenic and anthropogenic isoprene in the near-surface urban  
489 atmosphere — A case study in Essen, Germany. *Science of The Total Environment*, 475:104 –  
490 115, 2014.

491 G. Yarwood, S. Rao, M. Yocke, and G. Z. Whitten. Updates to the Carbon Bond Chemical  
492 Mechanism: CB05. Technical report, U. S Environmental Protection Agency, 2005.

1 The Influence of Temperature on Ozone Production under  
2 varying NO<sub>x</sub> Conditions – a modelling study: Supplementary  
3 Material

4 J. Coates<sup>1</sup>, K. Mar<sup>1</sup>, N. Ojha<sup>2</sup> and T. Butler<sup>1</sup>

5 <sup>1</sup>Institute for Advanced Sustainability Studies, Potsdam, Germany

6 <sup>2</sup>Atmospheric Chemistry Department, Max Planck Institute for Chemistry, Mainz,  
7 Germany

8 March 24, 2016

9 **S1 Vertical Mixing with Diurnal Boundary Layer Height**

10 The MECCA box model used in Coates and Butler (2015) included a constant boundary layer  
11 height of 1 km and no interactions (vertical mixing) with the free troposphere. In reality,  
12 the planetary boundary layer (PBL) height varies diurnally and affects chemistry by diluting  
13 emissions after sunrise when the PBL rises.

14 The evolution of the PBL leads to vertical mixing of the near surface air with the free  
15 tropospheric air mass. When the PBL collapses in the evening, pollutants are trapped in the  
16 PBL. The mixing layer height was measured as part of the BAERLIN campaign (Bonn et al.,  
17 2016) over Berlin, Germany. The profile of mean mixing layer height during the campaign period  
18 (June – August 2014) was used in the box model to represent the diurnal cycle of the mixing layer  
19 height. We implemented the vertical mixing scheme into the boxmodel following the approach of  
20 Lourens et al. (2016).

21 The mixing ratios of O<sub>3</sub>, CO and CH<sub>4</sub> in the free troposphere were respectively set to  
22 50 ppbv, 116 ppbv and 1.8 ppmv. These conditions were taken from the MATCH-MPIC chemical  
23 weather forecast model on the 21st March (the start date of the simulations). The model results  
24 (<http://cwf.iass-potsdam.de/>) at the 700 hPa height were chosen and the daily average was

25 used as input into the boxmodel.

## 26 **S2 Allocation of Benelux AVOC emissions to Mechanism** 27 **Species**

28 Anthropogenic NMVOC emissions over Benelux specified by the TNO\_MACCIII emission  
29 inventory (Kuenen et al., 2014) were translated to MCM v3.2 emissions (Table S1). The  
30 MCM v3.2 emissions for each initial species were translated to emissions of mechanism species  
31 into CRI v2, MOZART-4 and RADM2 chemical mechanisms by weighting with the carbon  
32 numbers (Tables S2 – S4). The allocation of MCM v3.2 emissions into CB05 species followed the  
33 recommendations of Yarwood et al. (2005) (Table S5).

Table S1: Speciated TNO\_MACCIII emissions for Benelux AVOC and BVOC emissions (molecules  $\text{cm}^{-2} \text{s}^{-1}$ ) mapped to MCM v3.2 species (Kuenen et al., 2014).

Type	MCM_Species	SNAP.1	SNAP.2	SNAP.34	SNAP.5	SNAP.6	SNAP.71	SNAP.72	SNAP.73	SNAP.74	SNAP.8	SNAP.9	BVOC	Total
Ethane	C2H6	9.85e+08	1668300000	9.18e+09			9.67e+08	2.96e+08	63860000		3.45e+08	210200000		1.3728e+10
	C3H8	2.886e+09	1086600000	2.573e+09	1.041e+11	9.72e+08	47090000	202400000	638600000	62710000	249700000	75200000		1.129e+11
Propane	NC4H10	2.127e+09	882870000	949270000	6.11e+11	3.61e+09	1.048e+09	2095000000		1037800000	315300000	42200000		6.21e+11
	IC4H10	258600000	309660000	232311000	1.486e+11	163700000	489100000	97500000		483900000	157900000	42200000		1.509e+11
Pentanes	NC5H12	1.783e+09	1014860000		4.548e+11		6.27e+08	8.4e+07		521500000	118200000	14890000		4.589e+11
	IC5H12	7.52e+08	544340000		2.718e+11		1.216e+09	163500000		1011700000	225600000	14890000		2.762e+11
NEOP	NEOP										14890000			14890000
	NC6H14	954100000	57390000	1.211e+09	6.49e+10	3.162e+09	2.207e+09	1.246e+09		193450000	4.26e+08	5160000		7.44e+10
M2PE	M2PE			156600000	9.98e+09	6.66e+08					7.08e+08	2215000		1.151e+10
	M3PE			117100000	4.989e+09	6.66e+08					4.26e+08			6.2e+09
NC7H16	NC7H16	409520000	98740000	5.71e+08	6.97e+10	1.146e+09	363500000	205300000		31790000	121900000	26040000		7.28e+10
	M2HEX					4.3e+08	2.83e+08	159500000		24710000	182900000			1.08e+09
M3HEX	M3HEX					4.3e+08	2.02e+08	1.14e+08		17634000	121900000			8.86e+08
	M22C4										141800000			141800000
M23C4	M23C4										141800000			141800000
	NC8H18			235300000	5.18e+10	1.25600000	319500000	179700000		27890000	6.95e+08	8900000		5.33e+10
NC9H20	NC9H20			131200000		3.02e+09						2969000		3.148e+09
	NC10H22			1.66e+08		5.85e+09	142200000	80300000		12458000		4460000		6.25e+09
NC11H24	NC11H24			64600000		2.387e+09	51830000	29280000		4536000	78100000	1625000		2.617e+09
	NC12H26					168500000	8.45e+08	476900000		74100000	71700000	1506000		1.637e+09
CHEX	CHEX			91490000	4e+07	6.82e+08								8.15e+08
	C2H4	212300000	3695700000	3.368e+10			5.341e+09	3.807e+09	342500000		4.62e+09	1.9e+08		5.188e+10
Propene	C3H6	141700000	868200000	6.59e+08			1.876e+09	634800000	151810000		7.86e+08	54500000		5.18e+09
	HEX1ENE	21050000	15773000									21810000		58703000
BUT1ENE	BUT1ENE		22154000	240400000							24510000			286604000
	MEPROPENE										12260000			12260000
TBUT2ENE	TBUT2ENE										12260000			12260000
	CBUT2ENE										12260000			12260000
CPENT2ENE	CPENT2ENE		6961000								4902000			11861000
	TPENT2ENE		6961000								4902000			11861000
PENTIENE	PENTIENE		6328000	6186000							19630000			32171000
	ME2BUT2ENE		3793000								9800000			13581000
ME3BUT1ENE	ME3BUT1ENE		3793000								9800000			13581000
	ME2BUT1ENE		2525500								9800000			2525500
Ethyne	C2H2	2697000	1252200000	426600000			4.975e+09	1.795e+09	134690000	252500000	1.614e+09	71500000		1.051e+10
	BENZENE	269600000	1.006e+09	8.3e+08	1.621e+10		1.197e+09	228300000		35380000	2.83e+08	36540000		2.014e+10

Table S1: Speciated TNO\_MACCIII emissions for Benelux AVOC and BVOC emissions (molecules  $\text{cm}^{-2} \text{s}^{-1}$ ) mapped to MCM v3.2 species (Kuenen et al., 2014).

Type	MCM_Species	SNAP.1	SNAP.2	SNAP.34	SNAP.5	SNAP.6	SNAP.71	SNAP.72	SNAP.73	SNAP.74	SNAP.8	SNAP.9	BVOC	Total
Toluene	TOLUENE	252700000	372760000	84400000	1.375e+10	6.8e+09	2.708e+09	1.45e+08	300300000	193900000	24100000	2.435e+10		2.435e+10
	MXYL	1.05e+08	21179000	1669300	1.994e+09	3.93e+09	5.77e+08	61040000	4735000	70200000	4880000	6.78e+09		6.78e+09
	OXYL	233300000	21179000	669700	1.994e+09	9.84e+08	5.77e+08	61040000	4735000	57100000	2924000	3.717e+09		3.717e+09
Xylenes	PXYL	21179000	21179000	669700	1.994e+09	9.84e+08	432900000	45800000	3551000	70200000	3909000	3.556e+09		3.556e+09
	TM123B	18550	1304500		6.6e+07		992000000		3330000	441000	170200000			170200000
Trimethylbenzenes	TM124B	18550	1304500	56100000	224600000	4.16e+08			7760000	589000	7.06e+08			7.06e+08
	TM135B	18550	1304500		6.6e+07		158600000		3330000	589000	229900000			229900000
	EBENZ	35100000		63400000	179400000	430600000	341600000	119530	8e+08	5250000	1.856e+09			1.856e+09
Other Aromatics	PBENZ				39600000	380600000	301500000	105570	128500000	2311000	8.53e+08			8.53e+08
	IPBENZ				145300000				128500000	2311000	276300000			276300000
	PETHTOL				13210000				257500000		270300000			270300000
	METHTOL				39600000				257500000		296300000			296300000
	OETHTOL								192800000		192800000			192800000
	DIET35TOL						8.05e+08	637600000	223800		1.443e+09			1.443e+09
	DIME35EB				224700000		99300000	78700000	27540		4.03e+08			4.03e+08
	STYRENE			64600000	45700000		91500000	72500000	25440		275100000			275100000
	BENZAL						153900000	121900000	42690		275900000			275900000
	PHENOL			71500000							71500000			71500000
Formaldehyde	HCHO	611400000	2195300000				1.177e+09	1.781e+09	85260000	2.9e+09	294900000			8.77e+09
	CH3CHO	11780000	130090000	73750000			318400000	7.39e+08	16383000	6.8e+08	6860000			1.976e+09
	C2H5CHO	6710000	98630000				53670000	124600000	2752000	257700000	5200000			5.49e+08
	C3H7CHO	38630	79420000							207600000	4190000			292100000
	IPRCHO	38630	79420000							138400000	4190000			222100000
Other Aldehydes	C4H9CHO	32340	66550000							3504000	70050000			70050000
	ACR	49770	102260000				83300000	193800000	4282000	5390000	388800000			388800000
	MACR	39730	81710000							4310000	86110000			86110000
	C4ALDB	39730	81710000				44510000	103300000	2287000	4310000	236100000			236100000
Alkadienes and Other Alkynes	MGLYOX									138500000	138500000			138500000
	C4H6	67600000	771300000	4.74e+09	2.221e+11		2.505e+09	7.78e+08	245800000	1.033e+09	52800000		1.435e+10	2.332e+11
Organic Acids	C5H8													1.435e+10
	HCOOH	4660000	1201400000							1.67e+08	69400000			1442400000
	CH3CO2H	3572000	9.21e+08	167700000						1.28e+08	53200000			1.274e+09
Organic Acids	PROPACID	2898000	746100000							1.04e+08	43100000			897100000
	ACO2H			140400000							140400000			140400000

Table S1: Speciated TNO\_MACCIII emissions for Benelux AVOC and BVOC emissions (molecules  $\text{cm}^{-2} \text{s}^{-1}$ ) mapped to MCM v3.2 species (Kuenen et al., 2014).

Type	MCM_Species	SNAP.1	SNAP.2	SNAP.34	SNAP.5	SNAP.6	SNAP.71	SNAP.72	SNAP.73	SNAP.74	SNAP.8	SNAP.9	BVOC	Total	
Alcohols	CH3OH	140000		3200000		6.38e+09				40419000	24020000			6.45e+09	
	C2H5OH	97400	1.687e+09	903000000		6.52e+09				28082900	63300000			8.39e+09	
	NPROPOL	74600				5.31e+08				21563500	7670000			5.61e+08	
	IPOPOL	74600		1135000		8.49e+08				21563500				8.73e+08	
	NBUTOL	60500				5.17e+08				17451500				5.34e+08	
	BUT2OL	60500				345400000				17451500	10360000			3.73e+08	
	IBUTOL	60500				215300000				17451500				232800000	
	TBUTOL	60500								17451500				17489700	
	PECOH	50900								14643300				14775400	
	IPEAOH	50900								14643300				14775400	
	ME3BUOL	50900								14643300				14775400	
	IPECOH	50900								14643300				14775400	
	IPEBOH	50900								14643300				14775400	
	CYHEXOL	44800								12938100					12966400
	MIBKAOH	38600					109900000			11132900					121100000
	ETHGLY	72300					154300000			20861500					175200000
	PROPGLY	59000					307800000			16950200					324800000
	C6H5CH2OH						88500000								88500000
	MBO	52100									15044300				15077200
	Ketones	CH3COCH3	384100	15896000	6.38e+08		6.66e+09	35750000	229900000		382100000	1414000			7.96e+09
MEK			12828000								1139000			3.236e+09	
MPRK			10745000			3.212e+09					954000			11705000	
DIEK			10745000								954000			11705000	
MIPK			10745000								954000			11705000	
HEX2ONE			9242000								820000			10062000	
HEX3ONE			9242000								820000			10062000	
MIBK			9242000			1.93e+09					820000			1.94e+09	
MTBK			9242000								820000			10062000	
CYHEXONE			9439000	34310000			157500000				837000			202200000	
APINENE											3050000		1.835e+09	1.839e+09	
BPINENE											3050000		1.835e+09	1.839e+09	
LIMONENE							209500000				4580000		1.835e+09	2.046e+09	
METHACET				64470000											64470000
ETHACET			7386000			4.44e+09								4.45e+09	
NBUTACET						3.113e+09								3.113e+09	
IPOACET						1.095e+09								1.095e+09	

Table S1: Speciated TNO\_MACCIII emissions for Benelux AVOC and BVOC emissions (molecules  $\text{cm}^{-2} \text{s}^{-1}$ ) mapped to MCM v3.2 species (Kuenen et al., 2014).

Type	MCM_Species	SNAP.1	SNAP.2	SNAP.34	SNAP.5	SNAP.6	SNAP.71	SNAP.72	SNAP.73	SNAP.74	SNAP.8	SNAP.9	BVOC	Total
	CH3OCHO			7229000								7950000		7229000
	NPROACET					4.1e+08								4.18e+08
	CH3OCH3	61750000	253500000		244300000									5.59e+08
	DIETHER	38360000	94510000											132360000
	MTBE	32330000												32330000
	DIIPRETER	27860000	68540000							19520000				115960000
	ETBE	27860000												27860000
	MO2EOL	37420000			295700000									3.33e+08
	EOX2EOL	31600000			249900000									281500000
	PR2OHMOX	31600000			5e+08									5.32e+08
	BUOX2ETOH	24117000			2.398e+09									2.422e+09
	BOX2PROL	21510000												21510000
	CH2CL2		6.74e+08		1.589e+09						1458000			2.262e+09
	CH3CH2CL		5.22e+08											5.22e+08
	CH3CCL3				1.113e+09						464000			1.114e+09
	TRICLETH				2.516e+09						471000			2.776e+09
	CDICLETH		256600000								951000			174800000
	TDICLETH		173100000								634000			174600000
	CH3CL		5.34e+08											5.34e+08
	CCL2CH2		173100000											173100000
	CHCL2CH3										715000			715000
	VINCL		1.62e+08											1.62e+08
	TCE		40500000			6.11e+08						927000		6.53e+08
	CHCL3		112800000											112800000
Total		1.192e+10	2.1806e+10	6.11e+10	2.049e+12	8.39e+10	3.33e+10	1.581e+10	1688300000	4.285e+09	2.059e+10	1.333e+09	1.9847e+10	2.32e+12

Table S2: Benelux AVOC and BVOC emissions (molecules  $\text{cm}^{-2} \text{s}^{-1}$ ) mapped from MCMv3.2 species to CRIv2 species by weighting with the carbon numbers of the respective species.

Type	MCMv3.2 Species	CRIv2 Species	Belgium	Netherlands	Luxembourg	Total
Ethane	C2H6	C2H6	4.91E+09	8.58E+08	7.96E+09	1.37E+10
Propane	C3H8	C3H8	3.35E+10	4.00E+10	3.94E+10	1.13E+11
Butanes	NC4H10	NC4H10	1.25E+11	3.49E+11	1.47E+11	6.21E+11
	IC4H10	IC4H10	3.03E+10	8.50E+10	3.56E+10	1.51E+11
Pentanes	NC5H12	NC5H12	8.89E+10	2.65E+11	1.05E+11	4.59E+11
	IC5H12	IC5H12	5.33E+10	1.60E+11	6.29E+10	2.76E+11
	NEOP	NEOP	1.11E+07	0.00E+00	3.79E+06	1.49E+07
Hexane and Higher Alkanes	NC6H14	NC6H14	1.52E+10	4.10E+10	1.82E+10	7.44E+10
	M2PE	M2PE	2.39E+09	6.28E+09	2.84E+09	1.15E+10
	M3PE	M3PE	1.34E+09	3.29E+09	1.57E+09	6.20E+09
	NC7H16	NC7H16	1.45E+10	4.12E+10	1.71E+10	7.28E+10
	M2HEX	M2HEX	2.74E+08	4.89E+08	3.17E+08	1.08E+09
	M3HEX	M3HEX	2.37E+08	3.90E+08	2.59E+08	8.86E+08
	M22C4	M22C4	3.47E+07	5.29E+07	5.42E+07	1.42E+08
	M23C4	M23C4	3.47E+07	5.29E+07	5.42E+07	1.42E+08
	NC8H18	NC8H18	1.04E+10	3.06E+10	1.23E+10	5.33E+10
	NC9H20	NC9H20	1.10E+09	1.07E+09	9.78E+08	3.15E+09
	NC10H22	NC10H22	2.15E+09	2.21E+09	1.89E+09	6.25E+09
	NC11H24	NC11H24	8.95E+08	9.26E+08	7.96E+08	2.62E+09
	NC12H26	NC12H26	3.07E+08	8.88E+08	4.42E+08	1.64E+09
	CHEX	CHEX	2.91E+08	2.44E+08	2.80E+08	8.15E+08
Ethene	C2H4	C2H4	3.66E+10	7.03E+09	8.25E+09	5.19E+10
Propene	C3H6	C3H6	1.82E+09	1.68E+09	1.68E+09	5.18E+09
Higher Alkenes	HEX1ENE	HEX1ENE	3.42E+07	5.03E+05	2.40E+07	5.87E+07
	BUT1ENE	BUT1ENE	9.99E+07	7.04E+05	1.86E+08	2.87E+08
	MEPROPENE	MEPROPENE	9.80E+06	0.00E+00	2.46E+06	1.23E+07
	TBUT2ENE	TBUT2ENE	9.80E+06	0.00E+00	2.46E+06	1.23E+07
	CBUT2ENE	CBUT2ENE	9.80E+06	0.00E+00	2.46E+06	1.23E+07
	CPENT2ENE	CPENT2ENE	9.57E+06	2.21E+05	2.07E+06	1.19E+07
	TPENT2ENE	TPENT2ENE	9.57E+06	2.21E+05	2.07E+06	1.19E+07
	PENT1ENE	PENT1ENE	2.68E+07	2.01E+05	5.17E+06	3.22E+07
	ME2BUT2ENE	ME2BUT2ENE	1.09E+07	1.21E+05	2.56E+06	1.36E+07
	ME3BUT1ENE	ME3BUT1ENE	1.09E+07	1.21E+05	2.56E+06	1.36E+07
	ME2BUT1ENE	ME2BUT1ENE	2.05E+06	8.05E+04	3.95E+05	2.53E+06
Ethyne	C2H2	C2H2	2.78E+09	4.51E+09	3.22E+09	1.05E+10

Table S2: Benelux AVOC and BVOC emissions (molecules  $\text{cm}^{-2} \text{s}^{-1}$ ) mapped from MCMv3.2 species to CRIv2 species by weighting with the carbon numbers of the respective species.

Type	MCMv3.2 Species	CRIv2 Species	Belgium	Netherlands	Luxembourg	Total
Benzene	BENZENE	BENZENE	4.52E+09	1.06E+10	5.02E+09	2.01E+10
Toluene	TOLUENE	TOLUENE	5.78E+09	1.22E+10	6.37E+09	2.44E+10
Xylenes	MXYL	MXYL	1.90E+09	3.00E+09	1.88E+09	6.78E+09
	OXYL	OXYL	8.61E+08	1.89E+09	9.66E+08	3.72E+09
	PXYL	PXYL	8.28E+08	1.82E+09	9.08E+08	3.56E+09
Trimethylbenzenes	TM123B	TM123B	4.49E+07	7.36E+07	5.17E+07	1.70E+08
	TM124B	TM124B	1.75E+08	2.89E+08	2.42E+08	7.06E+08
	TM135B	TM135B	5.58E+07	1.03E+08	7.11E+07	2.30E+08
Other Aromatics	EBENZ	EBENZ	3.99E+08	8.28E+08	6.29E+08	1.86E+09
	PBENZ	PBENZ	1.59E+08	4.63E+08	2.31E+08	8.53E+08
	IPBENZ	IPBENZ	7.88E+07	1.04E+08	9.35E+07	2.76E+08
	PETHTOL	PETHTOL	6.03E+07	1.05E+08	1.05E+08	2.70E+08
	METHTOL	METHTOL	6.93E+07	1.14E+08	1.13E+08	2.96E+08
	OETHTOL	OETHTOL	4.19E+07	7.47E+07	7.62E+07	1.93E+08
	DIET35TOL	DIET35TOL	2.45E+08	8.42E+08	3.56E+08	1.44E+09
	DIME35EB	DIME35EB	1.06E+08	1.88E+08	1.09E+08	4.03E+08
	STYRENE	STYRENE	6.01E+07	1.13E+08	1.02E+08	2.75E+08
	BENZAL	BENZAL	4.68E+07	1.61E+08	6.81E+07	2.76E+08
	PHENOL	AROH14	1.86E+07	0.00E+00	5.29E+07	7.15E+07
Formaldehyde	HCHO	HCHO	2.35E+09	3.04E+09	3.38E+09	8.77E+09
Other Aldehydes	CH3CHO	CH3CHO	5.53E+08	8.88E+08	5.35E+08	1.98E+09
	C2H5CHO	C2H5CHO	1.78E+08	1.97E+08	1.74E+08	5.49E+08
	C3H7CHO	C3H7CHO	1.19E+08	6.71E+07	1.06E+08	2.92E+08
	IPRCHO	IPRCHO	9.60E+07	4.57E+07	8.04E+07	2.22E+08
	C4H9CHO	C4H9CHO	4.25E+07	2.45E+06	2.51E+07	7.01E+07
	ACR	UCARB10	8.33E+07	1.35E+08	7.33E+07	2.92E+08
	MACR	UCARB10	5.23E+07	3.01E+06	3.08E+07	8.61E+07
	C4ALDB	UCARB10	7.67E+07	9.70E+07	6.24E+07	2.36E+08
MGLYOX	CARB6	4.52E+07	2.85E+07	3.36E+07	1.07E+08	
Alkadienes and Other Alkynes	C4H6	C4H6	4.36E+10	1.34E+11	5.56E+10	2.33E+11
	C5H8	C5H8	3.35E+09	1.10E+10	0.00E+00	1.44E+10
Organic Acids	HCOOH	HCOOH	9.28E+08	4.04E+07	4.74E+08	1.44E+09
	CH3CO2H	CH3CO2H	7.55E+08	3.10E+07	4.88E+08	1.27E+09
	PROPACID	PROPACID	5.77E+08	2.51E+07	2.95E+08	8.97E+08
	ACO2H	PROPACID	3.64E+07	0.00E+00	1.04E+08	1.40E+08

Table S2: Benelux AVOC and BVOC emissions (molecules  $\text{cm}^{-2} \text{s}^{-1}$ ) mapped from MCMv3.2 species to CRIv2 species by weighting with the carbon numbers of the respective species.

Type	MCMv3.2 Species	CRIv2 Species	Belgium	Netherlands	Luxembourg	Total
Alcohols	CH3OH	CH3OH	2.20E+09	2.40E+09	1.85E+09	6.45E+09
	C2H5OH	C2H5OH	3.30E+09	2.51E+09	2.58E+09	8.39E+09
	NPROPOL	NPROPOL	2.06E+08	2.00E+08	1.55E+08	5.61E+08
	IPROPOL	IPROPOL	3.08E+08	3.19E+08	2.46E+08	8.73E+08
	NBUTOL	NBUTOL	1.91E+08	1.94E+08	1.49E+08	5.34E+08
	BUT2OL	BUT2OL	1.41E+08	1.30E+08	1.02E+08	3.73E+08
	IBUTOL	IBUTOL	8.97E+07	8.09E+07	6.22E+07	2.33E+08
	TBUTOL	TBUTOL	1.74E+07	0.00E+00	8.97E+04	1.75E+07
	PECOH	PECOH	1.47E+07	0.00E+00	7.54E+04	1.48E+07
	IPEAOH	IPEAOH	1.47E+07	0.00E+00	7.54E+04	1.48E+07
	ME3BUOL	ME3BUOL	1.47E+07	0.00E+00	7.54E+04	1.48E+07
	IPECOH	IPECOH	1.47E+07	0.00E+00	7.54E+04	1.48E+07
	IPEBOH	IPEBOH	1.47E+07	0.00E+00	7.54E+04	1.48E+07
	CYHEXOL	CYHEXOL	1.29E+07	0.00E+00	6.64E+04	1.30E+07
	MIBKAOH	MIBKAOH	4.80E+07	4.13E+07	3.18E+07	1.21E+08
	ETHGLY	ETHGLY	7.26E+07	5.80E+07	4.46E+07	1.75E+08
	PROPGLY	PROPGLY	1.20E+08	1.16E+08	8.88E+07	3.25E+08
	C6H5CH2OH	BENZAL	2.31E+07	2.59E+07	1.99E+07	6.89E+07
MBO	PENT1ENE	1.50E+07	0.00E+00	7.72E+04	1.51E+07	
Ketones	CH3COCH3	CH3COCH3	2.67E+09	2.75E+09	2.54E+09	7.96E+09
	MEK	MEK	1.11E+09	1.20E+09	9.26E+08	3.24E+09
	MPRK	MPRK	8.03E+06	3.75E+05	3.30E+06	1.17E+07
	DIEK	DIEK	8.03E+06	3.75E+05	3.30E+06	1.17E+07
	MIPK	MIPK	8.03E+06	3.75E+05	3.30E+06	1.17E+07
	HEX2ONE	HEX2ONE	6.90E+06	3.22E+05	2.84E+06	1.01E+07
	HEX3ONE	HEX3ONE	6.90E+06	3.22E+05	2.84E+06	1.01E+07
	MIBK	MIBK	6.67E+08	7.17E+08	5.56E+08	1.94E+09
	MTBK	MTBK	6.90E+06	3.22E+05	2.84E+06	1.01E+07
	CYHEXONE	CYHEXONE	6.99E+07	5.89E+07	7.34E+07	2.02E+08
Esters	METHACET	METHACET	6.18E+07	0.00E+00	2.67E+06	6.45E+07
	ETHACET	ETHACET	1.48E+09	1.68E+09	1.29E+09	4.45E+09
	NBUTACET	NBUTACET	1.03E+09	1.18E+09	9.03E+08	3.11E+09
	IPROACET	IPROACET	3.63E+08	4.14E+08	3.18E+08	1.10E+09
	CH3OCHO	CH3OCHO	6.93E+06	0.00E+00	2.99E+05	7.23E+06
	NPROACET	NPROACET	1.42E+08	1.55E+08	1.21E+08	4.18E+08

Table S2: Benelux AVOC and BVOC emissions (molecules  $\text{cm}^{-2} \text{s}^{-1}$ ) mapped from MCMv3.2 species to CRIv2 species by weighting with the carbon numbers of the respective species.

Type	MCMv3.2 Species	CRIv2 Species	Belgium	Netherlands	Luxembourg	Total
Ethers	CH3OCH3	CH3OCH3	3.59E+08	9.30E+07	1.07E+08	5.59E+08
	DIETETHER	DIETETHER	1.11E+08	1.46E+06	1.99E+07	1.32E+08
	MTBE	MTBE	1.76E+07	1.23E+06	1.35E+07	3.23E+07
	DIIPREETHER	DIIPREETHER	9.56E+07	1.06E+06	1.93E+07	1.16E+08
	ETBE	ETBE	1.52E+07	1.06E+06	1.16E+07	2.79E+07
	MO2EOL	MO2EOL	1.21E+08	1.11E+08	1.01E+08	3.33E+08
	EOX2EOL	EOX2EOL	1.02E+08	9.39E+07	8.56E+07	2.82E+08
	PR2OHMOX	PR2OHMOX	1.87E+08	1.87E+08	1.58E+08	5.32E+08
	BUOX2ETOH	BUOX2ETOH	8.27E+08	8.90E+08	7.05E+08	2.42E+09
	BOX2PROL	BOX2PROL	1.17E+07	8.20E+05	8.99E+06	2.15E+07
Chlorinated Hydrocarbons	CH2CL2	C2H2	4.17E+08	2.04E+08	5.12E+08	1.13E+09
	CH3CH2CL	C2H2	1.36E+08	0.00E+00	3.86E+08	5.22E+08
	CH3CCL3	C2H2	4.61E+08	2.86E+08	3.67E+08	1.11E+09
	TRICLETH	C2H4	1.11E+09	6.46E+08	1.02E+09	2.78E+09
	CDICLETH	C2H4	4.58E+07	0.00E+00	1.29E+08	1.75E+08
	TDICLETH	C2H4	4.56E+07	0.00E+00	1.29E+08	1.75E+08
	CH3CL	C2H2	6.93E+07	0.00E+00	1.97E+08	2.66E+08
	CCL2CH2	C2H4	4.51E+07	0.00E+00	1.28E+08	1.73E+08
	CHCL2CH3	C2H2	5.35E+05	0.00E+00	1.80E+05	7.15E+05
	VINCL	C2H4	4.20E+07	0.00E+00	1.20E+08	1.62E+08
	TCE	C2H4	2.64E+08	1.57E+08	2.32E+08	6.53E+08
	CHCL3	C2H4	1.47E+07	0.00E+00	4.17E+07	5.64E+07
Terpenes	APINENE	APINENE	4.22E+08	1.27E+09	1.47E+08	1.84E+09
	BPINENE	BPINENE	4.22E+08	1.27E+09	1.47E+08	1.84E+09
	LIMONENE	APINENE	4.96E+08	1.34E+09	2.10E+08	2.05E+09
Total			5.15E+11	1.25E+12	5.64E+11	2.32E+12

Table S3: Benelux AVOC and BVOC emissions (molecules  $\text{cm}^{-2} \text{s}^{-1}$ ) mapped from MCMv3.2 species to MOZART-4 species by weighting with the carbon numbers of the respective species.

Type	MCMv3.2 Species	MOZART-4 Species	Belgium	Netherlands	Luxembourg	Total
Ethane	C2H6	C2H6	4.91E+09	8.58E+08	7.96E+09	1.37E+10
Propane	C3H8	C3H8	3.35E+10	4.00E+10	3.94E+10	1.13E+11
Butanes	NC4H10	BIGALK	1.00E+11	2.79E+11	1.17E+11	4.96E+11
	IC4H10	BIGALK	2.42E+10	6.80E+10	2.85E+10	1.21E+11
Pentanes	NC5H12	BIGALK	8.89E+10	2.65E+11	1.05E+11	4.59E+11
	IC5H12	BIGALK	5.33E+10	1.60E+11	6.29E+10	2.76E+11
	NEOP	BIGALK	1.11E+07	0.00E+00	3.79E+06	1.49E+07
Hexane and Higher Alkanes	NC6H14	BIGALK	1.82E+10	4.92E+10	2.18E+10	8.92E+10
	M2PE	BIGALK	2.87E+09	7.54E+09	3.41E+09	1.38E+10
	M3PE	BIGALK	1.61E+09	3.94E+09	1.89E+09	7.44E+09
	NC7H16	BIGALK	2.02E+10	5.77E+10	2.39E+10	1.02E+11
	M2HEX	BIGALK	3.83E+08	6.84E+08	4.44E+08	1.51E+09
	M3HEX	BIGALK	3.31E+08	5.45E+08	3.63E+08	1.24E+09
	M22C4	BIGALK	4.16E+07	6.34E+07	6.51E+07	1.70E+08
	M23C4	BIGALK	4.16E+07	6.34E+07	6.51E+07	1.70E+08
	NC8H18	BIGALK	1.67E+10	4.89E+10	1.97E+10	8.53E+10
	NC9H20	BIGALK	1.99E+09	1.93E+09	1.76E+09	5.68E+09
	NC10H22	BIGALK	4.31E+09	4.42E+09	3.78E+09	1.25E+10
	NC11H24	BIGALK	1.97E+09	2.04E+09	1.75E+09	5.76E+09
	NC12H26	BIGALK	7.37E+08	2.13E+09	1.06E+09	3.93E+09
	CHEX	BIGALK	3.49E+08	2.93E+08	3.36E+08	9.78E+08
Ethene	C2H4	C2H4	3.66E+10	7.03E+09	8.25E+09	5.19E+10
Propene	C3H6	C3H6	1.82E+09	1.68E+09	1.68E+09	5.18E+09
Higher Alkenes	HEX1ENE	BIGENE	5.13E+07	7.55E+05	3.60E+07	8.81E+07
	BUT1ENE	BIGENE	9.99E+07	7.04E+05	1.86E+08	2.87E+08
	MEPROPENE	BIGENE	9.80E+06	0.00E+00	2.46E+06	1.23E+07
	TBUT2ENE	BIGENE	9.80E+06	0.00E+00	2.46E+06	1.23E+07
	CBUT2ENE	BIGENE	9.80E+06	0.00E+00	2.46E+06	1.23E+07
	CPENT2ENE	BIGENE	1.20E+07	2.77E+05	2.58E+06	1.49E+07
	TPENT2ENE	BIGENE	1.20E+07	2.77E+05	2.58E+06	1.49E+07
	PENT1ENE	BIGENE	3.34E+07	2.52E+05	6.47E+06	4.01E+07
	ME2BUT2ENE	BIGENE	1.37E+07	1.51E+05	3.20E+06	1.71E+07
	ME3BUT1ENE	BIGENE	1.37E+07	1.51E+05	3.20E+06	1.71E+07
	ME2BUT1ENE	BIGENE	2.57E+06	1.01E+05	4.93E+05	3.16E+06
Ethyne	C2H2	C2H2	2.78E+09	4.51E+09	3.22E+09	1.05E+10

Table S3: Benelux AVOC and BVOC emissions (molecules  $\text{cm}^{-2} \text{s}^{-1}$ ) mapped from MCMv3.2 species to MOZART-4 species by weighting with the carbon numbers of the respective species.

Type	MCMv3.2 Species	MOZART-4 Species	Belgium	Netherlands	Luxembourg	Total
Benzene	BENZENE	TOLUENE	3.87E+09	9.05E+09	4.30E+09	1.72E+10
Toluene	TOLUENE	TOLUENE	5.78E+09	1.22E+10	6.37E+09	2.44E+10
Xylenes	MXYL	TOLUENE	2.17E+09	3.43E+09	2.14E+09	7.74E+09
	OXYL	TOLUENE	9.85E+08	2.16E+09	1.10E+09	4.25E+09
	PXYL	TOLUENE	9.46E+08	2.08E+09	1.04E+09	4.07E+09
Trimethylbenzenes	TM123B	TOLUENE	5.78E+07	9.47E+07	6.65E+07	2.19E+08
	TM124B	TOLUENE	2.25E+08	3.72E+08	3.12E+08	9.09E+08
	TM135B	TOLUENE	7.17E+07	1.32E+08	9.14E+07	2.95E+08
Other Aromatics	EBENZ	TOLUENE	4.57E+08	9.46E+08	7.19E+08	2.12E+09
	PBENZ	TOLUENE	2.04E+08	5.95E+08	2.97E+08	1.10E+09
	IPBENZ	TOLUENE	1.01E+08	1.34E+08	1.20E+08	3.55E+08
	PETHTOL	TOLUENE	7.76E+07	1.34E+08	1.36E+08	3.48E+08
	METHTOL	TOLUENE	8.90E+07	1.47E+08	1.45E+08	3.81E+08
	OETHTOL	TOLUENE	5.39E+07	9.61E+07	9.80E+07	2.48E+08
	DIET35TOL	TOLUENE	3.84E+08	1.32E+09	5.60E+08	2.26E+09
	DIME35EB	TOLUENE	1.52E+08	2.68E+08	1.56E+08	5.76E+08
	STYRENE	TOLUENE	7.72E+07	1.45E+08	1.31E+08	3.53E+08
	BENZAL	TOLUENE	6.01E+07	2.07E+08	8.76E+07	3.55E+08
	PHENOL	TOLUENE	1.59E+07	0.00E+00	4.54E+07	6.13E+07
	Formaldehyde	HCHO	CH2O	2.35E+09	3.04E+09	3.38E+09
Other Aldehydes	CH3CHO	CH3CHO	5.53E+08	8.88E+08	5.35E+08	1.98E+09
	C2H5CHO	CH3CHO	2.67E+08	2.95E+08	2.61E+08	8.23E+08
	C3H7CHO	CH3CHO	2.37E+08	1.34E+08	2.11E+08	5.82E+08
	IPRCHO	CH3CHO	1.92E+08	9.14E+07	1.61E+08	4.44E+08
	C4H9CHO	CH3CHO	1.06E+08	6.13E+06	6.27E+07	1.75E+08
	ACR	MACR	8.33E+07	1.35E+08	7.33E+07	2.92E+08
	MACR	MACR	5.23E+07	3.01E+06	3.08E+07	8.61E+07
	C4ALDB	MACR	7.67E+07	9.70E+07	6.24E+07	2.36E+08
	MGLYOX	CH3COCHO	4.52E+07	4.28E+07	5.05E+07	1.39E+08
Alkadienes and Other Alkynes	C4H6	BIGENE	4.36E+10	1.34E+11	4.45E+10	2.22E+11
	C5H8	ISOP	3.35E+09	1.10E+10	0.00E+00	1.44E+10
Organic Acids	HCOOH	HCOOH	9.28E+08	4.04E+07	4.74E+08	1.44E+09
	CH3CO2H	CH3COOH	7.55E+08	3.10E+07	4.88E+08	1.27E+09
	PROPACID	CH3COOH	8.65E+08	3.77E+07	4.42E+08	1.34E+09
	ACO2H	CH3COOH	5.46E+07	0.00E+00	1.56E+08	2.11E+08

Table S3: Benelux AVOC and BVOC emissions (molecules  $\text{cm}^{-2} \text{s}^{-1}$ ) mapped from MCMv3.2 species to MOZART-4 species by weighting with the carbon numbers of the respective species.

Type	MCMv3.2 Species	MOZART-4 Species	Belgium	Netherlands	Luxembourg	Total
Alcohols	CH3OH	CH3OH	2.20E+09	2.40E+09	1.85E+09	6.45E+09
	C2H5OH	C2H5OH	3.30E+09	2.51E+09	2.58E+09	8.39E+09
	NPROPOL	C2H5OH	3.08E+08	3.00E+08	2.33E+08	8.41E+08
	IPROPOL	C2H5OH	4.61E+08	4.79E+08	3.69E+08	1.31E+09
	NBUTOL	C2H5OH	3.82E+08	3.89E+08	2.98E+08	1.07E+09
	BUT2OL	C2H5OH	2.82E+08	2.59E+08	2.04E+08	7.45E+08
	IBUTOL	C2H5OH	1.79E+08	1.62E+08	1.24E+08	4.65E+08
	TBUTOL	C2H5OH	3.48E+07	0.00E+00	1.79E+05	3.50E+07
	PECOH	C2H5OH	3.66E+07	0.00E+00	1.88E+05	3.68E+07
	IPEAOH	C2H5OH	3.66E+07	0.00E+00	1.88E+05	3.68E+07
	ME3BUOL	C2H5OH	3.66E+07	0.00E+00	1.88E+05	3.68E+07
	IPECOH	C2H5OH	3.66E+07	0.00E+00	1.88E+05	3.68E+07
	IPEBOH	C2H5OH	3.66E+07	0.00E+00	1.88E+05	3.68E+07
	CYHEXOL	C2H5OH	3.87E+07	0.00E+00	1.99E+05	3.89E+07
	MIBKAOH	C2H5OH	1.44E+08	1.24E+08	9.53E+07	3.63E+08
	ETHGLY	C2H5OH	7.26E+07	5.80E+07	4.46E+07	1.75E+08
	PROPGLY	C2H5OH	1.80E+08	1.73E+08	1.33E+08	4.86E+08
	C6H5CH2OH	C2H5OH	1.04E+08	1.17E+08	8.94E+07	3.10E+08
	MBO	C2H5OH	3.75E+07	0.00E+00	1.93E+05	3.77E+07
Ketones	CH3COCH3	CH3COCH3	2.67E+09	2.75E+09	2.54E+09	7.96E+09
	MEK	MEK	1.11E+09	1.20E+09	9.26E+08	3.24E+09
	MPRK	MEK	1.00E+07	4.69E+05	4.12E+06	1.46E+07
	DIEK	MEK	1.00E+07	4.69E+05	4.12E+06	1.46E+07
	MIPK	MEK	1.00E+07	4.69E+05	4.12E+06	1.46E+07
	HEX2ONE	MEK	1.04E+07	4.84E+05	4.25E+06	1.51E+07
	HEX3ONE	MEK	1.04E+07	4.84E+05	4.25E+06	1.51E+07
	MIBK	MEK	1.00E+09	1.08E+09	8.34E+08	2.91E+09
	MTBK	MEK	1.04E+07	4.84E+05	4.25E+06	1.51E+07
	CYHEXONE	MEK	1.05E+08	8.83E+07	1.10E+08	3.03E+08
Esters	METHACET	BIGALK	3.71E+07	0.00E+00	4.08E+08	4.45E+08
	ETHACET	BIGALK	1.18E+09	1.35E+09	5.15E+07	2.58E+09
	NBUTACET	BIGALK	1.24E+09	1.41E+09	5.15E+07	2.70E+09
	IPROACET	BIGALK	3.63E+08	4.14E+08	7.90E+07	8.56E+08
	CH3OCHO	BIGALK	6.93E+06	0.00E+00	5.14E+07	5.83E+07
	NPROACET	BIGALK	1.42E+08	1.55E+08	7.22E+04	2.97E+08

Table S3: Benelux AVOC and BVOC emissions (molecules  $\text{cm}^{-2} \text{s}^{-1}$ ) mapped from MCMv3.2 species to MOZART-4 species by weighting with the carbon numbers of the respective species.

Type	MCMv3.2 Species	MOZART-4 Species	Belgium	Netherlands	Luxembourg	Total
Ethers	CH3OCH3	BIGALK	1.44E+08	3.72E+07	1.47E+08	3.28E+08
	DIETETHER	BIGALK	8.92E+07	1.17E+06	1.47E+08	2.37E+08
	MTBE	BIGALK	1.76E+07	1.23E+06	2.10E+08	2.29E+08
	DIIPREETHER	BIGALK	1.15E+08	1.27E+06	1.60E+06	1.18E+08
	ETBE	BIGALK	1.82E+07	1.27E+06	1.03E+09	1.05E+09
	MO2EOL	BIGALK	7.25E+07	6.67E+07	1.08E+09	1.22E+09
	EOX2EOL	BIGALK	8.16E+07	7.51E+07	3.18E+08	4.75E+08
	PR2OHMOX	BIGALK	1.49E+08	1.49E+08	2.99E+05	2.98E+08
	BUOX2ETOH	BIGALK	9.92E+08	1.07E+09	1.21E+08	2.18E+09
	BOX2PROL	BIGALK	1.64E+07	1.15E+06	4.28E+07	6.04E+07
Chlorinated Hydrocarbons	CH2CL2	BIGALK	1.67E+08	8.16E+07	1.60E+07	2.65E+08
	CH3CH2CL	BIGALK	5.42E+07	0.00E+00	1.35E+07	6.77E+07
	CH3CCL3	BIGALK	1.84E+08	1.14E+08	2.32E+07	3.21E+08
	TRICLETH	BIGALK	4.43E+08	2.58E+08	1.40E+07	7.15E+08
	CDICLETH	BIGALK	1.83E+07	0.00E+00	6.08E+07	7.91E+07
	TDICLETH	BIGALK	1.82E+07	0.00E+00	6.85E+07	8.67E+07
	CH3CL	BIGALK	2.77E+07	0.00E+00	1.26E+08	1.54E+08
	CCL2CH2	BIGALK	1.80E+07	0.00E+00	8.46E+08	8.64E+08
	CHCL2CH3	BIGALK	2.14E+05	0.00E+00	1.26E+07	1.28E+07
	VINCL	BIGALK	1.68E+07	0.00E+00	2.05E+08	2.22E+08
	TCE	BIGALK	1.06E+08	6.27E+07	1.54E+08	3.23E+08
	CHCL3	BIGALK	5.86E+06	0.00E+00	1.47E+08	1.53E+08
Terpenes	APINENE	C10H16	4.22E+08	1.27E+09	4.78E+07	1.74E+09
	BPINENE	C10H16	4.22E+08	1.27E+09	9.26E+07	1.78E+09
	LIMONENE	C10H16	4.96E+08	1.34E+09	1.67E+07	1.85E+09
Total			5.05E+11	1.21E+12	5.39E+11	2.25E+12

Table S4: Benelux AVOC and BVOC emissions (molecules  $\text{cm}^{-2} \text{s}^{-1}$ ) mapped from MCMv3.2 species to RADM2 species by weighting with the carbon numbers of the respective species.

Type	MCMv3.2 Species	RADM2 Species	Belgium	Netherlands	Luxembourg	Total
Ethane	C2H6	ETH	4.91E+09	8.58E+08	7.96E+09	1.37E+10
Propane	C3H8	HC3	3.47E+10	4.13E+10	4.08E+10	1.17E+11
Butanes	NC4H10	HC3	1.73E+11	4.81E+11	2.02E+11	8.56E+11
	IC4H10	HC3	4.18E+10	1.17E+11	4.91E+10	2.08E+11
Pentanes	NC5H12	HC5	9.26E+10	2.76E+11	1.09E+11	4.78E+11
	IC5H12	HC5	5.55E+10	1.66E+11	6.55E+10	2.87E+11
	NEOP	HC3	1.91E+07	0.00E+00	6.54E+06	2.56E+07
Hexane and Higher Alkanes	NC6H14	HC5	1.89E+10	5.12E+10	2.28E+10	9.29E+10
	M2PE	HC5	2.99E+09	7.85E+09	3.55E+09	1.44E+10
	M3PE	HC5	1.67E+09	4.11E+09	1.97E+09	7.75E+09
	NC7H16	HC5	2.11E+10	6.01E+10	2.49E+10	1.06E+11
	M2HEX	HC8	2.42E+08	4.33E+08	2.81E+08	9.56E+08
	M3HEX	HC8	2.10E+08	3.45E+08	2.30E+08	7.85E+08
	M22C4	HC3	7.18E+07	1.09E+08	1.12E+08	2.93E+08
	M23C4	HC5	4.34E+07	6.61E+07	6.78E+07	1.77E+08
	NC8H18	HC8	1.06E+10	3.10E+10	1.25E+10	5.41E+10
	NC9H20	HC8	1.26E+09	1.22E+09	1.11E+09	3.59E+09
	NC10H22	HC8	2.73E+09	2.80E+09	2.39E+09	7.92E+09
	NC11H24	HC8	1.25E+09	1.29E+09	1.11E+09	3.65E+09
	NC12H26	HC8	4.66E+08	1.35E+09	6.71E+08	2.49E+09
	CHEX	HC8	2.21E+08	1.85E+08	2.13E+08	6.19E+08
Ethene	C2H4	OL2	3.66E+10	7.03E+09	8.25E+09	5.19E+10
Propene	C3H6	OLT	1.43E+09	1.32E+09	1.32E+09	4.07E+09
Higher Alkenes	HEX1ENE	OLT	5.40E+07	7.94E+05	3.79E+07	9.27E+07
	BUT1ENE	OLT	1.05E+08	7.41E+05	1.96E+08	3.02E+08
	MEPROPENE	OLI	8.17E+06	0.00E+00	2.05E+06	1.02E+07
	TBUT2ENE	OLI	8.17E+06	0.00E+00	2.05E+06	1.02E+07
	CBUT2ENE	OLI	8.17E+06	0.00E+00	2.05E+06	1.02E+07
	CPENT2ENE	OLI	9.97E+06	2.31E+05	2.15E+06	1.24E+07
	TPENT2ENE	OLI	9.97E+06	2.31E+05	2.15E+06	1.24E+07
	PENT1ENE	OLT	3.52E+07	2.65E+05	6.81E+06	4.23E+07
	ME2BUT2ENE	OLI	1.14E+07	1.26E+05	2.66E+06	1.42E+07
	ME3BUT1ENE	OLT	1.44E+07	1.59E+05	3.36E+06	1.79E+07
	ME2BUT1ENE	OLI	2.14E+06	8.39E+04	4.11E+05	2.63E+06
Ethyne	C2H2	HC3	1.92E+09	3.11E+09	2.22E+09	7.25E+09

Table S4: Benelux AVOC and BVOC emissions (molecules  $\text{cm}^{-2} \text{s}^{-1}$ ) mapped from MCMv3.2 species to RADM2 species by weighting with the carbon numbers of the respective species.

Type	MCMv3.2 Species	RADM2 Species	Belgium	Netherlands	Luxembourg	Total
Benzene	BENZENE	TOL	3.82E+09	8.93E+09	4.24E+09	1.70E+10
Toluene	TOLUENE	TOL	5.69E+09	1.21E+10	6.28E+09	2.41E+10
Xylenes	MXYL	XYL	1.71E+09	2.69E+09	1.69E+09	6.09E+09
	OXYL	XYL	7.74E+08	1.70E+09	8.68E+08	3.34E+09
	PXYL	XYL	7.44E+08	1.63E+09	8.16E+08	3.19E+09
Trimethylbenzenes	TM123B	XYL	4.54E+07	7.45E+07	5.23E+07	1.72E+08
	TM124B	XYL	1.77E+08	2.93E+08	2.45E+08	7.15E+08
	TM135B	XYL	5.64E+07	1.04E+08	7.19E+07	2.32E+08
Other Aromatics	EBENZ	TOL	4.50E+08	9.33E+08	7.08E+08	2.09E+09
	PBENZ	TOL	2.01E+08	5.86E+08	2.93E+08	1.08E+09
	IPBENZ	TOL	9.99E+07	1.32E+08	1.18E+08	3.50E+08
	PETHTOL	XYL	6.10E+07	1.06E+08	1.07E+08	2.74E+08
	METHTOL	XYL	7.00E+07	1.16E+08	1.14E+08	3.00E+08
	OETHTOL	XYL	4.24E+07	7.56E+07	7.71E+07	1.95E+08
	DIET35TOL	XYL	3.02E+08	1.04E+09	4.41E+08	1.78E+09
	DIME35EB	XYL	1.19E+08	2.11E+08	1.23E+08	4.53E+08
	STYRENE	TOL	7.61E+07	1.43E+08	1.29E+08	3.48E+08
	BENZAL	CSL	6.38E+07	2.20E+08	9.29E+07	3.77E+08
	PHENOL	CSL	1.69E+07	0.00E+00	4.81E+07	6.50E+07
Formaldehyde	HCHO	HCHO	2.35E+09	3.04E+09	3.38E+09	8.77E+09
Other Aldehydes	CH3CHO	ALD	4.61E+08	7.40E+08	4.46E+08	1.65E+09
	C2H5CHO	ALD	2.23E+08	2.46E+08	2.18E+08	6.87E+08
	C3H7CHO	ALD	1.98E+08	1.12E+08	1.76E+08	4.86E+08
	IPRCHO	ALD	1.60E+08	7.62E+07	1.34E+08	3.70E+08
	C4H9CHO	ALD	8.86E+07	5.10E+06	5.23E+07	1.46E+08
	ACR	ALD	1.39E+08	2.25E+08	1.22E+08	4.86E+08
	MACR	ALD	8.71E+07	5.02E+06	5.14E+07	1.44E+08
	C4ALDB	ALD	1.28E+08	1.62E+08	1.04E+08	3.94E+08
MGLYOX	MGLY	4.52E+07	2.85E+07	3.36E+07	1.07E+08	
Alkadienes and Other Alkynes	C4H6	OLI	3.64E+10	1.12E+11	4.63E+10	1.95E+11
	C5H8	ISO	3.35E+09	1.10E+10	0.00E+00	1.44E+10
Organic Acids	HCOOH	ORA1	9.28E+08	4.04E+07	4.74E+08	1.44E+09
	CH3CO2H	ORA2	7.55E+08	3.10E+07	4.88E+08	1.27E+09
	PROPACID	ORA2	8.65E+08	3.77E+07	4.42E+08	1.34E+09
	ACO2H	OLT	2.87E+07	0.00E+00	8.19E+07	1.11E+08

Table S4: Benelux AVOC and BVOC emissions (molecules  $\text{cm}^{-2} \text{s}^{-1}$ ) mapped from MCMv3.2 species to RADM2 species by weighting with the carbon numbers of the respective species.

Type	MCMv3.2 Species	RADM2 Species	Belgium	Netherlands	Luxembourg	Total
Alcohols	CH3OH	HC3	7.59E+08	8.27E+08	6.37E+08	2.22E+09
	C2H5OH	HC3	2.27E+09	1.73E+09	1.78E+09	5.78E+09
	NPROPOL	HC5	1.29E+08	1.25E+08	9.70E+07	3.51E+08
	IPROPOL	HC5	1.92E+08	2.00E+08	1.54E+08	5.46E+08
	NBUTOL	HC8	9.67E+07	9.84E+07	7.55E+07	2.71E+08
	BUT2OL	HC8	7.14E+07	6.56E+07	5.17E+07	1.89E+08
	IBUTOL	HC8	4.54E+07	4.10E+07	3.15E+07	1.18E+08
	TBUTOL	HC3	2.40E+07	0.00E+00	1.24E+05	2.41E+07
	PECOH	HC8	9.27E+06	0.00E+00	4.77E+04	9.32E+06
	IPEAOH	HC8	9.27E+06	0.00E+00	4.77E+04	9.32E+06
	ME3BUOL	HC8	9.27E+06	0.00E+00	4.77E+04	9.32E+06
	IPECOH	HC3	2.53E+07	0.00E+00	1.30E+05	2.54E+07
	IPEBOH	HC8	9.27E+06	0.00E+00	4.77E+04	9.32E+06
	CYHEXOL	HC8	9.79E+06	0.00E+00	5.04E+04	9.84E+06
	MIBKAOH	KET	7.39E+07	6.36E+07	4.89E+07	1.86E+08
	ETHGLY	HC8	1.84E+07	1.47E+07	1.13E+07	4.44E+07
	PROPGLY	HC8	4.57E+07	4.39E+07	3.37E+07	1.23E+08
	C6H5CH2OH	HC8	2.64E+07	2.95E+07	2.26E+07	7.85E+07
MBO	OLT	1.97E+07	0.00E+00	1.02E+05	1.98E+07	
Ketones	CH3COCH3	KET	2.05E+09	2.11E+09	1.95E+09	6.11E+09
	MEK	KET	1.14E+09	1.23E+09	9.49E+08	3.32E+09
	MPRK	KET	1.03E+07	4.81E+05	4.23E+06	1.50E+07
	DIEK	KET	1.03E+07	4.81E+05	4.23E+06	1.50E+07
	MIPK	KET	1.03E+07	4.81E+05	4.23E+06	1.50E+07
	HEX2ONE	HC5	8.63E+06	4.03E+05	3.55E+06	1.26E+07
	HEX3ONE	HC5	8.63E+06	4.03E+05	3.55E+06	1.26E+07
	MIBK	HC5	8.34E+08	8.96E+08	6.95E+08	2.43E+09
	MTBK	KET	1.06E+07	4.96E+05	4.36E+06	1.55E+07
	CYHEXONE	HC5	8.73E+07	7.36E+07	9.18E+07	2.53E+08
Esters	METHACET	HC3	6.39E+07	0.00E+00	2.76E+06	6.67E+07
	ETHACET	HC3	2.04E+09	2.32E+09	1.78E+09	6.14E+09
	NBUTACET	HC5	1.29E+09	1.47E+09	1.13E+09	3.89E+09
	IPROACET	HC3	6.26E+08	7.14E+08	5.48E+08	1.89E+09
	CH3OCHO	HC3	1.19E+07	0.00E+00	5.16E+05	1.24E+07
	NPROACET	HC3	2.45E+08	2.68E+08	2.09E+08	7.22E+08

Table S4: Benelux AVOC and BVOC emissions (molecules  $\text{cm}^{-2} \text{s}^{-1}$ ) mapped from MCMv3.2 species to RADM2 species by weighting with the carbon numbers of the respective species.

Type	MCMv3.2 Species	RADM2 Species	Belgium	Netherlands	Luxembourg	Total
Ethers	CH3OCH3	HC3	2.48E+08	6.41E+07	7.38E+07	3.86E+08
	DIETETHER	HC8	5.64E+07	7.40E+05	1.01E+07	6.72E+07
	MTBE	HC3	3.03E+07	2.12E+06	2.32E+07	5.56E+07
	DIIPREETHER	HC8	7.26E+07	8.06E+05	1.47E+07	8.81E+07
	ETBE	HC8	1.15E+07	8.06E+05	8.83E+06	2.11E+07
	MO2EOL	HC8	4.59E+07	4.22E+07	3.85E+07	1.27E+08
	EOX2EOL	HC8	5.16E+07	4.75E+07	4.33E+07	1.42E+08
	PR2OHMOX	HC8	9.46E+07	9.45E+07	8.00E+07	2.69E+08
	BUOX2ETOH	HC8	6.28E+08	6.76E+08	5.35E+08	1.84E+09
	BOX2PROL	HC8	1.04E+07	7.26E+05	7.97E+06	1.91E+07
Chlorinated Hydrocarbons	CH2CL2	HC3	2.87E+08	1.41E+08	3.53E+08	7.81E+08
	CH3CH2CL	HC3	9.35E+07	0.00E+00	2.66E+08	3.60E+08
	CH3CCL3	HC3	3.18E+08	1.97E+08	2.53E+08	7.68E+08
	TRICLETH	HC3	7.64E+08	4.45E+08	7.03E+08	1.91E+09
	CDICLETH	HC3	3.16E+07	0.00E+00	8.88E+07	1.20E+08
	TDICLETH	HC3	3.14E+07	0.00E+00	8.87E+07	1.20E+08
	CH3CL	HC3	4.78E+07	0.00E+00	1.36E+08	1.84E+08
	CCL2CH2	HC8	1.14E+07	0.00E+00	3.25E+07	4.39E+07
	CHCL2CH3	HC3	3.69E+05	0.00E+00	1.24E+05	4.93E+05
	VINCL	HC8	1.06E+07	0.00E+00	3.03E+07	4.09E+07
	TCE	HC3	1.82E+08	1.08E+08	1.60E+08	4.50E+08
	CHCL3	HC3	1.01E+07	0.00E+00	2.88E+07	3.89E+07
Terpenes	APINENE	OLI	8.78E+08	2.65E+09	3.05E+08	3.83E+09
	BPINENE	OLI	8.78E+08	2.65E+09	3.05E+08	3.83E+09
	LIMONENE	OLI	1.03E+09	2.80E+09	4.38E+08	4.27E+09
Total			5.83E+11	1.44E+12	6.42E+11	2.66E+12

Table S5: Benelux emissions (molecules  $\text{cm}^{-2} \text{s}^{-1}$ ) of AVOC and BVOC species in CB05, determined by translating the MCMv3.2 emissions from Table S1 into CB05 species using Yarwood et al. (2005).

CB05 Species	Belgium	Luxembourg	Netherlands	Total
PAR	1.80E+12	4.90E+12	2.10E+12	8.80E+12
OLE	8.96E+10	2.70E+11	1.13E+11	4.73E+11
TOL	6.55E+09	1.39E+10	7.51E+09	2.80E+10
XYL	4.39E+09	8.50E+09	4.87E+09	1.78E+10
FORM	2.41E+09	3.09E+09	3.44E+09	8.94E+09
ALD2	5.64E+08	8.88E+08	5.37E+08	1.99E+09
ALDX	7.21E+08	6.35E+08	6.27E+08	1.98E+09
MEOH	2.20E+09	2.40E+09	1.85E+09	6.45E+09
ETOH	3.30E+09	2.51E+09	2.58E+09	8.39E+09
FACD	9.28E+08	4.04E+07	4.74E+08	1.44E+09
AACD	1.33E+09	5.61E+07	7.83E+08	2.17E+09
ETH	3.78E+10	7.68E+09	9.39E+09	5.49E+10
ETHA	4.91E+09	8.58E+08	7.96E+09	1.37E+10
IOLE	3.87E+07	4.43E+05	9.05E+06	4.82E+07
ISOP	3.35E+09	1.10E+10	0.00E+00	1.44E+10
TERP	1.34E+09	3.89E+09	5.03E+08	5.73E+09
Total	1.96E+12	5.23E+12	2.25E+12	9.44E+12

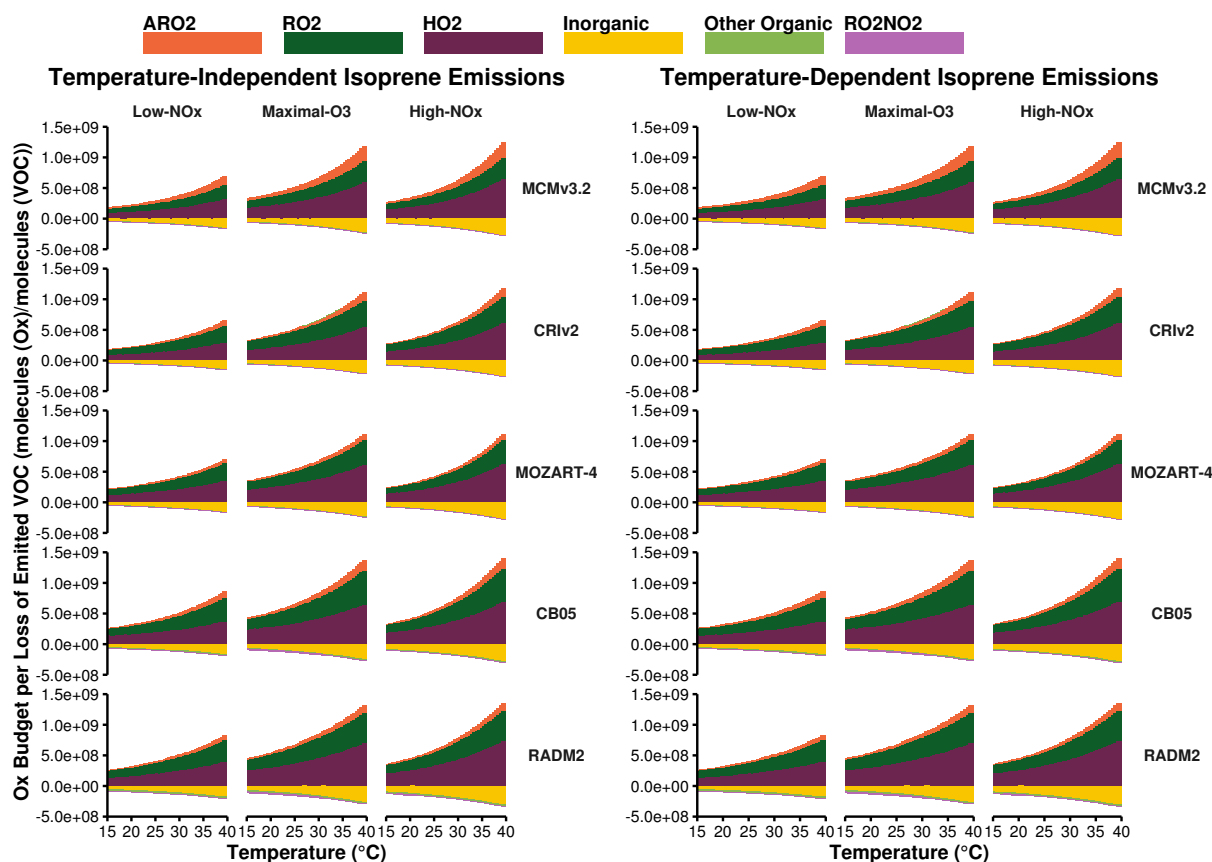
### S3 Ozone Production and Consumption Budgets

Section 3.2 of the research article analysed the  $\text{O}_x$  production and consumption budgets normalised by the total loss rate of the emitted VOCs. The absolute  $\text{O}_x$  production and consumption budgets are included to support the conclusion that the increased OH-reactivity of the emitted VOCs caused the increase of ozone with temperature in our study. As in Fig. 4 of the research article the production and consumption of  $\text{O}_x$  are allocated to the net contributions of major categories: ‘ARO2’, ‘RO2’ and ‘HO2’ represent the reaction of acyl peroxy radicals, alkyl peroxy radicals and  $\text{HO}_2$  with NO. ‘Inorganic’ represents the net contribution of inorganic reactions, ‘RO2NO2’ the net contribution of peroxy nitrates and any other reactions were allocated to the ‘Other Organic’ category. Figure S1a represents the absolute production and consumption budgets of  $\text{O}_x$  for each chemical mechanism, each  $\text{NO}_x$ -regime and using a temperature-independent and temperature-dependent source of isoprene emissions.

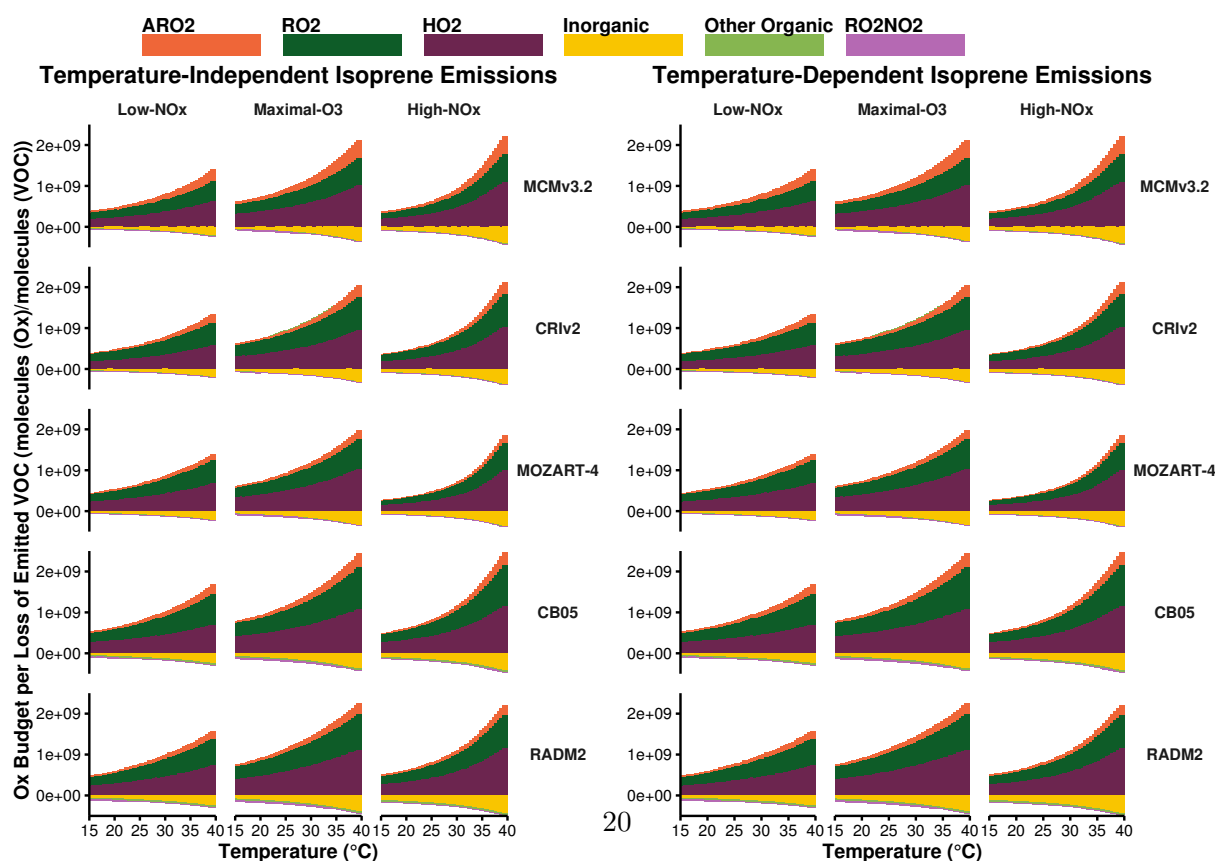
The absolute production and consumption budgets of  $\text{O}_x$  in the box model simulations without mixing, described in Section 3.3 of the research article, are illustrated in Fig. S1b. Similar to Fig. S1a, the increase in  $\text{O}_x$  with temperature is due to the increased OH-reactivity of emitted VOCs. The increased  $\text{O}_x$  with temperature led to the faster rate of increase in ozone with temperature than the original box model setup that included mixing, this is presented in Sect. 3.3 of the research article.

Figure S1: Day-time budgets of  $O_x$  allocated to the  $NO_x$ -regimes allocated to the net contribution of reactions to  $O_x$  budgets are allocated to categories of inorganic reactions, peroxy nitrates (RO2NO2), reactions of NO with HO2, alkyl peroxy radicals (RO2) and acyl peroxy radicals (ARO2). All other reactions are allocated to the 'Other Organic' category.

(a)  $O_x$  production and consumption budgets with box model setup including mixing.



(b)  $O_x$  production and consumption budgets with box model setup without including mixing.



## 52 References

- 53 B. Bonn, E. von Schneidmesser, D. Andrich, J. Quedenau, H. Gerwig, A. Lüdecke, J. Kura,  
54 A. Pietsch, C. Ehlers, D. Klemp, C. Kofahl, R. Nothard, A. Kerschbaumer, W. Junkermann,  
55 R. Grote, T. Pohl, K. Weber, B. Lode, P. Schönberger, G. Churkina, T. M. Butler, and M. G.  
56 Lawrence. BAERLIN2014 - The influence of land surface types on and the horizontal heterogeneity  
57 of air pollutant levels in Berlin. *Atmospheric Chemistry and Physics Discussions*, 2016:1–62,  
58 2016.
- 59 J. Coates and T. M. Butler. A comparison of chemical mechanisms using tagged ozone production  
60 potential (TOPP) analysis. *Atmospheric Chemistry and Physics*, 15(15):8795–8808, 2015.
- 61 J. J. P. Kuenen, A. J. H. Visschedijk, M. Jozwicka, and H. A. C. Denier van der Gon.  
62 TNO-MACC\_II emission inventory; a multi-year (2003–2009) consistent high-resolution european  
63 emission inventory for air quality modelling. *Atmospheric Chemistry and Physics*, 14(20):  
64 10963–10976, 2014.
- 65 A. S. M. Lourens, T. M. Butler, J. P. Beukes, P. G. van Zyl, G. D. Fourie, and M. G. Lawrence.  
66 Investigating atmospheric photochemistry in the Johannesburg-Pretoria megacity using a box  
67 model. *South African Journal of Science*, 112(1/2), 2016.
- 68 G. Yarwood, S. Rao, M. Yocke, and G. Z. Whitten. Updates to the Carbon Bond Chemical  
69 Mechanism: CB05. Technical report, U. S Environmental Protection Agency, 2005.

# Chapter 10

## Publication List

### 10.1 Scientific Articles

J. Coates and T. M. Butler. A comparison of chemical mechanisms using tagged ozone production potential (TOPP) analysis. *Atmospheric Chemistry and Physics*, 15(15):8795–8808, 2015.

E. von Schneidmesser, J. Coates, H. D. van der Gon, A. Visschedijk, and T. Butler. Variation of the NMVOC speciation in the solvent sector and the sensitivity of modelled tropospheric ozone. *Atmospheric Environment*, 135:59 – 72, 2016.

J. Coates, K. A. Mar, N. Ojha, and T. M. Butler. The influence of temperature on ozone production under varying NO<sub>x</sub> conditions – a modelling study. *Atmospheric Chemistry and Physics Discussions*, Submitted, 2016.

### 10.2 Presentations

J. Coates and T. M. Butler, Comparing chemical mechanisms using Tagged Ozone Production Potentials. 2013 American Geophysical Union Fall Meeting, 10th December 2013.

J. Coates and T. M. Butler, Comparing how chemical mechanisms treat VOC degradation and impact on ozone production. 2014 PhD Conference on Earth System Science, 13th March 2014.

J. Coates and T. M. Butler, The influence of atmospheric conditions on the production of ozone during VOC oxidation. 2015 American Geophysical Union Fall Meeting, 15th December 2015.

### 10.3 Posters

J. Coates and T. M. Butler, Comparing how chemical mechanisms treat VOC degradation and impact on ozone production. 2014 PhD Conference on Earth System Science, 13th March 2014.

J. Coates and T. Butler, Understanding ozone pollution: a comparison of chemical mechanisms. 2014 Our Climate Our Future Conference, 7th October 2014.

# Appendix

## Contribution to Paper I:

The experimental setup was designed by Tim Butler, the tagging of all chemical mechanisms and all model simulations performed by myself at the IASS. All analysis and graphical plotting of the model output data was performed by myself. The paper was written by myself assisted by Tim Butler.

## Contribution to Paper II:

The experimental setup was formulated by Erika von Schneidemesser, Tim Butler and myself. Translating the NMVOC emissions into chemical mechanism species was performed by myself aided by Erika von Schneidemesser and colleagues at TNO. All model simulations and analysis of model data was performed by myself at the IASS. I prepared an initial draft of the paper which was further updated by Erika von Schneidemesser and the other co-authors.

## Contribution to Paper III:

The experimental setup was designed by Tim Butler and myself. I updated the box model setup to include vertical mixing and a diurnal PBL height, and performed all model simulations at the IASS. Observational data was provided by Noelia Otero Felipe and WRF-Chem model output by Kathleen A. Mar and Narendra Ojha. Analysis and graphical plotting of the box model output data was performed by myself. The paper was written by myself aided by the co-authors.